Status of muon catalysis of nuclear fusion reactions

L. I. Men'shikov and L. N. Somov

I. V. Kurchatov Institute of Atomic Energy, Moscow and Joint Institute of Nuclear Research, Dubna
Usp. Fiz. Nauk **160**, 47–103 (August 1990)

The results of research on muon catalysis of nuclear fusion reactions are presented. A new direction is examined—muon catalysis in plasma. Possible applications of muon catalysis are discussed.

INTRODUCTION

In the last few years new experiments on muon catalysis of nuclear fusion reactions of hydrogen isotopes have been conducted and are being planned in virtually every laboratory in the world that has a source of muons. This field of research is of interest for the following reasons.

First, the possibilities of creating alternative sources of energy at ordinary temperatures based on muon catalysis of the fusion reactions

$$t\mu+d\rightarrow dt\mu\rightarrow {}^4He+n+\mu^-+17{,}6\ \text{MeV}$$

are being considered. One scheme under consideration is the muon-catalyzed fusion reaction mentioned above combined with neutron multiplication by high-energy protons ($E_p \sim 1$ GeV) in uranium-238 targets (see the review of S. S. Gershteĭn *et al.* in this issue of Soviet Physics Uspekhi. We believe, however, that such a system for producing energy, like the use of muonic processes in general for producing energy, is unrealisitic; it would be more realistic to use muon catalysis to produce neutrons.

Second, mu-atomic and mu-molecular processes in hydrogen have played a large role in the determination of the value of the muon–nucleon weak interaction constant from experiments on nuclear capture of muons by protons $\mu^- + p \rightarrow n + \nu_\mu$. This has stimulated the study of mu-atomic and mu-molecular processes in hydrogen.

Finally, nuclear fusion reactions of hydrogen isotopes catalyzed by muons and mu-atomic and mu-molecular reactions occurring in matter (muonic chemistry) comprise the physics of exotic atoms, which is of interest from both fundamental and applied standpoints.

Several reviews[1-4] on mu-atomic and mu-molecular processes occurring in hydrogen and in materials with nuclear charge greater than unity have now been published. In this review we examine the latest experimental and theoretical achievements in this field. In particular, we shall discuss a new direction in muon physics, namely, the investigation of mu-atomic and mu-molecular processes in a dense, low-temperature, hydrogen plasma.[5-7] For certain parameters of a DT plasma the number of cycles X_c, i.e., the number of fusion reactions of deuterium and tritium catalyzed by one muon, is an order of magnitude larger than in a cold molecular DT mixture, and can reach $X_c \sim 1500$. This theoretical result gives a new perspective on the problem of the practical application of the phenomenon of muon catalysis and, what is more realistic, it raises the possibility of creating based on this a monochromatic ($E_n \sim 14$ MeV) and high-intensity source of neutrons. We also studied possible experiments on determining the characteristics of muon catalysis in plasma.

This review is organized as follows. In Sec. 1 we briefly describe the basic processes involved in muon catalysis of nuclear reactions of hydrogen isotopes in cold hydrogen and we discuss the latest publications in this field. In Sec. 2 we present the results of calculations of the effective coefficient of sticking of a muon to the products of a fusion reaction—the mu-ions and μ^3He and μ^4He. In Sec. 3 we consider elementary mu-atomic and mu-molecular processes in plasma. Section 4 is devoted to the kinetics of these processes in a nonuniform plasma. Finally, in Sec. 5 we discuss possible experiments. It is our happy duty to thank R. B. Baksht, V. B. Belyaev, Vit. M. Bystritskiĭ, D. P. Grechukhin, S. V. Zakharov, M. V. Kazarnoskiĭ, S. L. Nedoseev, L. I. Rudakov, V. P. Smirnov, B. A. Trubnikov, A. V. Fedyunin, K. V. Chukbar, and V. A. Shakirov for numerous and fruitful discussions.

1. MUON CATALYSIS OF NUCLEAR REACTIONS IN COLD HYDROGEN

The study of muon catalysis started in 1947 with Frank's hypothesis[8] about the possible formation of a muonic molecule $pd\mu$ followed by a nuclear fusion reaction in it. Frank stated this hypothesis in connection with his interpretation of experiments performed by Lattes, Occhialini, and Powell,[9] in which the decay $\pi^- \rightarrow \mu^- + \nu_\mu$ was studied.

The phenomenon of muon catalysis was first observed experimentally in 1957 by Alvarez's group[10] in the mixture $H_2 + D_2$. The discovery of this phenomenon stimulated a large number of theoretical and experimental investigations of this subject.

The sequence of mu-atomic and mu-molecular processes occurring when negative muons stop in mixtures of hydrogen isotopes, is as follows. Mu-atoms of hydrogen isotopes form as a result of Coulomb capture of the muons and they are small (the Bohr radius of a hydrogen mu-atom is $a_\mu \hbar^2/m_\mu e^2 \approx 2.56 \cdot 10^{-11}$ cm; $m_\mu = 206 m_e$; and, m_μ and m_e are the muon and electron mass). They penetrate freely through the electronic shells of the molecules of the medium and approach their nuclei to distances of the order of the mu-atomic unit of length a_μ. This close approach is accompanied by a number of mu-atomic and mu-molecular processes: elastic scattering of muonic atoms by the nuclei of hydrogen isotopes; transitions between the levels of the hyperfine structure of the muonic atoms; transfer of muons from light to heavy hydrogen isotopes (isotopic exchange reaction); transfer of muons from hydrogen isotope nuclei to nuclei of elements with charge $Z > 1$; and, formation of the muonic molecules $pp\mu$, $pd\mu$, $dd\mu$, $dt\mu$, and $pt\mu$.

 0038-5670/90/080616-31$01.00

In muonic molecules subbarrier nuclear fusion reactions of hydrogen isotopes occur. As a result of these reactions of muon can be released and can therefore once again initiate the next chain of muon catalysis. Thus in a DT mixture, with which we shall be primarily concerned, the following reactions occur:

$$\mu^-[D_2+T_2]\to\begin{bmatrix}d\mu\\ t\mu\downarrow\end{bmatrix}\xrightarrow[\lambda_{dt\mu}]{\lambda_{dt}}dt\mu\xrightarrow{\lambda_f^{dt}}\begin{matrix}(1-\omega_s)\,{}^4He+n+\mu^-,\\ \omega_s\,\mu\,{}^4He+n.\end{matrix} \tag{1.1a}$$

(1.1b)

Here we have introduced the following notation: λ_f^{dt} is the rate of nuclear fusion reactions in $dt\mu$ molecules, λ_{dt} is the rate of transfer of muons from d nuclei to t nuclei, and ω_s is the coefficient of sticking of muons to He nuclei formed as a result of the fusion reactions.

We shall examine in greater detail the processes occurring when a muon enters a mixture of hydrogen isotopes.

1.1 Formation of mu-atoms

Relativistic muons with $v_\mu \sim c$ (v_μ, $E_\mu \approx m_\mu v_\mu^2/2$, and m_μ, that are the velocity, energy, and mass of the muons) entering a molecular D_2T_2 mixture decelerate to $v_\mu \sim 0.1 v_0$ ($v_0 = e^2/\hbar \approx 2.2\times 10^8$ cm/s is the atomic unit (a.u.) of velocity) over a time $\sim 3\times 10^{-9}/\varphi$,[11,12] where here and below all quantities are given in CGS units, $\varphi = N/N_0$ and N and $N_0 = 4.25\times 10^{22}$ cm^{-3} are the number of nuclei per 1 cm^3 in the mixture of $D_2 + T_2$ and in liquid hydrogen, respectively. To simplify expressions, atomic units $\hbar = m_e = e = 1$ are also employed. The atomic units of mass, length, and time are, respectively, $m = m_e \approx 10^{-27}$ g, $l = a_0 = \hbar/m_e e^2 \approx 0.5\cdot 10^{-8}$ cm, $\tau = \tau_0 = \hbar/m_e e^4 = a_0/v_0 \approx 2.5\cdot 10^{-17}$ s. The density of liquid hydrogen in these units is $N_0 = 6.3\times 10^{-3}$ a.u.

After the muons slow down to $v_\mu \leqslant 0.1$ ($E_\mu \leqslant 30$ eV) muatoms start to form by Wightman's mechanism[13,14] of Coulomb capture of muons. For $E_\mu \leqslant I_H = 13.6$ eV a muon approaching an atom knocks an electron out of it, after which the total energy of the muon in the field of the nucleus a = d, t, or p (kinetic + potential) is negative. A mu-atom $(a\mu)_n$ in an excited Rydberg state with the principal quantum number $n \sim (m_\mu/m_e)^{1/2} \sim 15$ and characteristic size of the muon orbit $r_\mu \sim a_0$ is formed. The cross section for the process of formation of a mu-atom is $\sigma_a \sim 10^{-16}$ cm^2 for $E_\mu \leqslant I_H$ and $\sigma_a \approx 0$ for $E_\mu \geqslant I_H$. The characteristic rate of Coulomb capture is $\lambda_a = N\langle v_\mu \sigma_a\rangle \sim 5\cdot 10^{13}\varphi$. In a D_2T_2 mixture with deuterium and tritium concentrations C_d and C_t excited mu-atoms $(t\mu)_n$ and $(d\mu)_n$ are formed with the probabilities C_t and $C_d = 1 - C_t$.

Next, cascade deexcitation of mu-atoms starts. The most important deexcitation processes are as follows:[15-23] Stark mixing of orbital angular momentum states (l, m) of the type $(t\mu)_{nlm} + D_2 \Rightarrow (t\mu)_{nl'm'} + D_2'$, where l and m are the orbital angular momentum of the muon and its projection on a stationary axis; the external Auger process ($K = 1, 2, \ldots$):

$$(t\mu)_n + D_2 \begin{cases}\longrightarrow (t\mu)_{n-K} + D_2^+ + e,\\ \longrightarrow (t\mu)_{n-K} + D_2^*;\end{cases} \tag{1.2}$$

transfer of muons to tritium in excited states of mu-atoms (this process is important, since the mu-molecules $dt\mu$ are formed only in the collisions $t\mu + d$ and the $d\mu$ atom is repelled from t (Ref. 24):

$$(d\mu)_n + t \to d + (t\mu)_n; \tag{1.3}$$

radiative transitions with emission of an x-ray are important at the lower levels $n \leqslant 3$:

$$(t\mu)_n \to (t\mu)_{n-K} + \gamma. \tag{1.4}$$

In an excited state a mu-atom has a nonzero dipole moment $\mathbf{d} \neq 0$ ($\mathbf{d} = 3n^2\mathbf{A}/(2m_\mu)$, $|\mathbf{A}| = e$ is the eccentricity of the muon orbit, and $\mathbf{A}$ is the Runge–Lenz vector). This is characteristic only for the Coulomb field (in any other fields the orbits precess and the average dipole moment is equal to zero). For this reason the character of the motion of excited mu-atoms ($n \geqslant 2$) in matter is qualitatively different from that of unexcited ($n = 1$, $\mathbf{d} = \langle \mathbf{d}\rangle = 0$) mu-atoms. A mu-atom in a 1s state is similar to a neutron and is scattered relatively weakly by nuclei and electrons in matter. The characteristic cross section for such scattering is $\sigma \sim 10^{-19}$ cm^2. The potential energy of an excited mu-atom in the electric field $\mathbf{E}$ of a molecule $U = -\mathbf{d}\cdot\mathbf{E}$ is greater than the kinetic energy. Indeed, within the electronic shell of the molecule, where $\mathbf{E} \sim 1$ a.u., even in the state $n = 2$, which has the smallest dipole moment $d \sim 0.02$ a.u., $U \sim 0.5$ eV $\gg T \leqslant 0.1$ eV. The trajectory of an excited mu-atom is strongly curved already at the periphery of the molecule and therefore the chartacteristic scattering cross section is large:[17-18] $\sigma_{el} \sim 3\times 10^{-16}$ cm^2. The rate of thermalization of the excited mu-atoms is very high: $\lambda_T \sim N v_T \sigma_{el} \sim (2\text{–}5)\cdot 10^{12}\varphi$, where $v_T \sim 4\times 10^5$ cm/s is the thermal velocity of a mu-atom. The rate λ_T is approximately an order of magnitude higher than the rate of ($\sim 10^{11}\,\varphi$) of the other inelastic processes (1.2) and (1.3), so that on the average the excited mu-atoms are thermalized, though in the case of the Auger transitions (1.2) they can accelerate.[21-22]

Let us sum up. A mu-atom formed in states with $n \sim 15$ reaches, as a result of Auger transitions, over a time $\sim 10^{-12}/\varphi$ s levels with $n \sim 3$–4. Then, $\sim 10^{-11}$ s later, it transfers into the 1s state; these latter transitions are radiative (1.8). In the excited states with $\varphi \geqslant 0.1$ the mu-atoms are practically thermalized. As φ decreases, the relative number of fast mu-atoms which have not been thermalized by the time the radiative transition into the 1s state occurs, increases.[21,22] From states with $n \leqslant 4$ the muons transfer from deuterium to tritium; the characteristic cross sections of this process are significant on mu-atomic scales: $\sigma_{trans} \sim 10^{-16}$ cm^2.

1.2. Muon transfer and scattering of mu-atoms

The charge-transfer process (1.3) is irreversible because the isotopic splitting of the levels of the $t\mu$ and $d\mu$ atoms is significant compared with the temperature: $\Delta\varepsilon_n = \varepsilon_n(d\mu) - \varepsilon_n(t\mu) = 48/n^2$ eV. the cross section of this process[17-18] $\sigma_{ct} \approx \sigma_{cap} W_{ct}$ is very large ($\sim 10^{-16}$ cm^2). This is explained by the large cross section σ_{cap} for capture of a mu-atom by a molecule on trajectories leading to nuclei, and the significant charge-transfer probability $W_{ct} \sim 0.1$–0.3. Charge-transfer occurs at small distances between the mu-atom and the nucleus of the molecule $R \sim r_\mu \sim n^2/m_\mu$, comparable to the size r_μ of the muon orbit and at which the

potential barrier separating the region of motion of the muon near each of the approaching nuclei vanishes. The results of detailed calculations of σ_{ct} are presented in Refs. 17–18 and 23.

Charge transfer occur primarily from states with $n \leqslant 4$. Indeed, the lifetimes of mu-atoms in higher energy levels is short, since the rates of the Auger processes are significant. In addition, for $n \geqslant 5$ the rate of an Auger transition for a mu-atom inside a molecule is so high ($\Gamma(R) \sim 10^{15}$) that the molecule breaks up before the mu-atom approaches the nuclei. After the mu-atom knocks out electrons, the nuclei of the molecules fly apart, because of the Coulomb repulsion within a time $\sim 10^{-15}$ s, much shorter than the approach time of the mu-atom to the nuclei. The mu-atom ($n \geqslant 5$) seemingly "explodes" the molecule, and because the explosion time is short and the mu-atom is small, the recoil of the mu-atom itself is insignificant.

Figure 1 shows the theoretical values of the probability q_{1s} that a mu-atom reaches the 1s state.[16] Evidently, under the typical conditions of muon catalysis $q_{1s} \ll 1$, i.e., the transfer muons from deuterium to tritium occurs primarily in the cascade process.

The formation of complexes in two-stage Auger processes

$$(t\mu)_n + D_2 \Rightarrow \begin{cases} [(t\mu)_{n-1}D_2^+] + e, \\ \longrightarrow (t\mu)_{n-2} + 2d + e \end{cases}$$

and in triple collisions of the type $(d\mu)_n + T_2 + D_2 \rightarrow [(d\mu)_n T_2] + D_2'$ additionally decrease q_{1s}.[18] Indeed, if within the lifetime of the complex the captured mu-atom collides several times with the constituent nuclei, the charge-transfer probability increases to $W_{ct} \sim 1$. Experiments[25–26] apparently do not confirm this conclusion, i.e., even though complexes do form, their formation has virtually no effect on q_{1s}. This can be explained by the high rate ($\Gamma \sim 10^{15}$) of the secondary Auger process leading to the decay of the complex.

We shall now study collisions with nuclei of unexcited mu-atoms. The temperatures of greatest interest for muon catalysis, in any case, fall into the range $T \leqslant 500$ eV. At these temperatures collisions of the type $(t\mu)_{1s} + d \rightarrow (t\mu)_n + d$ with nuclei and with excitation of mu-atoms are insignificant. For this reason we shall ignore them.

In the case of different nuclei ($a \neq b$, a, b = d, t, p) elastic scattering and charge transfer are possible:

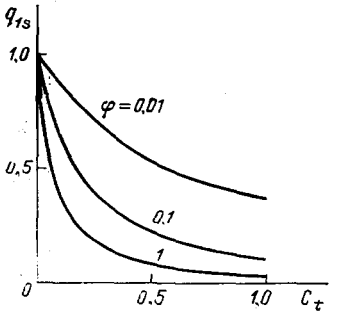

FIG. 1. The probability that a $(d\mu)_n$ atom reaches the 1s state. The numbers on the curves indicate the values of φ.

$$a\mu + b \begin{cases} \longrightarrow a\mu + b, & (1.5a) \\ \longrightarrow a + b\mu. & (1.5b) \end{cases}$$

In the case of identical nuclei (a = b) at temperatures $T \leqslant 1$ eV, which are of greatest interest for muon catalysis, the hyperfine splitting $\Delta\varepsilon_{hf}$ of the 1s levels of the mu-atoms, which is caused by the interaction of the magnetic moments of the muon and the nucleus, is significant. For mu-atoms $p\mu$, $d\mu$, and $t\mu$, respectively, we have (in eV) $\Delta\varepsilon_{hf} = \varepsilon(F=1) - \varepsilon(F=0) = 0.183$; $\varepsilon(F=3/2) - \varepsilon(F=1/2) = 0.049$, $\varepsilon(F=1) - \varepsilon(F=0) = 0.241$, where $\mathbf{F} = \mathbf{S}_\mu + \mathbf{S}_a$ and $\mathbf{S}_\mu$ and $\mathbf{S}_a$ are the spins of the muon and the nucleus. During the collisions elastic scattering ($F' = F$) and spin flip ($F' \neq F$) are possible:

$$(a\mu)_F + a \frac{\sigma_{FF}}{\sigma_{FF'}} \begin{cases} \longrightarrow (a\mu)_F + a, & (1.6) \\ \longrightarrow (a\mu)_{F \neq F'} + a. & (1.7) \end{cases}$$

In addition, in the last case the muon is transferred to the other nucleus (charge transfer), forming with it a different spin state $F' \neq F$. Spin flip in collision with "foreign" nuclei of the type $(t\mu)_F + d \Rightarrow (t\mu)_{F' \neq F} + d$ is unlikely,[1] since it is caused by the relativistic spin–spin and spin–orbital interactions.

In the most interesting range of collision energies the two-level approximation (TLA) below is applicable. In this approximation only two adiabatic states of the muon $|1s\sigma\rangle \equiv \varphi_g$, and $|2p\sigma\rangle \equiv \varphi_u$, which are eigenstates of the Hamiltonian h describing the motion of a muon in the field of stationary nuclei $\hbar\varphi_{g,u} = E_{g,u}(R)\varphi_{g,u}$ (see the review of Ref. 27), where R is the separation of the nuclei, participate. The wave functions (WF below) of the muon $\varphi_a = (\varphi_g - \varphi_u)/\sqrt{2}$ and $\varphi_b = (\varphi_g + \varphi_u)/\sqrt{2}$ corresponds to the correct boundary conditions in the limit $R \rightarrow \infty$. In the states φ_a and φ_b the muon in the limit $R \rightarrow \infty$ is localized on the a and b nuclei, respectively. In the two-level approximation the wave function of the system in the center-of-mass system (CM below) is $\Psi = \varphi_a\chi_a(R) + \varphi_b\chi_b(R)$. The transfer reactions (1.5b) in which muons in the 1s states are transferred, $d\mu + t \rightarrow d + t\mu$, $p\mu + d \rightarrow p + d\mu$, and $p\mu + t \rightarrow p + t\mu$, are significant for small values of φ and C_t. In these reactions energy corresponding to the significant isotopic splitting $\Delta E_{ab} = \varepsilon_{1s}(a\mu) - \varepsilon_{1s}(b\mu)$ is released: $\Delta\varepsilon_{dt} = 4.8$ eV, $\Delta\varepsilon_{ab} = 135$ eV, $\Delta\varepsilon_{pt} = 183$ eV. For low collision energies ε [$\varepsilon \leqslant 0.2$ eV for the pair dt and $\varepsilon \leqslant 5$ eV for the pairs pd and pt (Ref. 28)], the cross sections for these inelastic processes satisfy Bethe's $1/v$ law, so that the rates $\lambda = Nv\sigma$ of the transfer processes at these energies are constant:[28–30] $\lambda_{dt} = 1.9 \cdot 10^8 \varphi C_t$, $\lambda_{pt} = 8 \cdot 10^9 \varphi C_t$, $\lambda_{pd} = 1.7 \cdot 10^{10} \varphi C_d$ (here and below primarily the theoretical values are given; the cross sections and rates are given in cm^2 and s^{-1}, respectively). For low energies the cross sections and rates of the reactions (1.6) and (1.7) are equal to[28]

$p\mu + p$: $\sigma_{11} = 1.2 \cdot 10^{-18}$, $\sigma_{00} = 4 \cdot 10^{-20}$,
$\lambda_{10}^0 = N_0\sigma_{10}v = 2 \cdot 10^{10}$,
$t\mu + t$: $\sigma_{11} = 1.3 \cdot 10^{-19}$, $\sigma_{00} = 2 \cdot 10^{-22}$, $\lambda_{10}^0 = 1.5 \cdot 10^9$,
$d\mu + d$: $\sigma_{3/2,3/2} = 1.8 \cdot 10^{-19}$,
$\sigma_{1/2,1/2} = 1.7 \cdot 10^{-19}$, $\lambda_{3/2,1/2}^0 = 4 \cdot 10^7$.

For collision energies $E < 1$ eV, the effect of the electronic shell[31–35] and chemical binding[35–36] of nuclei in the

molecule on the cross sections of the processes (1.5)–(1.7) become significant.

For mu-atom energies in the range $0.01 \leqslant E \leqslant 0.3$ eV, which determines their energy distribution function, taking the chemical bond of the nuclei in the molecule into account reduces to premulitplying by the factor $\eta \sim 1.2$–1.4 the cross sections σ_b^0 for elastic scattering of mu-atoms $a\mu$ by nuclei b. In the analysis of the kinetics of retardation of mu-atoms the matter may be assumed, to a reasonable approximation, to be atomic, taking for the cross section for elastic scattering of mu-atoms $a\mu$ by atoms of the type $B = H$, D, and T the expression $\sigma_B = \eta\sigma_b^0 + \sigma_{el}^B$, where $\sigma_{el}^B \approx \sigma_0[1 + p^2 + (p^4/3)]/(1 + p^2)^3$ is the cross section (in a.u.) for scattering by the electron shell, $\sigma_0 = 4\pi\mu_a^2/m_\mu^4 \sim 10^{-18}$ cm^2, $\mu_a^{-1} = m_{a\mu}^{-1} + M_b^{-1}$, and $p = (2\mu_a E)^{1/2}$ is the relative momentum of $a\mu$ and B. For $E \geqslant \omega \sim 0.3$ eV, where ω is the vibrational quantum of the molecule, η must be set equal to unity.

The cross sections for the inelastic processes (spin flip and charge transfer) remain practically unchanged, since these processes occur at small separations R between the nuclei, where the effect of the electrons is insignificant.

1.3. Formation of mu-molecules

The bound states of mu-molecules are numbered by the quantum numbers (J,v), where $\mathbf{J} = \mathbf{L} + \mathbf{1}$ is the total orbital angular momentum of the mu-molecule, $\mathbf{L}$ and $\mathbf{1}$ are the orbital angular momenta of the nuclei and the muon, v is the vibrational quantum number, which numbers, starting with $v = 0$, in order of decreasing binding energy the states of the mu-molecule with fixed J. The mu-molecules $pp\mu$, $pd\mu$, and $pt\mu$ have two bound states $(J,v) = (0,0)$ and $(1,0)$, the $dd\mu$ and $dt\mu$ molecules have five bound states ($(0,0)$, $(0,1)$, $(1,1)$, and $(2,0)$), and the $tt\mu$ molecule has six bound states—the state $(3,0)$ is added to those listed.[27]

In the two-level approximation, in which only the σ states of the muon are taken into account, the total angular momentum J is equal to L, i.e., the nuclei carry the entire angular momentum. Indeed, φ_a and φ_b depend on the arguments r_0, R, and $\hat{\mathbf{r}}_0 \cdot \hat{\mathbf{R}}$, where $\hat{\mathbf{r}}_0 = \mathbf{r}_0/r_0$, $\hat{\mathbf{R}} = \mathbf{R}/R$, and $\mathbf{r}_0$ are the coordinates of the muon measured from the midpoint between the nuclei. Since $[\mathbf{J}^2, \hat{\mathbf{r}}_0 \cdot \hat{\mathbf{R}}] = 0$, we have $(J^2\varphi_a\chi_a = \varphi_a J^2\chi_a(R) = \varphi_a \mathbf{L}^2\chi_a(\mathbf{R})$, whence it follows that $J = L$, since $\mathbf{L}^2\chi_{a,b} = L(L+1)\chi_{a,b}$. Taking this into account and remaining within the two-level approximation, we shall not distinguish below between J and L. Transitions of nuclei into states with $L \neq J$ become possible only if states of the muon with nonzero projection $\mathbf{1} \cdot \hat{\mathbf{R}}$ of the angular momentum on the internuclear axis are taken into account. The probability of such transitions is small: $\sim (m_\mu/M_0)^2 \ll 1$.

Depending on the binding energy $\varepsilon \equiv \varepsilon_{Jv}$, two mechanisms of formation of mu-molecules are possible: nonresonant[1,37] if $|\varepsilon| \geqslant I_H$ and resonant[38–41] if $|\varepsilon| \leqslant D$, where $I_H \approx 4.5$ eV is the dissociation energy of a hydrogen isotope molecule. In the case of a deep level $|\varepsilon| \geqslant I_H$ in the conversion process

$$a\mu + BX \rightarrow [(ab\mu)Xe]^+ + e. \tag{1.8}$$

the electron carries away the excess energy ($\approx |\varepsilon|$). Here X = p, d, t, H, D, or T. The molecular ion $[(ab\mu)Xe]^+$, analogous to H_2^+, in which one of the nuclei (b) is replaced by a practically point ($\sim 5 \times 10^{-11}$ cm) mu-molecule $ab\mu$ with the same charge (+1) is formed in the reaction (1.8).

The reaction (1.8) is caused primarily by the dipole E1 interaction of the mu-molecule with electrons:[37]

$$V_d = -\mathbf{dE}, \tag{1.9}$$

where $\mathbf{d}$ is the dipole moment operator of the mu-operator of the mu-molecule and $\mathbf{E}$ is the electric field of the electrons at the location of the mu-molecule.

Finding the rate $\mu_{ab\mu}^n$ of the nonresonant formation of the mu-molecules in the conversion process (1.8), according to Fermi's golden rule, reduces to calculating the matrix element of the dipole moment of the mu-molecule[37]

$$d^2 = \sum_{M_J} |\langle vJM_J | \mathbf{d} | \mathbf{p} \rangle|^2,$$

where M_J is the projection of J on the stationary z axis, $\Psi_{vJM_J} \equiv |vJM_J\rangle = [\varphi_a\chi_a(R) + \varphi_b\chi_b(R)]Y_{JM_J}(\hat{\mathbf{R}})/R$ is the wave function of $ab\mu$ in the two-level approximation, and ψ_J is the wave function of the system $a\mu + b$ with relative momentum $\mathbf{p}$. The electronic part of the matrix element of the transition can be expressed in terms of the cross section for photoionization of the hydrogen molecule,[42] for which there are extensive experimental data.

In the case of identical nuclei $(aa\mu)$ we have

$$\Psi_{vJM_J} = \varphi_g\chi_{Jv}(R)\, Y_{JM_J}(\hat{\mathbf{R}})\, R^{-1}, \tag{1.10}$$

and in addition because of Pauli's principle $(-1)^{I+J} = 1$, where I is the total spin of the nuclei. When mu-molecules are formed I, is conserved, since $[\mathbf{I}, \mathbf{V}_d] = 0$. For identical nuclei $\mathbf{d} = -[1 + (m_\mu/m_{aa\mu})]\mathbf{r}_0$, so that only terms in the continuum wave functions ψ_p that are proportional to φ_u contribute to $\lambda_{aa\mu}^n$. When the nuclei are perrmuted $(\mathbf{R} \rightarrow -\mathbf{R})\mathbf{P}\varphi_u = -\varphi_u$, so that at low energies ($E \leqslant 10$ eV), when only the S waves are significant in the wave functions $\chi_{a,b}(\mathbf{R})$ describing the motion of the nuclei, according to Pauli's principle the spin I must be odd, since the spin wave function of the nuclei has the property $\mathbf{Pe} = (-1)^{2s_a + J}\mathbf{e}$. Then we conclude from Eq. (1.10) that the mu-molecules $aa\mu$ form predominantly in states with odd J.[2,43] For $tt\mu$, therefore, $J = 1$ and $J = 3$, while for $pp\mu$ and $dd\mu$ $J = 1$.

We note that the identity of the nuclei in large molecules with B = X does not play any role in the formation of mu-molecules. The reason is that the overlap integral of the wave functions ψ_1 and ψ_2, corresponding to the complexes $[(ab\mu)Xe]^+$ and $[b(aX\mu)e]^+$ is negligibly small (X = b).

The rate of formation of the mu-molecules $ab\mu$ can evidently be written in the form $\lambda_{ab\mu} = \lambda_{ab\mu}^0 \varphi C_b$. The typical values of the reduced nonresonant formation rates are $\lambda_n^0 \sim 10^6$–10^7 and for $dd\mu$ $\lambda_n^0 = 4.6 \times 10^4$.[37] It has been found that it is important to calculate $\lambda_{pp\mu}^n$ when choosing the experimental conditions for experiments on determining the muon-proton weak interaction constants.[43–46] The resonant mechanism gives much higher rates.

The resonant formation of the mu-molecules $dt\mu$ and $dd\mu$ in the reactions (Vesman's mechanism)

$$t\mu + DX \rightarrow [(dt\mu)^* Xee]_{vK'} \tag{1.11a}$$

$$d\mu + DX \rightarrow [(dd\mu)^* Xee]_{vK} \tag{1.11b}$$

plays the key role in the chain of muon catalysis processes.[47]

The processes (1.11a) and (1.11b) are made possible by the existence of quasistationary states of the mu-molecular complexes [(dtμ)*Xee] and [(ddμ)*Xee], one nucleus of which is the mu-molecule formed in the excited weakly bound state with quantum numbers $(J,v) = (1,1)$. According to this resonant mechanism[38,39] the energy released when the mu-molecule is formed goes into excitation of the vibrational-rotational levels (v,K) of the molecular complexes [(dtμ)Xee] and [(ddμ)Xee]. This is followed either by deexcitation of the mu-molecule with conversion to an electron (see Sec. 1.4) or the nuclear reaction in the (1,1) state or decay of the complex[48,49] into the starting fragments according to the scheme

$$[(dt\mu)^*Xee]_{vK} \begin{cases} \longrightarrow [(dt\mu)^+ Xe] + e^-, \\ \longrightarrow {}^4He + n + \mu^+, & (1.12a) \\ \longrightarrow t\mu + DX, & (1.12b) \end{cases}$$

$$[(dd\mu)^*Xee]_{vK} \begin{cases} \longrightarrow [(dd\mu)^+ Xe] + e^-, & (1.13a) \\ \longrightarrow {}^3He + n + \mu^-, \\ \longrightarrow d\mu + DX. & (1.13b) \end{cases}$$

The rate λ of resonant formation of the mu-molecules $dt\mu$ and $dd\mu$ in the reactions (1.11a) and (1.11b), expressed in terms of the squared matarix element of the perturbation operator **V** with respect to the wave functions of the initial and final states of the system, $\lambda \sim |\langle f|\mathbf{V}|i\rangle|^2$, was first evaluated in Refs. 38 and 39. However, further investigation of the process of resonant formation of mu-molecules and the acquisition of extensive experimental data required a more detailed study of the choice of the wave functions ψ_i and ψ_f of the initial and final states as well as the operator **V** connecting them.[40,41,50-52]

The rate of formation λ of mu-molecules in the reactions (1.11) and the decay rate Γ_e of the complex (1.12b) and (1.13b) (the elastic width of the level of the complex) are related by the principle of detailed balance:[48]

$$\lambda = \frac{2\pi}{p_r^2} N v_r f(\varepsilon_r) \Gamma_e, \qquad (1.14)$$

where $(v_r = (2\varepsilon_r/\mu_1)^{1/2}, p_r = \mu_1 v_r = (2\mu_1\varepsilon_r)^{1/2}$, μ_1 is the reduced mass of $t\mu$ and D_2, ε_r is the resonance energy (the difference of the internal energies of the complex and the system consisting of the mu-atom and molecule), $f(\varepsilon_p) \equiv f(\varepsilon_p, T)$ is the Maxwellian distribution function over the collision energies ε_p, and **p** is the relative momentum of $t\mu$ and DX.

Thus the problem of calculating the rate of the resonant formation of a mu-molecule reduces to finding the decay width Γ_e of the quasistationary state of the molecular complex in a reaction of the type (1.12b). According to Refs. 40, 50, and 51, the expression for Γ_e looks like the golden rule of perturbation theory:

$$\Gamma_e = 2\pi \int |\langle f|\hat{V}|i\rangle|^2 \delta(E_f - E_i)\, dv_f. \qquad (1.15)$$

where E_i and E_f are the total energies of the initial and final states of the complex [(dtμ)Xee], $\hat{V}$ is the perturbation operator giving rise to the transition between the initial $|i\rangle$ and final $|f\rangle$ states, and dv_f is the density of final states of the system $t\mu + DX$.

The wave functions $\Psi_{i,f}$ are the eigenfunctions of the Hamiltonian H_i and H_f (we note that $H_i \neq H_f$, so that Eq. (1.15) is not a perturbation-theory formula), i.e., $H_{i,f}\Psi_{i,f} = E_{i,f}\Psi_{i,f}$. The expressions for H_i and H_f are obtained from the complete Hamiltonian H of the system, if it is represented in the form

$$H = H_i + V_i = H_f + V_f. \qquad (1.16)$$

In Eq. (1.16) H_i corresponds to the approximation of a point mu-molecule, i.e., it describes a stationary process, and V_i includes all terms describing the interaction between the internal degrees of freedom of the complex and the mu-molecule. When V is "switched on" the stationary complex becomes quasistationary. The Hamiltonian H_f is obtained from the complete Hamiltonian H when all terms V_f corresponding to the interaction between the mu-atom and the molecule are dropped. The transition operator V is equal to either V_i or V_f (for $E_i = E_f$ $\langle f|V_i|i\rangle = \langle f|V_f|i\rangle$). In particular, keeping only the dipole term in the multipole expansion of V_i in powers of the small parameter $\eta_0 = a_m/a_0 \leqslant 0.1$, where a_m is the characteristic size of the mu-molecule in the weakly bound state, we obtain for V_i the expression (1.9), in which $\mathbf{E} = \nabla_\rho U(\rho) = \hat{\boldsymbol{\rho}}\, dU/d\rho$, where $\boldsymbol{\rho}$ are the coordinates of the nucleus X measured from the center of mass of the $dt\mu$ mu-molecule (for definiteness, in what follows we shall study this mu-molecule), $\hat{\boldsymbol{\rho}} = \boldsymbol{\rho}/\rho$, and $U(\rho)$ is the Σ term of the H_2 molecule. The wave functions $\Psi_{i,f}$ have the form $\Psi_i = \Phi(\rho)\Psi_{vJM}$ and $\Psi_f = \exp(i\mathbf{pp}_1)\Phi\Psi_{1s}$, where Φ is the wave function describing the relative motion of $dt\mu$ and the nucleus X in the complex, $\tilde{\Phi}$ is the wave function of the molecule (D + X), Ψ_{vJM_J} is the wave function of the $dt\mu$ molecule, ψ_{1s} is the wave function of the $t\mu$ atom in the 1s state, $\boldsymbol{\rho}_1$ are the coordinates of the center of mass of DX, and **p** is the relative momentum of $t\mu$ and DX. The formula (1.15) is valid, if in the limit $\rho_1 \to \infty$ V_f decreases more rapidly than $1/\rho_1$, which happens in our case. The error in the approximate formula (1.15) is of the order of $\delta\Gamma/\Gamma \sim D \sim \exp(-2v)$, where D is the penetration factor of the effective potential barrier through which the mu-atom tunnels when the complex decays (see below). For $dt\mu$ $v = 2$ and $\delta\Gamma/\Gamma \sim 0.02$ and for $dd\mu v = 6$ and $\delta\Gamma/\Gamma \sim 10^{-4}$.

Since a rigorous proof of the formula (1.15) has not been published, we shall present it here. Following Refs. 40, 50, and 51 we shall study a simpler model, analogous to our case. When the complex at the point of the mu-molecule vibrates there arises an electric field $\hat{\mathscr{E}} = \hat{\rho}\, dU(\rho)/d\rho$. This field "pulls out" a deuteron from the mu-molecule, causing the mu-molecule to decay. It is obvious that this problem is analogous to the one-dimensional (for simplicity) problem of the pulling of a charged particle by a weak electric field out of a potential well $U_0(x)$ by the field of the potential $V_1(x)$. Near the well $(x \approx 0)$ $V_1 \approx -\mathscr{E}x$, as $x \to -\infty$ $V_1(x) \to +\infty$, and as $x \to +\infty$ $V_1(x) \to V_0 < 0$. The specific form of $U_0(x)$ and $V(x)$ are not important. It is important that there exist a wide potential barrier preventing the particle from escaping from the well $U_0(x)$ $|x|U_0(x) \to 0$ is $|x| \to \infty$. The only difference between this model and our case is the number of dimensions of the configuration space in a complex of no longer independent coordinates.

Since the decay width is small ($\Gamma_e \ll \varkappa^2/2m = \varepsilon_0$, the binding energy of the particle in the well $U_0(x)$), we shall calculate Γ_e by the method described, for example, in Ref. 53. Assume that as $t \to -\infty$, the particle is in a bound state

($\hbar = 1$): $\Psi(x,t) \to \varphi_0(x,t) = \Psi_0(x)\exp(-iE_i t)$, $H_i\Psi_0(x) = E_i\Psi_0(x)$, $H_i = H - V_i = T + U_0(x)$, $T = -(1/2)\partial^2/\partial x^2$, $E_i = \varepsilon_0$. Since the field $\mathscr{E}$ is weak, near the well $\Psi(x,t) \approx \varphi_0(x,t)$, which makes it possible to solve instead of the exact Schroedinger equation $i\partial\Psi/\partial t = H\Psi$, where $H = T + U_0 + V_i$, the approximate equation

$$L\Psi(x,t) = U_0(x)\varphi_0(x,t), \tag{1.17}$$

where $L = i\partial/\partial t + (1/2)\partial^2/\partial x^2 - V_i(x)$. Equation (1.17) does not conserve the number of particles. The number of particles created per unit time in the region of the well is equal to the particle flux at infinity $\Gamma_e = j(x \to +\infty)$, which is what we must calculate.

Dropping in $\Psi(x,t)$ the term that spreads as $t \to +\infty$—the solution Ψ_0 of the "free" equation $L\Psi_0(x,t) = 0$, which in the limit $t \to -\infty$ is equal to $\varphi_0(x,t)$ (obviously, as $t \to +\infty$, $\Psi_0(x,t)$ does not contribute to j)—we write the solution of Eq. (1.17) in the form (compare with Ref. 53)

$$\Psi(x,t) = \int_{-\infty}^{t} G(x,x';\ t-t')\,\varphi_0(x',t')\,dx'\,dt', \tag{1.18}$$

where G is the retarded Green's function: $LG(x,x',t-t') = \delta(x-x')\times\delta(t-t')$.

From Eq. (1.18), the definition of $\varphi_0(x,t)$, and the expression

$$G(x,x',\tau) = (2\pi i)^{-1}\Theta(\tau)\int_0^\infty \Psi_K(x)\,\Psi_K^*(x')\exp(-iE_K\tau)\,dK,$$

where $\Psi_\kappa(x)$ is the real wave function describing the motion of a particle with momentum K (as $x \to +\infty$) and energy $E_\kappa = K^2/2m$ in the potential $V_i(x)$ and has the asymptotic form $\Psi_\kappa(x) \to \sqrt{2}\sin(kx + \delta_K)$ $(x \to +\infty)$, we obtain for $\Psi(x,t)$ the asymptotic expression $\Psi(x,t) \to 2^{1/2}p^{-1}V_{fi}\exp(ipx + i\delta_p - iE_i t)$. Here,

$$p = (2mE_f)^{1/2}, \quad E_f = E_i = -\varepsilon_0,$$

$$V_{fi} = \langle f|V_f|i\rangle = \int \Psi_k^*(x)\,U_0(x)\,\Psi_0(x)\,dx = \langle f|V_i|i\rangle = \int \Psi_k^*(x)\,V_i(x)\,\Psi_0(x)\,dx.$$

In the calculation we took into account the property that $\exp(ikx)/(k^2 - p^2 - i0) \to \pi ip^{-1}\exp(ipx)\times\delta(k-p)$. For Γ_e we obtain the expression $\Gamma_e = j(x \to +\infty) = 2p^{-1}|V_{fi}|^2$, which is identical to Eq. (1.15), since for the asymptotic wave function Ψ_κ indicated above $d\nu_f = dK/\pi$.

As we have already mentioned, the quite general computational scheme presented above for calculating the width Γ_e is valid only in those cases when the interaction energy between the fragments of the system for large separations R decreases more rapidly than R^{-1}. This scheme can be used, for example, to calculate the rate of decay of a negative ion in an electric field, but this cannot be done in the case of an atom—in this case the preexponential factor will be incorrect.

To obtain an accuracy of $\sim 1\%$ it is sufficient to use an approximation with two σ-terms for the wave function of the mu-molecule, which for the state $J = 1$ has the form (linear combinations of the functions ψ_{ijm}, forming a vector, are taken)

$$\Psi(\mathbf{r},\mathbf{R}) = R^{-1}(\chi_a(R)\varphi_a + \chi_b(R)\varphi_b)\cdot\left(\frac{3}{4\pi}\right)^{1/2}\hat{\mathbf{R}}_j, \tag{1.19}$$

where $\hat{\mathbf{R}} = \mathbf{R}/R$ and $j = \{x,y,z\}$.

The region of coordinates

$$R \sim A_0 \sim \nu^{1/2}\varkappa^{-1} \gg 1 \text{ m. a. u.}, \tag{1.20}$$

where m.a.u. denotes mu-atomic units $\hbar = e = \mu_3 = 1$ and $\mu_3^{-1} = m_\mu^{-1} + M_t^{-1}$, $A_0 \sim (\mu_2\omega)^{-1/2} \sim 40$ m.a.u. is the amplitude of zero-point vibrations of the molecule, $p_2^{-3} = M_d^{-1} + M_x^{-1}$, $\varkappa \equiv \varkappa_a = (2\mu_a|\varepsilon_{11}|)^{1/2}$, $\mu_a^{-1} = m_{a\mu}^{-1} + M_b^{-1}$. The estimate (1.20) follows from the relations $dU(\rho)/d\rho \sim \mu\Omega^2 A_0$ and $\mu\Omega^2 A_0^2 \sim \Omega\nu \sim |\varepsilon_{11}|$ and from the calculation of Γ for the model studied above. At the separations (1.20) the interaction between the mu-atom and the nucleus can be neglected.

The asymptotic ($R \gg 1$ m.a.u.) expressions for the wave functions $\chi_{a,b}$ of weakly bound states with $J = 1$ have the form[40,54]

$$\chi_{a,b}(R) = \frac{c_{a,b}}{R\varkappa_{a,b}^{1/2}}(1 + \varkappa_{a,b}R)\,e^{-\varkappa_{a,b}R}. \tag{1.21}$$

For the $dt\mu$ mu-molecule $c_a = 0.574$, $c_b = 4.7$, $\varkappa_a = 0.0518$ m.a.u $= 10.3$ a.u., $\varkappa_b = 0.445$ m.a.u. $= 88.7$ a.u.; for the $dd\mu$ mu-molecule $c_a = c_b = 0.678$, $\varkappa_a = \varkappa_b = 0.0831$ m.a.u. $= 16.3$ a.u. The expression (1.21) is valid in a wide range of values of R. The wave functions (1.21) differ from the numerical results[27] by $\geqslant 5\%$ only for $R \leqslant 7$ m.a.u. Because of the relations (1.20) the expression (1.21) can obviously be used for calculating the resonant-formation rate, and in addition the wave function χ_b in Eq. (1.19) can be neglected. All this greatly simplifies the calculation.

The rate of resonant formation of mu-molecules in the nth spin state in collisions between mu-atoms with spin F and molecules of the type α ($\alpha = D_2$, DT) is given by the expression (Refs. 39, 40, 51, and 54; compare with Eqs. (1.14) and (1.15))

$$\lambda_{Fn}(\alpha) = 2\pi N_\alpha W_{Fn} \times \int f(p) \sum_{K_i,K_f} w(K_i)\,\delta(\varepsilon_p + \bar{E}_{K_i0} + |\varepsilon_{j1}| + \Delta\varepsilon_{Fn} - E_{K_f\nu})\,V_{fi}^2\,d^3p, \tag{1.22}$$

where N_α is the number of deuterons per cm^3, which are constituents of the molecules of the type α; W_{fn} is the spin factor; $f(p)$ is the distribution function over the momenta p, $\int f(p)d^3p = 1$, $w(K_i)$ is the probability of finding the molecule DX in the state with orbital angular momentum K_i, $E_{K\nu}$ and $\bar{E}_{K_i0}$ are the energy levels of MD and DX in the state (K_f, ν) and $(K_i, 0)$, respectively, where $M \equiv dt\mu$ and $dd\mu$; $\Delta\varepsilon_{Fn} = \Delta\varepsilon(F) - \Delta\varepsilon(n)$, $\Delta\varepsilon(F)$, $\Delta\varepsilon(n)$ are the corrections to the levels of the mu-atom and the mu-molecule, owing to the hyperfine interaction, F and n are the quantum numbers of the spin states,

$$V_{fi}^2 = (2K_i + 1)^{-1}\sum_{j,m_i,m_f}|V_j|^2, \tag{1.23}$$

$$V_j = \int \Psi_f^*\hat{V}_j\Psi_i\,d^3r\,d^3R\,d^3\rho. \tag{1.24}$$

where $\hat{V}_j = -d\mathscr{E}$.

To avoid misunderstandings we note that in Eqs. (1.22) and (1.23) and below we assume the left sides of the reactions (1.11) to be the initial states and the right sides to be

the final states, which in this case is more natural.

The calculation of V_{fi} reduces to calculating on a computer a double integral,[54] since, for example, in the region (1.20) the integration over the coordinates of the muon is trivial and can be performed analytically.

We have seen that instead of the matrix element V_j of the operator $\hat{V}_j$ (1.24) studied above it would be possible to calculate equally successfully the matrix element V_2 and V_f, which includes all terms describing the interaction of a $t\mu$ atom with a DX molecule. In practice, however, such a calculation cannot be performed, since to calculate V_2 in contrast to V_i, it is necessary to calculate numerically an integral over an eight-dimensional region; in addition, the integrand is not given in an analytic form and requires additional numerical calculation. The approximate analytical calculation of V_i performed in Ref. 40 makes it possible to indicate reliably the integration limits and steps necessary for the numerical calculation as well as the position, in configuration space, of the region making the main contribution to V_i. Thus in the case with V_i the situation is completely clear and high numerical accuracy is achieved.

The decay of the complexes (1.12b) causes the observed rates $\tilde{\lambda}_{dt\mu}$ and $\tilde{\lambda}_{dd\mu}$ of the resonant formation of mu-molecules, i.e., the total rates of the inelastic reactions (1.12a) and (1.13a), to differ from the rates, studied in this section, of the resonant formation of mu-molecules in the reactions (1.11a) and (1.11b).

We shall first study $dt\mu$. Obviously, $\tilde{\lambda}_{dt\mu} = w_f \lambda_{dt\mu}$, where $\omega_f = \tilde{\lambda}_f/(\tilde{\lambda}_f + \Gamma_e)$ is the probability of a nuclear reaction in the mu-molecule formed, $\tilde{\lambda}_f = \lambda_f^{11} + \lambda_{dex} \sim 10^{12}$ is the rate at which the upper level (1,1) is depopulated as a result of the nuclear reaction ($\lambda_f^{11} \sim 10^8$) and deexcitation of the mu-molecule ($\lambda_{dex} \sim 10^{12}$). The vibrational relaxation processes $(MX)_{Kv} + DX \to (MX)_{K'v'} + DX$ increase w_f, since of these processes stabilize the complex—decay of the states $v' < v$ is forbidden according to energy. The relaxation rate becomes significant ($\sim\tilde{\lambda}_f + \Gamma_e$) only for $T \geqslant 0.2$ eV, so that it is insignificant in the region $T \leqslant 0.2$ eV of interest to us here.

The rotational relaxation $(MX)_{Kv} + DX \to (MX)_{K'v} + DX$ does not stabilize the complex, but causes w_f to depend on φ and T, since the decay rate Γ_e depend on $K_i v_i$ and $K_f v_f$. In the region $T \geqslant 0.2$ eV the formation of complexes with $v_f = 3, 4, \ldots$ as well as collisions with vibrationally excited molecules ($v_i \neq 0$) become significant. In these cases Γ_e increases ($\sim\tilde{\lambda}_f$), so that w_f decreases. For $T \geqslant 0.2$ eV $w_f \sim 0.99$, since $\Gamma_e \sim 10^{10}$.[41,55]

The observed rates $\lambda^0_{dt\mu-X}$ of formation of the mu-molecules $dt\mu$ in the reactions (1.11a) are presented in Fig. 2 (high temperatures) and Fig. 3 (average temperatures). As usual, $\tilde{\lambda}_{dt\mu-x} = \tilde{\lambda}^0_{dt\mu-X}\varphi C_d$, where λ^0 are the reduced rates. According to what was said above for $T \leqslant 0.2$ eV there is no need to distinguish between λ and $\tilde{\lambda}$. The rates at high temperatures were calculated based on the data of Refs. 41, 55, and 54. Figure 3 was taken from Ref. 57 and corresponds to the binding energy[57-59] $|\varepsilon_{11}| = 0.632 \pm 0.002$ eV, which agrees best with experiment.[60]

When the mu-molecules $dt\mu$ form and decay the spin F of the $t\mu$ atom is conserved[40] primarily owing to the smallness of the magnetic moment of the deuteron. In contradistinction to this case, a mu-atom $d\mu$ having spin F when the

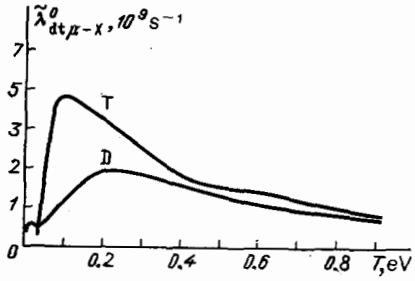

FIG. 2. The rates of resonant formation $\lambda^0_{dt\mu-X}$ ($\varphi = 1$) of the mu-molecules $dt\mu$ in the processes $t\mu + DX \Rightarrow [(dt\mu)Xee]$ at high temperatures. The curves D and T correspond to X = D and X = T.

complex $[(dd\mu)_s Xee]$, where S is the spin of $dd\mu$, forms may turn out to be in a different spin state $F' \neq F$ after the complex decays. For this reason the resonant processes change the rates of the spin-flip reactions $\lambda_{FF'}$ by the amount[52]

$$\Delta\lambda_{FF'} = \sum_S \lambda_{FS}\omega_{SF'},$$

where λ_{FS} is the rate of formation of the mu-molecules $dd\mu$ with spin S from mu-atoms $d\mu$ with spin F, $\omega_{ss'} = \Gamma_{SF'}/(\lambda_f + \Gamma_s)$ is the probability that the complex decays in the channel $S \to F'$, $\Gamma_{SF'}$ is the rate of this decay, and $\Gamma_s = \Sigma_F \Gamma_{SF}$ is the total elastic width.

The observed rates $\tilde{\lambda}_F$ of formation of the mu-molecules $dd\mu$ from the mu-atoms with spin F are equal to

$$\tilde{\lambda}_F = \sum_S \lambda_{FS}\omega_t^s + \lambda^H_{dd\mu}. \qquad (1.25)$$

where $\omega_t^s = \tilde{\lambda}_f/(\tilde{\lambda}_f + \Gamma_s)$. The second term in Eq. (1.25) describes the nonresonant formation of the mu-molecules $dd\mu$ in lower levels, for which $w_f \approx 1$.

The observed formation rate of mu-molecules $dd\mu$ $\tilde{\lambda}_{dd\mu}$ can be expressed taking into account the hyperfine structure of $d\mu$ and $dd\mu$, in terms of the partial rates[52] (the first attempt to take into account the hyperfine structure was made in Ref. 61):

$$\tilde{\lambda}_{dd\mu} = \sum_F \tilde{\lambda}_F N_F \left(\sum_F N_F\right)^{-1} = (\tilde{\lambda}_{1/2} + \tilde{\gamma}\tilde{\lambda}_{3/2})(1 + \tilde{\gamma})^{-1},$$

where $\tilde{\gamma} = (\tilde{\lambda}_{1/2,3/2} + 3\tilde{\lambda}_{3/2,1/2}/4)/(\tilde{\lambda}_{3/2,1/2} + \tilde{\lambda}_{1/2,3/2}/4)$.

The rates $\tilde{\lambda}_{dd\mu}$ (Refs. 52 and 57) and $\tilde{\lambda}_{3/2}$ and $\tilde{\lambda}_{1/2}$ (Ref. 57) are presented in Fig. 4 of this paper and Fig. 15b of the review by S. S. Gershteĭn *et al.* (in this issue of Uspekhi Fizicheskikh Nauk). In the calculations the values $|\varepsilon_{11}| = 1.9656$ eV, $\lambda_f = 0.39 \cdot 10^9$ $\lambda^0_H = 4.8 \cdot 10^4$, for which

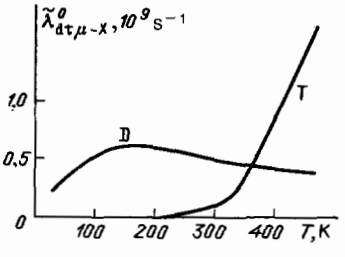

FIG. 3. The rates of resonant formation $\lambda^0_{d\mu-X}$ at moderate temperatures. The curves D and T correspond to X = D and X = T.

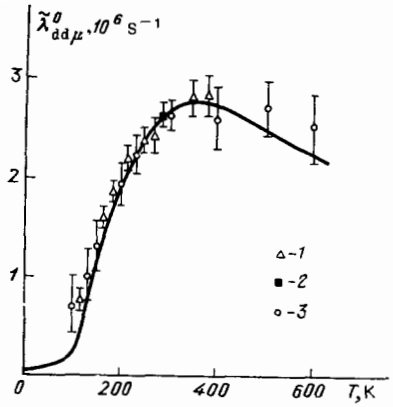

FIG. 4. The temperature dependence of the observed rate $\tilde{\lambda}^0_{dd\mu}(T)$ of the process $d\mu + D_2 \Rightarrow [(dd\mu)dee]$. *1*) Dubna,[131] *2*) Gatchina,[104] *3*) Los Alamos[26] (the Dubna data were renormalized to the value of $\lambda^0_{dd\mu}$ ($T = 293$ K) measured in Gatychina). The solid line shows the calculation of Ref. 52 with $|\varepsilon_{11}| = 1.9656$ eV, $\lambda_f = 3.9 \cdot 10^8\ s^{-1}$, and $\lambda^0_H = 4.8 \times 10^4\ s^{-1}$.

the best agreement with experiment is obtained,[62] were used. We note that the probabilities w_f^s of nuclear reactions in a $dd\mu$ molecule are much less than one (~ 0.2).

The agreement between the theoretical and experimental values of $\lambda_{dd\mu}(T)$ indicates both that the computational method employed is on the whole correct (choice of wave functions, transition operator, averaging method, etc.) and that the accuracy of the theoretical calculations[63] of the structure of the energy levels of the mu-molecules and mu-molecular complexes is high. In the case with $dt\mu$ the significant error ($\sim 50\%$) in the theoretical and experimental values of the probability q_{1s} (see Sec. 1.5) makes it difficult to make comparisons with experiment in the entire temperature range.

As the density of the mixture increases ($\varphi \geqslant 0.1$) the quasiresonant mechanism[64]

$$t\mu + D_2 + X \xrightarrow{\lambda_{qr}} C + X, \quad \lambda_{qr} \sim \varphi^2,\ X = D_2,\ DT,\ T_2, \tag{1.26}$$

as well as the additional broadening of the resonances caused by collisions between X molecules and D_2 and the molecular complex $C \equiv MD$ become important, so that for $\varphi \geqslant 0.1$ the width of the resonance is equal to (Ref. 65) $\Gamma = \Gamma_\nu + \Gamma_\varphi$, where Γ_φ is the collisional width.

The role of collisions in the resonance formation of mu-molecules is analyzed in Refs. 66 and 67. The starting point in these investigations was the analogy between the reaction of interest to us

$$t\mu + D_2 \to C \to t\mu + D_2 \tag{1.27}$$

and the resonant fluorescence process

$$\gamma + A \to A^* \to \gamma + A. \tag{1.28}$$

This analogy makes it possible to apply to the reaction (1.27) the well-developed methods of the theory of collision broadening of spectral lines TCB, which is presented, for example, in Refs. 68–79. The analysis is valid in the "gas" limit $\tau\nu_c \leqslant 1$, where τ is the duration of a collision, i.e., the time during which the interaction potential energy of the molecules is of the order of their kinetic energy ($\sim T$, where T is the temperature of the mixture) and ν_c is the collision frequency, i.e., the average time interval between collisions. The collision frequency ν_c is determined by the size $R_0 \sim 6$ a.u. and the duration τ of a collision is determined by a much smaller $\Delta R \sim (2\eta)^{-1} \sim 0.6$ a.u., where the index $\eta = 0.85$ determines the interaction potential $U(R) \approx U_0 \exp(-2\eta R)$ between the hydrogen isotope molecules;[70] for this reason the main assumption employed in Refs. 66 and 67, regarding the fact that collisions with different molecules are independent, is valid not only for a dense gas ($\varphi \leqslant 1$) but also for a liquid. Thus collective phonon effects, which are important in the solid phase, were ignored. Such effects include, for example, transfer of the momentum of the mu-atom not to a separate molecule D_2, but rather to the entire crystal lattice, analogously to the Mössbauer effect.

In Refs. 66 and 67 it is shown that the two currently known nonlinear (with respect to the gas density) mechanisms of formation of mu-molecules in triple[64] and pair[65] collisions, which at first glance appear to be of a completely different physical nature, are in reality two different limiting cases of the same mechanism of formation of mu-molecules, which extends the mechanism of É. Vesman[38] to the case of a high-density gas or liquid. It is also shown there that the form of the resonances $I_{K_i K_f}(\varepsilon_p)$ in the center of mass system of $t\mu + D_2$ is an adequate physical quantity that permits taking into account accurately collisions with gas molecules, and expressions are derived for $I(\varepsilon_p)$ in different approximations.

For a low-density deuterium-tritium mixture ($\varphi \leqslant 0.1$) the resonances have a Lorentzian form, and for $\varphi \geqslant 0.1$ the resonances deviate significantly from a Lorentzian form.[66] For $\phi \geqslant 0.1$ the functions $I(\varepsilon_p)$ have three characteristic regions: resonance, quasiresonance, and vacuum. In the resonance region the form of $I(\varepsilon_p)$ is approximately Lorentzian. The collisional width of the resonance Γ_φ is determined solely by collisions of the complex with gas molecules and does not depend on the character of the motion of the D_2 molecule. This is explained by the effect of recoil when the mu-atom and the D_2 molecule form a complex. This is what makes the reactions (1.27) and (1.28) significantly different. Recoil leads to a unique "forgetting" of the initial state. For $t\mu + D_2$ energies far from the resonance energy ($|\varepsilon_p - \varepsilon_r| \geqslant \Gamma/2$) the quasiresonance mechanism (1.26) plays the main role.

In Ref. 64 the approximation of structureless molecules, applicable at low temperatures ($T \leqslant 40$ K) was used to describe triple collisions (1.26). To describe more accurately the reactions forming $dt\mu$ molecules with $\varphi \sim 1$ and at temperatures $40 \leqslant T$ (K) $\leqslant 150$ it is necessary to perform a complicated and reliable calculation of the rates of formation $\lambda_{K_i K_f}$ of mu-molecules in triple collisions (1.26) taking into account the rotational degrees of freedom of the molecules D_2 and X and the complex, though it is hardly possible to do this.

It is also of interest to calculate the form of the resonance in the approximation of structureless molecules with finite mass for arbitrary ε_p, i.e., to extend the results of Refs. 66 and 67. In optics the profile of a spectral line is expressed in terms of the two-particle Green's function of the excited and unexcited atoms.[71] In our case, the calculation is com-

plicated by the momentum transfer (recoil) effect mentioned above.

1.4. Nuclear reaction and cascade transitions in a mu-molecule

The rates of nuclear fusion reactions, for example, λ_f^{dt}, in mu-molecules and the cross sections of these reactions between colliding bare nuclei can be expressed in terms of the same nuclear matrix element. This makes it possible to express λ_f in terms of the cross sections of the fusion reactions measured in the experiments of Refs. 1, 2, 4, and 72–75. In the case of different nuclei ($a \neq b$)

$$\lambda_f(ab\mu) = K_s \int \Psi_J^2(r_0, R=0)\, d^3r_0, \tag{1.29}$$

where

$$K_s = \lim_{v\to 0} \frac{\sigma_f(v)v}{f(v)},$$

$f(v) = (2\pi/v)[\exp(2\pi/v) - 1]$, and v is the relative velocity of the nuclei.

In the states $J = 0$ of the mu-molecules $pd\mu$, $pt\mu$, $dd\mu$, and $dt\mu$ the rates of the nuclear reactions are, respectively, equal to $\lambda_f^{pd} = (0.25 \pm 0.06)\cdot 10^6$, $\lambda_f^{pt} = 0.7\cdot 10^5$, $\lambda_f^{dd}\lambda_f^{dt} \sim 10^{12}$.[1,2,4,72–74] For $J = 1$ the rate of a nuclear reaction decreases as a result of the centrifugal barrier: in states with $(J,v) = (1,1)$ and $(1,0)$ in $dd\mu$ $\lambda_f^{dd} = 4.3\times 10^8$ and 1.5×10^9.[75] In $dt\mu$, in the same states, $\lambda_f^{dt} = 5.2\times 10^7$ and 1.3×10^8.[74] According to the experiment of Ref. 76, for states with $J = 1$ of the $tt\mu$ molecule $\lambda_f^{tt} = 1.5\times 10^7$ (by analogy to $dd\mu$ from here it may be concluded that for $J = 0$ $\lambda_f^{tt} \sim 10^{10}$). The rate of nuclear reactions in states with $J = 2$ is even slower: $\lambda_f^{dt} = 1\times 10^5$.[74]

Intense conversion Auger transitions occur between the bound states of mu-molecules:[1,72,77]

$$[(ab\mu)_{Jv}\, Xee] \to [(ab\mu)_{J'v'}\, Xe]^+ + e. \tag{1.30}$$

The fastest is the dipole E1 transition, whose characteristic rate is $\lambda_{dex} \sim 10^{12}$. This transition is due to the interaction (1.9). In the case of identical nuclei $\langle \varphi_g | \mathbf{d} | \varphi_g \rangle = 0$. From here and from Eq. (1.10) we conclude that the E1 transition is forbidden. In this case E2 and E0transitions occur. These transitions are determined by operators that are second-order infinitesimals with respect to the parameter η_0—quadrupole V_q and monopole V_m. For V_d, V_q, and V_m the selection rules $J' = J \pm 1$, $J' = J \pm 2$, and $J' = J$, respectively, hold.

The characteristic rate of the E0 and E2 transitions is $\lambda_{dex} \sim 2\cdot 10^8$.[78] The E0 transition $(1,1) \to (1,0)$ out of the weakly bound state (1,1) in the $dd\mu$ molecule, whose rate is low [2.2×10^7 (Ref. 78)], is an exception. The explanation lies in the following (for simplicity we shall study transitions in the atom $[(ab\mu)e]$.[54] The characteristic period of the vibrations of a mu-atom and a nucleus in the mu-molecule $\tau_{ab\mu} \sim 1/|\varepsilon_{11}|$ is long compared with the period of revolution of an electron in the atom $\tau_e \sim 1/I_H$. For this reason there is enough time for the electron to adjust to these vibrations and the electron always follows the charged nucleus and virtually does not interact with the small neutral mu-atom; this is the physical meaning of the effect. Formally, however, the matrix elements of V_q and V_m are significantly compensated by the second-order perturbation theory in the operator V_d from (1.9).

The mu-molecules $dd\mu$ and $dt\mu$ form, with overwhelming probability, by the resonant mechanism in the weakly bound states (1,1). Since for $dd\mu$ λ_{dex} is small we conclude that in the mu-molecule $dd\mu$ the nuclear reaction proceeds only in the upper (1,1) state.

It may seem that a mu-molecule, having undergone two Auger transitions $(1,1) \Rightarrow 0,1) \to (1,0)$ or $(1,1) \to (2,0) \to (1,0)$ and having exhausted all electrons of the mu-molecular complex $[(dt\mu)Xee]$ on this, arrives in the state (1,0) in which the rate of the nuclear reaction is low. This rate, in any case, would then appear in the expression for the muon catalysis cycle rate (see below), and the annihilation of muons in the (1,0) state would significantly reduce the number of cycles per muon X_c. In reality, however, the electrons are practically instantaneously ($\lambda \sim 3\cdot 10^{13}\varphi$) replenished owing to ion-molecular reactions[79] analogous to $H_2^+ + H_2 \to H_3^+ + H$. Muons practically never decay in the cascade process in a mu-molecule, since the characteristic lifetime of the molecule $\sim 5\times 10^{-11}$ s is short compared with the lifetime of a muon.

1.5. The kinetics of muon catalysis. Results of experiments up to the end of the 1980s

The basic processes in the mixture $D_2 + T_2$, determining the spectrum of $t\mu$ atoms, are presented in Fig. 5.

In the absence of muon-loss channels (muon decay and muon sticking to the nuclei of fusion products), within a period of time of the order of the thermalization time of mu-atoms $\tau_T \sim 10^{-9}/\varphi$ s after a μ^- meson stops in $D_2 + T_2$ mixture a stationary state, characterized by a constant number of nuclear fusion reactions per unit time, would be established. In reality, however, because of losses instead of a stationary state there is established a quasistationary state in which the number of particles participating in muon-catalysis reactions (mu-atoms, mu-molecules, and others) decreases with time exponentially with the decay constants $\lambda \sim \lambda_0$ (see below). The energy distribution functions $f_F(E,t)$ (t is the time after the muon stops) of $t\mu$ atoms with spin F in this regime factorizes (Refs. 55 and 56): $f_F(E,t) = N_F(t)\Phi_F(E,T)$ where $N_F(t)$ is the number (population) of mu-atoms with spin F and

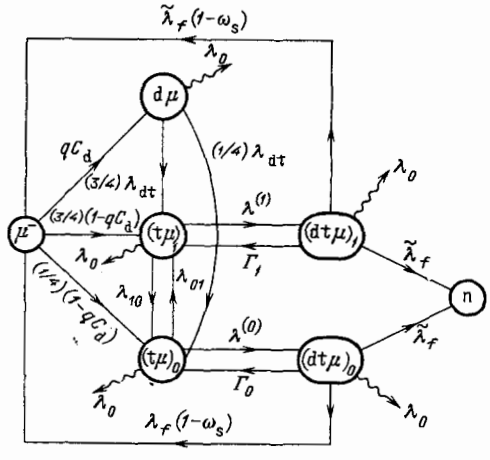

FIG. 5. Diagram of the main processes determining the spectrum of $t\mu$ atoms. The indices 0 and 1 indicate the spin F of the states of $t\mu$ and $dt\mu$, respectively.

$$\int_0^\infty \Phi_F(E, T)\,dE = 1,$$

The kinetic equations in the quasistationary state simplify and reduce to the standard kinetic equations for the numbers of mu-atoms and mu-molecules (populations), in which the observed velocities appear:

$$\lambda^{(F)}(T) = \int_0^\infty \lambda^{(F)}(E)\,\Phi_F(E, T)\,dE. \tag{1.31}$$

where $\lambda^{(F)}(E)$ are the rates of formation of mu-molecules from mu-atoms with spin F and energy E in the laboratory coordinate system. Most fusion reactions occur in the quasistationary regime.

The number of mu-atoms in the quasistationary regime decreases as $N_F(t) = N_F^{(0)} e^{-\lambda t}$ and $N_{d\mu}(t) = N_{d\mu}^0 e^{-\lambda t}$, and the time distribution of neutrons which arise from one muon has the form[55,56]

$$\frac{dN_n}{dt} = \lambda_c e^{-\lambda t}, \quad \lambda = \lambda_0 + W\lambda_c. \tag{1.32}$$

where

$$\lambda_c = \left(\frac{qC_d}{\lambda_{dt}} + \frac{B}{A}\right)^{-1} \tag{1.33}$$

is the cycle rate,

$$q \equiv q_{1s},$$
$$A = \lambda^{(1)}\lambda^{(0)} + \lambda^{(1)}\lambda^{01} + \lambda^{(0)}\lambda_{10},$$
$$B = \eta_0\lambda^{(1)} + \eta_1\lambda^{(0)} + \lambda_{01} + \lambda_{10}, \quad \eta_0 = \frac{1}{4}, \quad \eta_1 = \frac{3}{4},$$
$$N_F^{(0)} = \frac{\lambda_c}{A}(\eta_F\lambda^{(F')} + \lambda_{F'F}),$$
$$F' \neq F,$$
$$N_{d\mu}^{(0)} = \frac{qC_d\lambda_c}{\lambda_{dt}},$$

$\lambda_{F'F}$ are the spin-flip rates, and

$$W = \omega_s + \frac{\beta q C_d \omega_d \lambda_{dd\mu}}{\lambda_{dt} C_t} + \frac{\lambda_{t(t\mu)\omega_t} B}{A} + C_{He}\left(\frac{qC_d\lambda_{dHe}}{\lambda_{dt}C_t} + \frac{\lambda_{tHeB}}{A}\right). \tag{1.34}$$

We note that the expressions (1.33) and (1.34) are valid if $\lambda_0 + \lambda_{dd\mu} \ll \lambda_{dt}$, where λ_{dHe} and λ_{tHe} are the rates of transfer of a muon to He nuclei from d and t nuclei, ω_d is the muon sticking coefficient in the dd-fusion reaction, and $\beta = 0.58$,[80] where β is the probability of a fusion reaction in a $dd\mu$ molecule with emission of a proton and tritium.

Physically λ_c is the rate of production of neutrons (for $t \ll \lambda^{-1}$). The formula for the total number of cycles X_c of muon-catalysis per mu-meson stopping in the mixture has the form

$$X_c = \int_0^\infty \frac{dN_n}{dt}\,dt, \quad X_c^{-1} = W + \frac{\lambda_0}{\lambda_c}. \tag{1.35}$$

We note that the formulas (1.32)–(1.35), describing the quasistationary regime, are valid in a wide range of densities $\varphi \geqslant 0.01$, in which $\lambda_0\tau_T \ll 1$.

The rates $\lambda^{(F)}$ appearing in the formula (1.32) are determined by the expression (1.31). Calculations show[55,56] that for $\varphi \geqslant 0.2$ the functions $\Phi_F(E)$ differ from the Maxwellian distribution by less than 10%.

For $T \leqslant 500$ K the rate λ_{01} can be neglected, and the expression for λ_c simplifies:

$$\lambda_c^{-1} = \left(\frac{qC_d}{\lambda_{dt}C_t} + \frac{0.75}{\lambda_{10}C_t} + \frac{1}{\lambda_{dt\mu}C_d}\right)\frac{1}{\varphi}. \tag{1.36}$$

This formula is used for analyzing the experimental data.

As an example of an experiment on investigation of muon catalysis of nuclear fusion reactions in a $dt\mu$ molecule we mention an experiment performed in Dubna,[81] where catalysis of a fusion reaction in this mu-molecule was first observed. This experiment is also notable in that the procedure for working with large amounts of tritium was first tested in the USSR.

The experiment was performed in a muon beam from the synchrophasotron at the Joint Institute of Nuclear Research. The beam of muons with an initial momentum of 130 MeV/c was extracted with the help of a meson channel into a low-background laboratory containing the main apparatus—the gas target together with the gas-supply system and the detectors. The arrangement of the target and the detectors in the muon beam is shown in Fig. 6.

The muons were recorded with monitor counters 1–3 (plastic scintillator), moderated in the moderator 6, detected with the counter 4, and entered the target 8. Some of the muons stopped in the target and give rise to the reaction (1.1). The neutrons produced in this reaction were detected with the help of detectors N_{1-4} arranged around the target and the electrons from muon decay were detected with the help of detectors E_{1-8} arranged in pairs.

The basic idea of the experiment, which made it possible to reduce significantly the background of random coincidences and the background associated with the stopping of muons in the target walls, consisted of detecting successively in a time interval of 10 μs ("gate") after the muon entered the target, first a neutron from the reaction (1.1) and then an electron from muon decay, i.e., the delayed coincidences muon-neutron-electron are used. Stopping of a muon in the

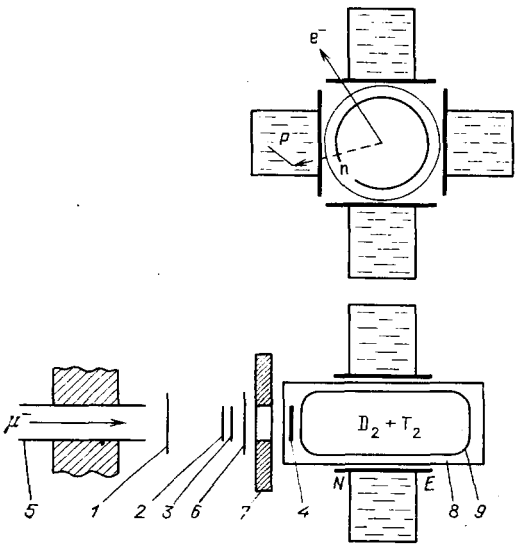

FIG. 6. Diagram of the experimental apparatus. *1–3*) Monitor counters with plastic scintillator, *4*) counter with CsI (Tl) crystal; *5*, *7*) collimators; *6*) filter, *8*) gas target, *9*) vacuum casing; N are neutron detectors; E are electron detectors.

material of the target walls (iron) results either in nuclear capture of a muon with emission of a neutron (there is no electron) or in muon-decay (no neutron); for this reason the use of neutron-electron coincidences made it possible to achieve a low background under these experimental conditions, when the number of muons stopping in the target walls was hundreds of times larger than the number stopping in the gas. In addition, the background level was also reduced by using a counter 4 with a CsI(T1) scintillator ($\varnothing 110\times 1$ mm^2), positioned after the moderator directly in front of the target.

The main part of the experimental apparatus consisted of a deuterium-tritium gas target. In designing the target the following requirements were taken into account: 1) the maximum pressure is 55 atm; 2) the working temperature range is -196 to 400 °C; 3) the amount of gas released from the walls in the working volume of the target is quite small ($<10^{-4}$ torr/h), which is necessary in order to maintain the purity of the gas mixture D_2+T_2 at a level $<10^{-6}$ volume fractions; and, 4) safety when working with large quantities of tritium (5000 Ci) must be ensured. The target housing consisted of a stainless steel cylindrical vessel ($\varnothing 130\times 250$ mm^2). The volume of the target was equal of 3.25 liters and the walls were 3 mm thick.

To ensure safety the target itself as well as the manometer and valves connected to it were enclosed in a vacuum-tight casing, connected with a ballast reservoir. The total volume of the casing and the reservoir, equal to 130 liters, was large enough so that if the target was accidently unsealed, the total pressure of the gas mixture in it would not exceed 0.6 atm.

The target was heated with the help of a wire coil, passing through a copper tube soldered to the target body. The target was cooled by blowing nitrogen vapor through another copper tube. The temperature of the target was by two thermocouples. The accuracy of the temperature measurements was $\pm$ 3°C.

With the help of the gas-supply system the target was filled with ultrapure deuterium and tritium. The required degree of purity of the hydrogen isotopes employed was determined by the ratio of the known rates of muon transfer (λ_Z) from hydrogen mu-atoms to the nuclei (Z) of possible impurities (N_2,O_2,CO_2) and the expected values of λ_{dt} and $\lambda_{dt\mu}$. In order that the background due to transfer to an impurity not exceed 1% the conditions $\lambda_z c_z/\lambda_{dt} c_t < 0.1$ and $\lambda_z c_z/\lambda_{dt\mu} c_d < 0.01$, where c_Z is the relative content of impurities, must be satisfied. Using the values $\lambda_Z^0 = \lambda_Z/\varphi = 5\cdot 10^{10}$ s^{-1}, $\lambda_{dt\mu}^0 = 10^8$ s^{-1}, and $\lambda_{dt}^0 = 3\cdot 10^8$ s^{-1}, we obtain the condition $c_Z < 10^{-6}$.

The deuterium was purified directly as the target was being filled with it by three serially connected zeolite absorbers, placed in liquid nitrogen. The tritium source consisted of titanium tritide TiT_2, placed in a stainless steel ampoule with a volume of 100 cm^3. The dissociation of TiT_2, i.e., the liberation of gaseous tritium, proceeds efficiently at temperatures of 750–800 °C. It is important that at this temperature TiT_2 actively absorbs gases of different chemical substances, including oxygen, nitrogen, and carbon dioxide and monoxide. As a result the residual content of these gases in tritium does not exceed 10^{-5}. The relative content of tritium in these experiments did not exceed 10%, so that the indicated tritium purity corresponds to the condition presented above.

It was necessary not only to purify the deuterium and tritium before the target was filled with them, but it was also necessary to maintain their purity at the required level (10^{-6}) during prolonged exposures (200 h), i.e., it was necessary to prevent gases of other substances released from the target walls and the pipes from contaminating the gas mixture. To this end the target and the pipes were subjected to vacuum-thermal conditioning, which was performed for three days before the target was filled. To monitor the parameters of the gas-supply system the target was filled with deuterium several times, after which the purity of the deuterium was checked. The results of these analyses indicate that the degree of purity of the gas was not worse than 2×10^{-7}.

The target was first filled with tritium. The amount of tritium in the target was determined from the known volume of the target and the partial pressure of tritium, measured with the help of a combined pressure and vacuum gauge. The maximum tritium pressure at a TiT_2 temperature of 800 °C was equal to 480 torr. The content of tritium in the target was determined with an accuracy of not worse than 1%. After the target was filled with tritium the tritium was absorbed with titanium from the input lines, after which the target was filled with deuterium up to the required pressure. At the end of the measurements the gas mixture D_2+T_2 present in the target was adsorbed in adsorbers, filled with TNT-4 titanium. The sorption capacity of each adsorbed was equal to 360 liters under normal conditions. The residual gas pressure in the target and the lines after adsorption of the mixture did not exceed 10^{-3} torr.

The electrons produced when the muons stopping in the target decayed were detected with scintillation detectors E_{1-8}. A plastic scintillator with the dimensions $340\times 200\times 10$ mm^3 and FÉU-30 photomultipliers were used in these detectors. To reduce the background random coincidences the electron detectors were connected pairwise for coincidence, thereby forming four telescopes. The geometric efficiency of all detectors for electrons leaving the volume of the target was equal to 60%.

Neutrons from the reaction (1.1) were detected with four highly efficient detectors N_{1-4} containing the liquid scintillator NE-213. Photoplastic windowless cells ($\varnothing 100\times 95$ mm^2) and a 56 AVP photomulitplier (at the photocathode $\varnothing 110$ mm) were used in the neutron detectors. The cells were pressed directly against the input window of the photomultiplier without any intervening transparent media. The use of a detector with this construction made it possible to improve the amplitude resolution by a factor of 1.5 compared with the usually employed neutron detectors with glass cells.

We shall briefly describe the block diagram of the experiment. The unit "Master," which selects the useful events, passed during the 10-μs wide gate pulse the signals from the E and N detectors to time-to-code and charge-to-code converters, which were triggered by a pulse from the coincidence of the signals from detectors 2 and 3. Fast (100 ns) anticoincidences $23(\overline{\Sigma E+\Sigma N})$ were used to suppress the "instantaneous" background associated with the stopping of muons in the scintillator of the N and E detectors and in the target walls. The efficiency with which the "neutron" events were extracted was increased by introducing "fast" anticoincidences ($N\bar{E}$).

To discriminate the background from the γ-rays detect-

ed by the N detectors n-γ separation was performed based on the form of the scintillation pulse. This was done with the help of an analog-commutator unit. Signals from an N detector were fed into the unit and two signals, whose amplitudes were proportional to the intensities of the fast (FC) and slow (SC) components of the scintillation pulse, were formed at the output of the unit. The neutrons and γ-rays were separated by analyzing the amplitudes of the signals of the fast and slow components.

Information about an event, including the time at which a signal from the N and E detectors appears, the amplitudes of the signals of the fast and slow components, and the number of the detector, was fed into a computer for analysis when a number of conditions were satisfied. It was required that signals from the E and N detectors be present throughout the entire gate pulse and that a signal from the counter 4 be present for 0.4 μs from the start of the gate pulse, and in addition it was required that there be no signal from the counter 1 (second muon) 5 μs before the start of the gate pulse. The monitor readings were recorded in the counting registers 10 μs after the gate pulse starts. Information was periodically transferred from the counting registers into a computer.

A total of 14 exposures were performed in the muon beam. The conditions under which the exposures were made differed by the temperature of the gas mixture $D_2 + T_2$ or the content of deuterium and tritium in the mixture. In each exposure the temporal and amplitude characteristics of the events recorded with the N and E detectors were measured.

Preliminary processing of the experimental data was performed directly in the course of the measurements and consisted of separating the neutron and electron events and constructing the temporal and amplitude distributions for each case of events. The electronic events were recorded in the electronic exposures. Neutron events were assumed to be events that were recorded in neutron exposures and fell within the neutron region in the two-dimensional distributions constructed from the amplitudes of the fast and slow components. In selecting the neutron events the criterion $E_n > 3$ MeV was used in order to suppress the background from the fusion reaction $dd\mu \rightarrow {}^3He + n + \mu$ (the neutron energy $E_n = 2.5$ MeV). In addition, to discriminate the background random coincidences and the background from the stopping of muons in the target walls an electron was required to be present for 10 μs (the gate) after the neutron.

At the first stage of analysis the relative values of the experimental neutron yield $Y = N_n/N_e$ obtained in different exposures were compared. In so doing the following was established. First, the relative neutron yield remains constant in a wide temperature interval $T = 93$–613 K. The dependence of the neutron yield on the temperature of the mixture $D_2 + T_2$ is shown in Fig. 7.

Second, Y remains virtually constant when only the tritium content in the target changes. On the other hand, when only the tritium content in the mixture is changed the neutron yield changes in proportion to the tritium content. The character of the neutron distributions as a function of time, obtained in different exposures, also agrees with the expression (1.32).

The complete analysis consisted of comparing by the method of least squares the experimental data on the yield and the temporal distributions of the neutrons obtained in each exposure with the expected theoretical expressions. The neutron yield was approximated in the form

$$\bar{Y}_n = \frac{N_n}{N_e} = \varepsilon_n Y_n(\lambda_{dt\mu}, \lambda_{dt}),$$

where Y_n is the absolute neutron yield and ε_n is the neutron detection efficiency.

The quantity ε_n was found by a computational method (the method of random tests). In determining it the interaction of neutrons not only with the detector scintillators but also with all intervening media in the path from the point of exit from the target to the scintillator (the walls of the target, casing, and detectors and the elements of the heating and cooling systems) was taken into account. In analyzing the interactions of neutrons with the NE-213 scintillator both single and double scattering by hydrogen and carbon nuclei were taken into account.

It seems obvious that the yield and temporal distribution of all neutrons by no means reflect all available information about the process of successive muon catalysis. It is also possible to measure the temporal distribution of the "first," "second," etc., neutrons and their yield or the yield of single, double, etc., neutrons. It has been found[82-86] that when such additional information is employed there is no need to know ε *a priori* (it can be found from the experimental data (see the Appendix)). The optimal values of $\lambda_{dt\mu}$ and λ_{dt} obtained in the course of the analysis were $\lambda_{dt\mu} > 10^8$ s^{-1} (90% reliability) and $\lambda_{dt} = (2.9 \pm 0.4) \times 10^8$ s^{-1}.

Most subsequent experiments were performed using the experimental procedure described above. We shall present the basic results of these investigations.

The experiments performed at Los Alamos[26,87] showed that, as in the case of formation of $dd\mu$ molecules, the formation rates of $dt\mu$ molecules are strongly temperature dependent (Fig. 8). It was found that the formation rate of $dt\mu$ molecules $\lambda_{dt\mu}^{D_2}$ depends quadratically on the density of the mixture $D_2 + T_2$ (Fig. 9). This is evidently explained by the contribution of tripole collisions to the process of formation of $dt\mu$ molecules (1.26). This result, however, is not unequivocal, since the accuracy of the theoretical and experimental values of the coefficient $q \equiv q_{1s}(C_t, \varphi, T)$ is low ($\sim 50\%$). The experiments of Refs. 25, 62, and 88 (Fig. 17 from the review by S. S. Gershteĭn *et al.* in this issue of Uspekhi Fizicheskikh Nauk confirms the conclusion that the dependence of the cycle rate on the density of the mixture is strongly nonlinear. It is obvious that for $\varphi > 0.2$ the cycle rate λ_c is a quadratic function of φ and that for $\varphi < 0.2$ the dependence on φ becomes even sharper; this is apparently

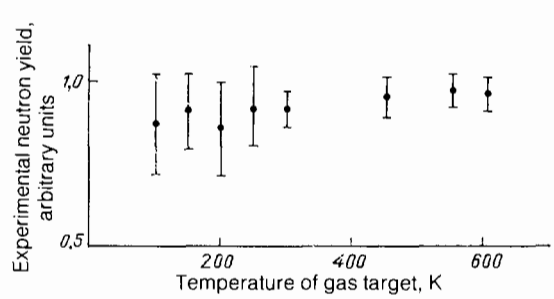

FIG. 7. The experimental neutron yield in relative units as a function of the temperature of the gas target.

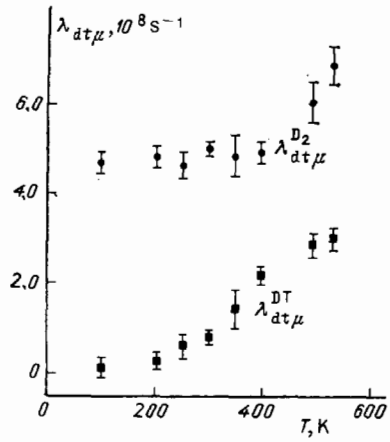

FIG. 8. $\lambda^{D_2}_{dt\mu}$ and $\lambda^{DT}_{dt\mu}$ as a function of the temperature of the mixture $D_2 + T_2$.[26,87]

explained by effects associated with the thermalization of $t\mu$ atoms.

The quasistationary approximation studied above is not applicable for $t \leqslant \tau_T$, when quasistationary equilibrium is being established. It is of great interest to study the kinetics of muon catalysis in such a transient regime, clearly observed in the experiment at low mixture densities $\varphi \leqslant 0.1$, because in this regime it is possible to measure numerous characteristics of muon catalysis, for example, the cross section for elastic scattering of mu-atoms and the spin-flip rate.

The existence of the transient regime is clearly illustrated in Figs. 10 and 11. Figure 10 shows the temporal spectrum of the primary detected neutrons from the fusion reaction in a $dt\mu$ molecule in a liquid deuterium-tritium mixture ($\varphi \sim 1.2$) at $T = 23$ K and with C_t 0.36. This spectrum was taken from the experiment of Refs. 62 and 88. One can see from the spectrum that the temporal distribution of the neutrons is described by a single exponential function with the decay constant $\lambda = \lambda_0 + W\lambda_c$ in the entire experimentally observed time interval, i.e., the quaistationary regime is realized. Figure 11 shows the temporal spectrum of neutrons in a gaseous deuterium-tritium mixture at $T = 300$ K and with $C_t = 0.9$ and $\varphi = 0.01$.[62,88] Two time regions ($0 < t < 1$ μs and $t \geqslant 1$ μs) can be clearly seen. In these regions the distribution of neutrons as a function of time is described by two different exponential functions, corresponding to the transient and quasistationary regimes. The curves 1 and 2 in the same figure show the results of the solution of the kinetic equations by the Monte Carlo method.[56] The theoretical values were used for all parameters. Curve 1 corresponds to the theoretical cross sections for elastic scattering. The decrease in these cross sections by a factor of two (curve 2) changes significantly the spectrum of dN/dt. Of course, the magnitude of the scattering cross sections cannot be estimated based on these curves, since the problem involves many parameters and requires further study.

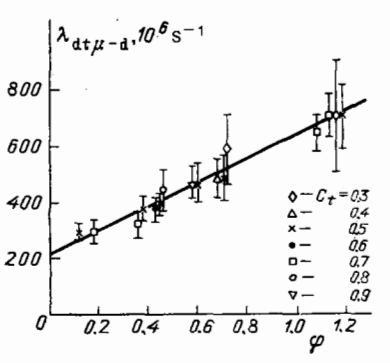

FIG. 9. $\lambda^{D_2}_{dt\mu}$ as a function of the density of the mixture $D_2 + T_2$.[26,87]

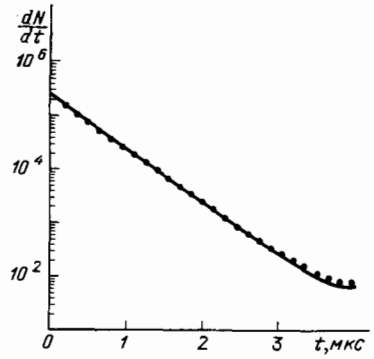

FIG. 10. The temporal spectrum of the first detected neutrons from a fusion reaction in a $dt\mu$ molecule in a liquid deuterium-tritium mixture.[25,62,88]

An increase of the thermalization time τ_T for small φ also changes substantially the main quantity pertaining to the quasistationary regime—the cycle rate λ_c (see Fig. 17 from the review by S. S. Gershteĭn *et al.* in this issue of Uspekhi Fizicheskikh Nauk), which is determined in the experiments from the slope of the slow exponential dN_n/dt. This can be seen from the two-group approximation, when the $t\mu$ atoms are divided into two groups—fast and slow:

$$\lambda_s^{-1} = \frac{qC_d}{\lambda_{dt}} + \frac{1}{\lambda_s}\left(1 - \frac{\lambda_f (N_f^0 + qC_d N_s^0)}{\tau^{-1} + \lambda_f}\right),$$

where λ_s and λ_f are the rates of formation of the mu-molecules $dt\mu$ from the slow and fast $t\mu$ atoms and N_s^0 and $N_f^0 = 1 - N_s^0$ are the initial relative numbers of these atoms immediately after the cascade processes. According to Refs.

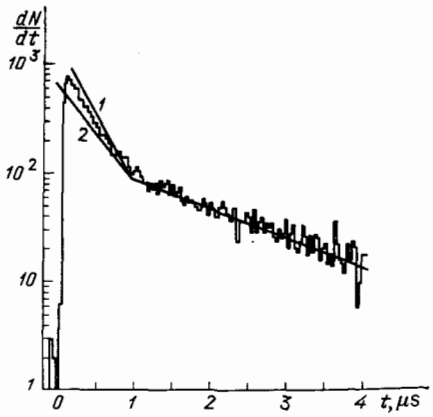

FIG. 11. The temporal spectrum of the first detected neutrons from a fusion reaction in a $dt\mu$ molecule in a gaseous deuterium-tritium mixture ($\varphi = 0.01$). The figure was taken from Refs. 25, 62, and 88. The curves *1* and *2* are theoretical curves (see text).

21 and 22 N_f^0 increases as φ decreases; q also increases (see Fig. 1).

The analysis made in this section shows that for $\varphi \leqslant 0.1$ the process of thermalization of mu-atoms must be taken into account for all t, and hence it must also be taken into account when calculating the integrated yield of fusion products.

2. THE EFFECTIVE COEFFICIENT OF STICKING OF MUONS TO THE PRODUCTS OF A NUCLEAR FUSION REACTION

2.1. The probability of sticking of a muon to the products of a fusion reaction in a mu-molecule

The effective coefficient of sticking (the probability) ω_s of muons to α particles in the reaction ($E_f = 17.6$ MeV)

$$(\mathrm{dt}\,\mu)_{Jv} \xrightarrow[1-\omega_s]{\omega_s} \begin{cases} \longrightarrow \alpha\mu + \mathrm{n} \\ \longrightarrow \alpha + \mathrm{n} + \mu \end{cases} + E_f, \tag{2.1}$$

determining the upper limit for the number of cycles ($X_c \leqslant 1/\omega_s$), is equal to[89,90]

$$\omega_s = \omega_s^0 (1 - R_0). \tag{2.2}$$

In Eq. (2.2) ω_s^0 is the initial probability of muon capture in all Rydberg bound states (n,l,m) of the ion $\alpha\mu$ and R_0 is the probability that muons are shaken off the $\alpha\mu$ ions stopping in the material in collisions with the nuclei b = d, t, p:

$$(\alpha\mu)_{nlm} + \mathrm{b} \xrightarrow[\sigma_b]{\sigma_i} \alpha + \mathrm{b} + \mu, \tag{2.3}$$

$$\xrightarrow{\sigma_{ct}} \alpha + (\mathrm{b}\mu)_{n'l'm'}, \tag{2.4}$$

where σ_i, σ_{ct}, and $\sigma_b = \sigma_i + \sigma_{ct}$ are the cross sections for ionization, charge transfer, and break-up of an $\alpha\mu$ ion in the state $\nu = (n,l,m)$.

The calculation of ω_s^0 (Ref. 91) is analogous to the well-known problem of the ionization of an atom when the nucleus of the atom is subjected to a sudden impact:[11]

$$\omega_s^0 = \sum_\nu \omega_\nu, \tag{2.5}$$

where the summation extends only over the bound states and ω_ν is the probability that a muon is captured in the νth state of the $\alpha\mu$ ion

$$\omega_\nu = (2J+1)^{-1} \sum_{M_J} |C_\nu|^2, \tag{2.6}$$

$$C_\nu = \langle \nu | e^{-iqr_0} | i \rangle = \int \Psi_\nu^*(\mathbf{r}_0) e^{-iqr} \Phi_i(\mathbf{r}_0)\, \mathrm{d}^3 r_0, \tag{2.7}$$

$$q = \frac{K m_\mu}{m_{\alpha\mu}} = m_\mu \{2E_f M_n [m_{\alpha\mu}(m_{\alpha\mu} + M_n)]^{-1}\}^{1/2},$$

$$\Phi_i(\mathbf{r}_0) = N \Psi_{vJM_J}(\mathbf{r}_0, 0), \quad N^{-2} = \int |\Psi_{vJM_J}(\mathbf{r}_0, 0)|^2 \, \mathrm{d}^3 r_0. \tag{2.8}$$

Calculation of ω_s^0 using the formulas (2.5)–(2.8) gives[91]

$$\begin{aligned} &\text{for } J=0,\ v=1 \quad \omega_s^0 = 0.00848, \\ &\text{for } J=0,\ v=0 \quad \omega_s^0 = 0.00845. \end{aligned} \tag{2.9}$$

The quantities ω_ν with different values of the quantum numbers ν are presented in Table I for the state with $J = 0$ and $v = 1$. The probability of capture in the level with $n = 5$ is equal to 0.000242. For the state with $J = v = 0$ the quantities ω_ν do not differ significantly from Eq. (2.9).

According to Ref. 89, in the Born-Oppenheimer approximation (the adiabatic approximation $M_0/m_\mu = \infty$) $\omega_s^0 = 0.01164$, i.e., nonadiabatic effects reduce ω_s by 27%. The result (2.9) agrees with the calculation of ω_s^0 by the Monte Carlo method.[92]

As the separation of nuclei in the mu-molecule $\mathrm{dt}\mu$ in states with $J \neq 0$ decreases the angular momentum of the entire molecule is transferred to the muon, which finds itself in a state with angular momentum J in the field of the united nucleus. The probability ω_s^0 for such states is extremely low. Thus for $J = 1$ in $\mathrm{dt}\mu$ $\omega_s^0\ (J=1)/\omega_s^0\ (J=0) \sim \omega_{2p}\ (J=0)/\omega_{1s}\ (J=0) = 0.037$. From here and from Eq. (2.9) we obtain the estimate $\omega_s^0\ (J=1) \sim 3 \cdot 10^{-4}$. One would think that if the mechanisms for deexcitation of the mu-molecule are "switched off," and the density is reduced to $\varphi \leqslant 10^{-4}$, then fusion reactions will occur in the state (1,1), where $\omega_s^0 \approx 0$, which suggests that X_c will increase. These hopes are not justified for several reasons. First, the rate of formation of mu-molecules is low when the density φ is low and the rate of the fusion reaction λ_f ($L = 0$) or states with $J = 1$, which proceeds from the S wave, is low. The contribution of the f wave increases λ_f: $\lambda_f(J=1) = \lambda_f(L=0) + \lambda_f(L=1)$. In the state with $J = 1$ and $L = 1$, when the nuclei merge the muon is primarily in the 1s state of the united atom, in which ω_s increases substantially. Thus the rate λ_f can exceed the previous estimate, but at the same time ω_s^0 also increases up to the value given in Eq. (2.9).

For $\mathrm{dd}\mu$ in states with $J = v = 1$ and $J = 1$, $v = 0$ the value

$$\omega_d^0 = 0{,}133 \tag{2.10}$$

was obtained for the initial sticking coefficient in the channel with formation of ^{3}He.[93] The effective sticking probability is equal to $\beta\omega_d^0$, since in the channel with formation of triton $\omega_d^0 \approx 0$. This is explained by the lower charge and higher velocity of particles in this channel.

2.2. Probability of muon shakeoff in the process of stopping of the mu-ions μ^3He and μ^4He in cold hydrogen

The dependences of the cross sections of the break-up and ionization processes (2.3) and (2.4) from the 1s ground state of $\alpha\mu$ ions and the effective stopping $\varkappa$ of $\alpha\mu$ ions in the molecular mixture $D_2 + T_2$ on the energy E of $\alpha\mu$ ions are presented in Fig. 12. A generalization of the experimental

ν	1s	2s	2p	3s	3p	3d	4s	4p
ω_ν, 10^{-2}	0.6526	0.0937	0.0239	0.0285	0.0086	0.0003	0.0122	0.0038

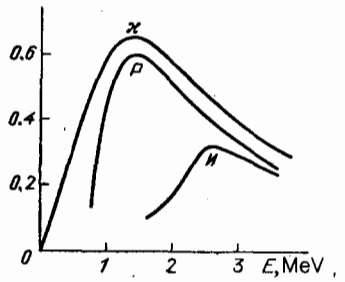

FIG. 12. The cross section (10^{-21} cm^2) for ionization σ_i (curve I) and break-up σ_b (curve *d*) of $(\alpha\mu)_{1s}$ ions in the 1s states as a function of the energy E (laboratory system) in collisions with stationary hydrogen isotopes nuclei. The curve $\varkappa$ is the effective stopping of $\alpha\mu$ ions in a molecular D–T mixture (in units of 10^{-20} MeV cm^2).

data on the stopping of protons in hydrogen was employed for $\varkappa$.[94,95] The ionization and break-up cross sections were calculated using the formulas

$$\sigma_i(v) = \tilde{\sigma}_H(v)\left(\frac{m_e}{m_\mu}\right)^2, \quad \sigma_b(v) = \tilde{\sigma}_p(v)\left(\frac{m_e}{m_\mu}\right)^2, \qquad (2.11)$$

where $\tilde{\sigma}$ is the cross section of analogous electronic processes, well known from experiments[96–98] on the break-up of helium ions by protons. The charge-transfer cross section and the cross sections of different inelastic processes in the excited states (n,l,m) were calculated using the formulas from Ref. 99. When $\alpha\mu$ ions stop they are also deexcited as a result of radiation and Auger processes.

To calculate the muon shakeoff probability R_0 it is necessary to solve a system of equations for the populations N_ν of the bound states of the mu-ion $\alpha\mu$ and the continuum N_c taking into account all possible transitions of the mu-ion:

$$\begin{aligned}
\frac{dN_\nu}{dt} &= -\left(\lambda_{\nu K} + \sum_{\nu'}\lambda_{\nu\nu'}\right)N_\nu + \sum_{\nu'}\lambda_{\nu'\nu}N_{\nu'},\\
\frac{dN_K}{dt} &= \sum_\nu \lambda_{\nu K}N_\nu, \qquad (2.12)\\
\frac{dE}{dt} &= -Nv\varkappa, \quad R_0 = N_K(v=0).
\end{aligned}$$

where $\lambda_{\nu\nu'}$ are the rates of the corresponding processes $\nu\to\nu'$ and $v = (2E/m_{\alpha\mu})^{1/2}$. The initial conditions have the form $N_c(0) = 0$, $N_\nu(0) = B\omega_\nu$, $E(0) = E_0$,

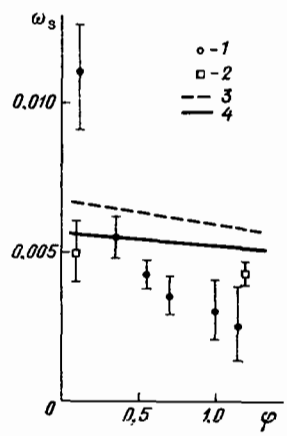

FIG. 13. The dependence of the muon sticking coefficients for the reaction $dt\mu\to\mu^4$He + n on the density of the DT mixture. Experiments: *1*—Ref. 26 and *2*—Ref. 62. Theory: *3*—Ref. 102 and *4*—Ref. 95.

$$B = \left(\sum_\nu \omega_\nu\right)^{-1}$$

is the normalization constant, and E_0 is the initial energy of the mu-ion. In particular, for the reactions d + t and d + d $E_0 = 3.5$ and 0.8 MeV, respectively.

The shakeoff probabilities R_0 in different approximations employed in Eqs. (2.12) were calculated in Refs. 89–91, 95, and 100–102. For $dt\mu$ the most accurate calculation[95] gives $R_0 = 0.35$ for $\varphi = 1$. Muon shakeoff occurs primarily from the 1s state, whose population is large. Step ionization processes $(\alpha\mu)_{1s} \to (\alpha\mu)_n \to \alpha + \mu$, as a result of which ω_s decreases slowly as φ increases, are also very significant.[100,102] Neglecting these processes, i.e., taking into account only the 1s state of the $\alpha\mu$ ion, we obtain[89] from Eq. (2.12)

$$R_0 = 1 - e^{-P}, \quad P = \int_0^{E_0} \delta(E)\,dE, \quad \delta(E) = \frac{\sigma_b(E)}{\varkappa(E)}. \qquad (2.13)$$

In this approximation $R_0 = 0.27$.[95]

The theoretical[95,102] and experimental[25,26,62,103] values of ω_s are presented in Fig. 13. The disagreement between the experiments is explained by the approximation $q_{1s} = 1$, used in Ref. 26 in the analysis of data based on a formula of the type (1.35)–(1.36).

For the mu-molecule $dd\mu$ $R_0 \approx 0.09$ for $\varphi = 1$,[89,93,100] so that from Eqs. (2.2) and (2.10) we find $\omega_d = 0.12$ ($\varphi = 1$). The experimental value (Ref. 104) $\omega_d = 0.124 \pm 0.004$ ($\varphi = 0.1$), converted to $\varphi = 1$ using the formulas from Ref. 100, is equal to $\omega_d = 0.118 \pm 0.004$ ($\varphi = 1$).

The cross sections $\tilde{\sigma}$ of electronic processes were measured with an insignificant error by the method of crossed beams. The existing discrepancy between the theoretical[95] and experimental[25,103] values of ω_s (see Fig. 13) cannot be eliminated by varying the cross sections $\tilde{\sigma}$ within the limits of experimental error (changing the cross sections of other processes within the limits of the errors in the theory has an even smaller effect on ω_s). The main reason for the discrepancy is the inaccuracy of the formulas (2.11) themselves. They are based on the description of the motion of nuclei in the reactions (2.3) and (2.4) by classical and, in addition, rectilinear trajectories. This approximation is correct for electronic processes, but it is incorrect for the reactions of interest to us in the case of low collision velocities $v \leqslant v_{max} \approx 1.6$ a.u., where $\tilde{\sigma}_b(v_{max}) = \max$.[6] Although for such velocities the motion of the nuclei remains quasiclassical, it depends to a significant degree on the state of the quantum subsystem—the muon.[105]

We shall trace the dependence of the cross section σ_b on the mass m of the light particle (muon). The most general formula has the form $\sigma_d = (\hbar^2/me^2)^2 F(mM, \hbar v/e^2)$, where $M^{-1} = M_a^{-1} + M_b^{-1}$ or in atomic units $\sigma_b = m^{-2}F(m/M, v)$. For the electronic process $\tilde{\sigma}_b \approx m_e^{-2}F(0,v)$. For the muonic process with a high collision velocity $\sigma_b \approx m_\mu^{-2}F(0,v)$, i.e., the formula (2.11) is valid. However for a low velocity $v \sim (m_\mu/M)^{1/2}$, i.e., $Mv^2 \sim m_\mu$, the argument m/M in the function F cannot be neglected, so that the formula (2.11) is no longer satisfied. It is difficult to make more definite theoretical assertions about σ_b at low energies without a numerical calculation.

It follows from the experiments of Refs. 25 and 103 that

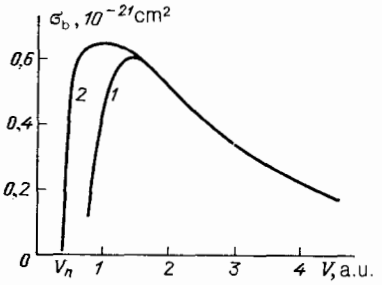

FIG. 14. The break-up cross section of $\alpha\mu$ ions in the 1s state as a function of the velocity of collisions with deuterium nuclei. Curve *1* was calculated using the formula (2.11) and curve *2* is the trial cross section used for calculating ω_s.

for low collision velocities the cross section for the break-up of an $\alpha\mu$ ion is higher (curve 2 in Fig. 14) than the cross section determined from the formula (2.11) (curve 1). When the shakeoff probability R_0 is calculated using this cross section agreement between theory and experiment is obtained. (We are grateful to V. A. Shakirov for acquainting us with the results of this calculation.) To resolve this question completely it is necessary to calculate by Faddeev's method the cross section for charge transfer (2.4) from the 1*s* state, which makes the main contribution to σ_d for $v \leqslant v_{max}$.

3. MUON CATALYSIS IN PLASMA

In the preceding section we indicated that $\omega_s \approx 0.005$, so that the number of cycles in a molecular DT mixture does not exceed ~ 150. The only real possibility of reducing ω_s lies in using the kinetic energy of the $\alpha\mu$ ions to increase the muon shakeoff probability R_0, i.e., choosing conditions under which $R_0 \sim 1$. Such conditions exist in a plasma with $T \sim$ 100–200 eV,[5] since at this temperature the friction force acting on the decelerating $\alpha\mu$ ion is appreciably weaker. As a consequence, the number of collisions with nuclei (2.3) and (2.4), as a result of which the $\alpha\mu$ ions lose muons, increases. This indicates that the diverse muonic processes in plasma deserve a more detailed study. Such a study was started in Refs. 5–7, 106, and 107.

3.1. Mechanisms of formation of mu-atoms in plasma

Mu-molecules form primarily from mu-atoms in 1s states. Actually, the formation of mu-molecules from excited mu-atoms is extremely unlikely, since the cascade time is short. In addition, because the excited mu-molecules are large the rates of nuclear reactions in them are negligibly low; the rates at which they break-up in collisions with nuclei and electrons are high (see Sec. 3.2) and the transitions $(dt\mu)^* \to (dt\mu)_{J_0} + \gamma$ are unlikely compared with the dissociative transitions $(dt\mu) \to t\mu + d + \gamma$ and $(dt\mu)^* \to d\mu + t + \gamma$.

Thus we are interested in the total rate λ_{mes} of the processes $\mu \to (t\mu)_{1s}$, as a result of which a mu-atom forms in the 1*s* state. In these processes three stages can be conditionally separated: 1) formation of a bound state $t + \mu + X \to (t\mu)_n + X'$; 2) diffusion along the Rydberg levels $(t\mu)_n + X \to (t\mu)_{n'} + X'$; and, 3) radiative transitions to lower levels $(t\mu)_n \to (t\mu)_{1s} + \gamma$. Here the third body X = e, t, p, or d. The time $\tau_{mes} = \lambda_{mes}^{-1}$ of the entire process is determined by the longest stage—diffusion along levels with binding energy of the mu-atom $|\varepsilon| \sim T$, which occurs over a time $\sim \tau$ (see below).

We shall estimate, starting from the well-known Thompson model, the rate λ_{mes}^{X} of formation of mu-atoms with a third body of the type *X*. In one collision of a mu-atom with an *X* particle, carrying energy $\sim T$, the energy of the mu-atom $\varepsilon_\mu = p^2/(2m_a) - r_a^{-1}$ (here and below $e = \hbar = m_e = 1$, $m_a^{-1} = m_\mu^{-1} + M_t^{-1}$, $\mathbf{p} = (M_t \mathbf{p}_\mu - m_\mu \mathbf{p}_t)/m_{t\mu}$ is the momentum of the mu-atom in the center of mass system) changes by the amount $|\Delta\varepsilon_\mu| \sim \eta T$. Thus $\sim 1/\eta$ collisions are required to pass through the diffusion region $|\varepsilon_\mu| \sim T$ (in the corresponding Fokker-Planck equation the terms describing the mobility and diffusion are of the same order of magnitude). For electrons $\eta = m_e/m_\mu \equiv \eta_e$, and for collisions with nuclei $\eta = m_\mu/m_n \sim m_\mu/M_t \equiv \eta_n$. After a collision with an *X* particle muons with kinetic energy $\varepsilon_\mu \leqslant \eta T$ and located at distances $r_a < r_{cr} \sim 1/\eta T$ from the nuclei are, with probability of the order of unity, in a bound state, forming with the nucleus (for definiteness a triton) an excited mu-atom with the binding energy $|\varepsilon_\mu| \sim \eta T$. The concentration of such muons $N'_\mu \sim WN_\mu$, where $W = W_1 W_2 \sim N_t T^3 \sim N_1 T^{-3}$, $W_1 \sim r_{cr}^3 N_t$ is the probability that a muon is located in the region $r_a < r_{cr}$, $W_2 \sim \eta_3$ is the relative number of muons with energy $\sim \eta T$, and N_t and N_μ are the numbers of tritons and muons in 1 cm^3.

We note two interesting facts: 1) excited mu-atoms are formed from slow muons ($\varepsilon_\mu/T \sim \eta \ll 1$) and 2) the details of this process are not important, since the parameter η drops out of *W*.

The density of mu-atoms in 1s states increases according to the law $dN_{t\mu}/dt \sim N'_\mu/\tau = \lambda_{mes} N_\mu$. From here and from the estimates $\tau \sim 1/(\eta_X V_{X\mu} \sigma_{X\mu}) \sim T^{3/2} \mu_{X\mu}$ (here $V_{X\mu} \sim (T/\mu_{X\mu})^{1/2}$ is the relative velocity of X and μ, $\mu_{X\mu}$ is their reduced mass, $\sigma_{X\mu} \sim 1/T^2$ is the cross section for scattering of X by μ) we obtain the estimate $\lambda_{mes}^{X} \sim \eta N_1^2 (\mu_{X\mu})^{-1/2} T^{-9/2}$ for the rate of formation of mu-atoms. In particular for the electronic mechanism (X = e)

$$\lambda_{mes}^{rel} \sim N_1^2 m_\mu^{-1} T^{-9/2}. \tag{3.1}$$

It follows from Eq. (3.1) that the reaction of the rates of the electronic and nuclear (X = d,t,p) mechanisms is of the order of $\lambda_{mes}^{el}/\lambda_{mes}^{nuc} \sim (m_e/m_\mu)^{1/2} (M_t/m_\mu) \sim 1$, but actually $\lambda_{mes}^{el} \gg \lambda_{mes}^{nuc}$. Actually, the estimates presented above correspond to the classical-trajectory approximation, which does not hold for muons undergoing quantum transitions induced by slowly moving nuclei. The Massey parameter for such transitions is large $\zeta \sim \Delta\varepsilon_\mu r_\mu / v_{nuc} \sim (M_t/m_\mu)^{1/2} \gg 1$, where $\Delta\varepsilon \approx m_\mu/n^3$ is the difference of the neighboring energy levels, $m_\mu/n^2 \sim T$, i.e., $n \sim (m_\mu/T)^{1/2}$; $r_\mu \sim a_\mu n^3 = n^2/m_\mu$ is the size of the muon orbit; and, $V_{nuc} \sim (T/M_t)^{1/2}$ is the velocity of the nuclei. Thus, adiabatic transitions of muons are unlikely, i.e, collisions with nuclei virtually never lead to diffusion of mu-atoms along the levels (in reality, such transitions, though they remain unlikely, still occur near the interactions of the muonic terms[21,22]).

Based on the estimates presented we conclude that in a plasma mu-atoms form primarily by the electronic mechanism (X = e). The theory of multiquantum electron-ion recombination, employed in our case, makes it possible to de-

rive an exact expression for $\lambda_{\text{mes}} \approx \lambda_{\text{mes}}^{\text{el}}$. According to this theory[108-110]

$$\lambda_{\text{mes}} = \lambda_{\text{d}\mu} + \lambda_{\text{i}\mu} = \alpha N, \quad \alpha = \left(\frac{\pi}{T}\right)^{3/2} (2J)^{-1},$$

$$J = \int_0^\infty \varepsilon^{5/2} e^{-\varepsilon/T} (B(\varepsilon))^{-1} \, d\varepsilon, \tag{3.2}$$

where $\varepsilon = |\varepsilon_\mu|$, $B(\varepsilon) = \langle (\Delta\varepsilon_\mu)^2/2\delta t \rangle$, $1/\delta t$ is the collision frequency, and averaging is performed over all possible collisions (see below). The density and temperature of the plasma in the case at hand are high, so that $T_e \approx T_i \equiv T$ (equilibrium) and $N_e \approx N_i \equiv N$ (quasineutrality, total ionization). Let us assume (this will be confirmed in the course of the calculation) that collisions of electrons with a mu-atom with large impact parameters $\eta \gg r_\mu \sim 1/|\varepsilon_\mu|$ make the main contribution to $B(\varepsilon)$. Since the velocity of the muon in a mu-atom is low ($v_\mu \ll v_e$), in a collision with an electron the muon can be assumed to be at rest. Therefore $\Delta\varepsilon_\mu \approx [(\mathbf{p} + \Delta\mathbf{p})^2 - p_\mu^2]/2m_\mu$, $\Delta\mathbf{p} = \int F\, dt = 2\rho/v_e\rho^2$, and F is the Coulomb repulsion force between the electron and the muon. From here $B(\varepsilon) = (1/2)N_e v_e \int d^2\rho (\Delta\varepsilon_\mu)^2 = (8/3)(2\pi/T)^{1/2}(\varepsilon/m_\mu)\Lambda_D(\varepsilon)N$, where $\Lambda_D(\varepsilon)\ln(\rho_{\max}/\rho_{\min}) \approx \ln(r_D/r_\mu) = \ln(r_D\varepsilon)$, and $r_D = (T/8\pi N)^{1/2}$ is the Debye radius. Finally we obtain[5] [compare with Eq. (3.1)]

$$\lambda_{\text{mes}} = \frac{16\sqrt{2}\,\pi^{3/2}N^2}{9m_\mu T^{9/2}} \Lambda_D(T) \text{ a.u.} = 2\cdot 10^9 \varphi^2 \tilde{T}^{-9/2} \text{s}^{-1} \tag{3.3}$$

here and below we employ the reduced temperature $\tilde{T} = T$ (eV)/10.

The expressions (3.2) are obtained by solving the Fokker-Planck equations[110]

$$\frac{\partial f}{\partial t} + \frac{\partial S}{\partial \varepsilon_\mu} = 0, \quad S = -Bf_0 \frac{\partial}{\partial \varepsilon_\mu}\left(\frac{f}{f_0}\right),$$

$$f_0 = \frac{1}{2} e^{-\varepsilon_\mu/T} \left(\frac{\pi}{T}\right)^{3/2} |\varepsilon_\mu|^{-5/2}, \tag{3.4}$$

from which the distribution function $f(\varepsilon_\mu, t)$ of mu-atoms over the binding energies $\varepsilon = |\varepsilon_\mu|$, $f(\varepsilon_\mu)\,d\varepsilon_\mu$ being the probability of finding a mu-atom in a state with binding energy in the interval $(\varepsilon, \varepsilon + d\varepsilon)$, is determined. Assume that at $t = 0$ $f(\varepsilon_\mu, 0) = \delta(\varepsilon_\mu - \varepsilon_0)$, i.e., the mu-atom formed in a state with energy ε_0. The probability of formation of a mu-atom (recombination) is obviously equal to

$$W_{\text{rec}} = -\int_0^\infty S(\varepsilon_0 - 0, t)\, dt.$$

Integrating Eq. (3.4) over t from 0 to $+\infty$ and solving the equation obtained we find

$$W_{\text{rec}}(\varepsilon_0) = \frac{4}{3\sqrt{\pi}} \int_0^{\varepsilon_0/T} x^{3/2} e^{-x} dx. \tag{3.5}$$

One can see from Eq. (3.5) that $W_{\text{rec}} \ll 1$ if $|\varepsilon_0| \ll T$ and $W_{\text{rec}} \sim 1$ if $|\varepsilon_0| \sim T$.

From here as well as from the expression (3.2), in which $\varepsilon \sim T$ make the main contribution to J, we conclude that the slowest limiting stage of recombination is diffusion along the levels with $\varepsilon \sim T$, as conjectured earlier. Compared with the electronic mechanism, radiative recombination $\mu + t = t\mu + \gamma$ is unlikely, so that we ignore it (and the nuclear mechanism also) below

3.2. Mechanisms of formation of mu-molecules in plasma

In a plasma mu-molecules form in three-particle collisions.[5] Depending on the type of third particle carrying away the excess energy the following mechanisms of formation are possible:

electronic

$$t\mu + d + e \to (dt\mu)_{Jv} + e', \tag{3.6}$$
$$t\mu + D + e \to (dt\mu)e + e', \tag{3.7}$$

neutral-ionic (X = D,T,H)

$$t\mu + d + X \to dt\mu + X', \tag{3.8}$$
$$t\mu + D + X^+ \to (dt\mu)e + (X^+)', \tag{3.9}$$

ion-ionic

$$t\mu + d + X^+ \to dt\mu + (X^+)', \tag{3.10}$$

neutral-neutral

$$t\mu + D + X \to (dt\mu)e + X'. \tag{3.11}$$

In addition, if molecules are present, then Vesman's mechanism must be taken into account (see Sec. 1.3).

As the temperature increases the break-up of mu-molecules formed in reactions that are the reverse of the reactions (3.6)–(3.11) becomes important. The observed (effective) rate of formation is equal to

$$\tilde{\lambda}_{dt\mu} = \lambda_{\text{form}} w_f, \tag{3.12}$$

where $\tilde{\lambda}_{\text{form}}$ is the rate of the direct reactions, $w_f/(\tilde{\lambda}_f + \lambda_b)$ is the probability of a nuclear reaction in the mu-molecule formed (compare with Sec. 1.3), λ_b is the rate of the reverse reactions (break-up), and $\tilde{\lambda}_f = \lambda'_{deex} + \lambda_f$ is the rate of depopulation of the upper level of the mu-molecule (see Sec. 1.4). The principle of detailed balance is satisfied ($\hbar = 1$):

$$\frac{\lambda_{\text{form}}}{\lambda_b} = (2J+1) N_d \cdot \left(\frac{2\pi}{\mu_a T}\right)^{3/2} e^{|\varepsilon_{Jv}|/T} \equiv K. \tag{3.13}$$

We conclude from Eqs. (3.12) and (3.13) that

$$\tilde{\lambda}_{dt\mu} \leqslant K\tilde{\lambda}_f, \tag{3.14}$$

and in addition $\lambda_{dt\mu} \to K\tilde{\lambda}_f$ as $\lambda_b/\tilde{\lambda}_f \to \infty$. We shall prove below that all the mechanisms enumerated above guarantee that $\lambda_b/\tilde{\lambda}_f \geqslant 1$, so that in Eq. (3.14) the equal sign can be used.

Because mu-molecules in the lower (J,v) states are small the rates λ_{rev} for them are low ($\lambda_{\text{form}} \sim 1/|\varepsilon_{Jv}|$; see below), so that the mu-molecules $dd\mu$ and $dt\mu$ in the reactions (3.6) and (3.11), like in the case of Vesman's mechanism, form primarily in weakly bound states $J = v = 1$, so that in what follows we set $J = v = 1$ in the formulas (3.13). From here and from Eqs. (3.13) and (3.14) we obtain $K \approx 4\cdot 10^{-4} \varphi T^{-3/2} \exp(0.64/T)$.

$$\tilde{\lambda}_{dt\mu} \sim 4\cdot 10^8 \varphi T^{-3/2} e^{0.64/T}, \tag{3.15}$$

where T is given in eV. In particular, for $\varphi \sim 5$ (this is the density of matter in drops compressed by the pressure of the plasma; see Sec. 4) it follows from Eq. (3.15) that

$$\tilde{\lambda}_{dt\mu} \geqslant 10^9 \quad \text{for} \quad T \leqslant 2 \text{ eV}. \tag{3.16}$$

Thus it is sufficient to study temperatures $T \leqslant 2$ eV—at high temperatures $\lambda_{dt\mu}$ is small.

We shall calculate λ_{form} for the electronic mechanism. It is simplest to determine λ_{form} from Eq. (3.13), calculating first the rate λ_b of the reverse reaction $e + d\text{-}t\mu \to e' + t\mu + d$.

We shall prove below that $R \sim 1/\varkappa$ make the main contribution to λ_b, so that the approximation $\chi_b \approx 0$ for the wave function of the mu-molecule (1.19) and (1.21) is applicable, i.e., the mu-atom can be regarded as a point particle. The initial and final wave functions have the form

$$\Psi_i = \Psi_k^{(+)}(\mathbf{r})\,\Psi_j(\mathbf{R}), \quad \Psi_j(\mathbf{R}) = \left(\frac{3}{4\pi}\right)^{1/2} \hat{\mathbf{R}}_j \chi_a(R)\,R^{-1}, \qquad (3.17)$$

$$\Psi_f = e^{i\mathbf{pR}}\Psi_{k'}^{(-)}(\mathbf{r}),$$

where $\mathbf{R}$ are the coordinates of the $t\mu$ atom with respect to the deuteron; $\mathbf{r}$ are the coordinates of the electron with respect to the center of mass of $dt\mu$; $\hat{\mathbf{R}} = \mathbf{R}/R; j = x,y,z$; $\Psi^{(\pm)}$ are the Coulomb wave functions of an electron in the field of the charge $Z = +1$ of a point mu-molecule;[11] $\mathbf{K}$ and $\mathbf{K}'$ are the momenta of the electron in the initial and final states; and, $\mathbf{p}$ is the relative momentum of $t\mu$ and d. The transition operator is defined in Eq. (1.9), and in addition $\mathbf{d} \approx -\beta\mathbf{R}$ ($\mathbf{r}_0 \approx \mathbf{R}/2$), $\vec{\mathscr{E}} = \mathbf{r}/r^3$, $\beta = M_{t\mu}/(M_{t\mu} + M_d)$, where we employed the fact that the mu-molecule is small: $R/r \ll 1$.

From perturbation theory, which is valid owing to the fact that $R/r \ll 1$, we obtain

$$\lambda_b = N_e \frac{\beta^2 C_a^2}{12\pi^3\varkappa^2} \int x^{1/2} \frac{3x^2 + 2x + 3}{(x+1)^4} \left\langle K'\theta \left(\frac{K^2}{2} - \omega\right) Q \right\rangle dx, \qquad (3.18)$$

where $\varepsilon_p = p^2/(2\mu_a)$, $x = \varepsilon_p/|\varepsilon_{11}|$, $\omega = \varepsilon_p + |\varepsilon_{11}| = |\varepsilon_{11}|(1+x)$, $K' = (K^2 - 2\omega)^{1/2}$, $Q = \int |(\mathbf{r}/r^3)_{K'K}|^2 d\Omega_{K'}$. In Eq. (3.18) the brackets denote averaging over the Maxwellian distribution of the electrons.

The quantity Q, expressed in terms of the hypergeometric function, has the following form in the case of greatest interest $K \ll 1$ (we recall that $T \leqslant 2$ eV) and $|\mathbf{K}' - \mathbf{K}|/\mathbf{K}^2 \gg 1$,:[111] $Q = 2^6\pi^4/\sqrt{3}\mathbf{K}'\mathbf{K}$.

The function θ in Eq. (3.18) indicates that after colliding with a mu-molecule the electron remains in the continuous spectrum and moves with the momentum $\mathbf{K}'$. However transitions into a quasicontinuum of Rydberg states are possible. Taking these transitions into account, we write in the following form the reaction by which the mu-molecules are broken up by electrons:

$$dt\mu + e \longrightarrow \begin{cases} \longrightarrow t\mu + d + e, & (3.19) \\ \longrightarrow t\mu + D^*. & (3.20) \end{cases}$$

The formation of excited D* atoms can be taken into account approximately by dropping the θ function in the expression (3.18):

$$\lambda_b \approx N_e \frac{20\pi^2\beta^2 C_a^2}{3\sqrt{3}\varkappa^2} \left\langle \frac{1}{K} \right\rangle = N_e \frac{20\pi^2\beta^2 C_a^2}{3\sqrt{3}\varkappa^2} \left(\frac{2}{\pi T}\right)^{1/2}. \qquad (3.21)$$

The following remark is in order regarding the choice of Ψ_f in Eq. (3.17). The process of interest is nonresonant. However, as in Sec. 1.3, it is sufficient to use a plane wave for the wave function of the system $t\mu + d$. A dipole transition out of the state $J = 1$ is possible only into an S and a D wave. For $J = 1$ and $J = 2$ the mu-molecule $dt\mu$ does not have weakly bound states, so that the partial scattering amplitudes are small: $f_{L=0} \sim f_{L=2} \sim a_\mu$. This means that in the region $R \sim 1/\varkappa \sim 20a_\mu$, which makes the main contribution to the matrix element, the exact wave function $\Psi_p^{(-)}(\mathbf{R})$, which should be used in reality, can be replaced by its asymptotic form $\Psi_p^{(-)}(\mathbf{R}) \approx \exp(i\mathbf{pR}) + f(\theta)\exp(i\mathbf{pR})/R$ and the small terms $f_{L=0}/R \sim f_{L=2}/R \ll 1$ can be dropped. This means that the plane wave $\exp(i\mathbf{p}\cdot\mathbf{R})$ can be used at the outset.

The rates of the reactions (3.6) and (3.7) are approximately equal to one another, so that the total rate of these reactions, i.e., of the electronic mechanism, according to Eqs. (3.13) and (3.21), is equal to

$$\lambda_{form} = \alpha_i \varphi^2 C_d \lambda_{form}^{(0)},$$

$$\lambda_{form}^{(0)} = N_0^2 \frac{80\pi^3\beta^2 C_a^2}{\sqrt{3}\,\mu^{3/2}\varkappa^2 T^2} e^{|\varepsilon_{11}|/T} \text{ a.u.} \approx 2 \cdot 10^{10} e^{0,64/T} \frac{1}{T^2} \text{ s}^{-1}, \qquad (3.22)$$

where α_i is the degree of ionization, $N_e = N_i = \alpha_i N$, and $N = \varphi N_0$ is the density of nuclei. In the last formula in Eq. (3.22) T is given in eV. Deuterium in the reactions (3.6) and (3.7) can be an atom or an ion or it can be a constituent of a molecular ion or molecule. The rates of the electronic mechanisms in all these cases differ insignificantly—the accuracy of our calculation is adequate for analyzing the kinetics of muon catalysis (see Sec. 4).

Because the degree of ionization of matter in drops is low (see below) the most important three-particle mechanism is the neutral-neutral mechanisms (3.11), which we shall now study. The reverse reaction proceeds according to the scheme

$$(dt\mu)e + X \longrightarrow \begin{cases} \longrightarrow t\mu + D + X', & (3.23) \\ \longrightarrow t\mu + (DX)^*, & (3.24) \end{cases}$$

where $(DX)^*$ is the DX molecule in an excited rotational-vibrational state [compare with Eqs. (3.19) and (3.20)]. The transition operator is determined by the formula (1.9) (compare with Sec. 1.3), in which according to the Feynman-Hellman theorem[112,113] $\vec{\mathscr{E}} = \nabla_r U(r) = \hat{\mathbf{r}} dU(r)/dr$, where r is now the distance between X and the center of mass of $dt\mu$, $\hat{\mathbf{r}} = \mathbf{r}/r$, and $U(r)$ is the interaction potential energy of the atoms (molecular term); with accuracy up to insignificant isotopic effects this interaction potential is identical to the term of the H_2 molecule.

The energy $U(r)$ depends on the total spin of the electrons S. For $S = 1$ the atoms repel one another (Fig. 15). The reactions (3.23) and (3.24) are adiabatically unlikely, since the Massey parameter $\zeta = |\varepsilon_{11}| r_2/\hbar v$ is large; here r_2 is the minimum separation of the atoms (distance of closest approach) and v is the collision velocity. Analogously, the ion + ion (3.10), neutral + molecule, and molecule + molecule processes are unlikely, and for this reason we shall ignore them. The cases in which these molecules are in excited vibrational states, when the interatomic separations can be small, are an exception. We shall not study below the complicated reactions in which excited molecules participate, but it should be borne in mind that for $T \sim 1$ eV, when there are many such molecules, these reactions make a con-

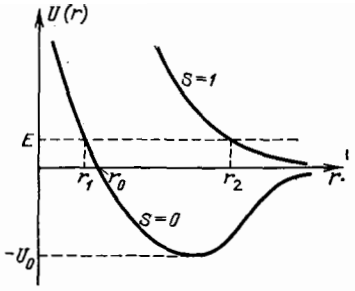

FIG. 15. The potential energy $U(r)$ of motion along the coordinate r in the reaction $(dt\mu)e + X$ (X = D, T, H). S is the total spin of the electrons.

tribution to λ_{form} that is comparable to the contribution of the neutral + neutral mechanism.

For $S = 0$ the stopping distance is short ($r_1 \approx r_0 \approx 0.7$ a.u.), and the nuclei acquire a high velocity ($\sim v_0 = (2U_0/M)^{1/2}$, $M^{-1} = M_{dt\mu}^{-1} + m_X^{-1}$), so that the mu-molecule breaks up with a significant probability. For $T \leqslant 3$ eV the estimate

$$\lambda_b(T) \sim \eta N_x \langle v\sigma_{cap}(v) W_b(v)\rangle, \tag{3.25}$$

where averaging over v is performed, is valid. The factor $\eta = 1/4$ is the probability of motion along an attractive term, corresponding to $S = 0$. In the formula (3.25) σ_{cap} is the cross section for capture of X atoms on a trajectory approaching $(dt\mu)e$, and $W_b(v)$ is the probability that a mu-molecule breaks up in a head-on collision, i.e., with a zero impact parameter and orbital angular momentum. In the case of the van-der-Waals interaction $U(r) = -c/R^6$ $(r \geqslant 3)$, $c = 6.5$,

$$\sigma_{cap}(E) \approx \pi \left(\frac{3}{2}\right)^{2/3} \left(\frac{3c}{E}\right)^{1/3}, \quad E = \frac{1}{2} M v^2. \tag{3.26}$$

The condition $|\varepsilon_{11}| \ll E + U_0$ is satisfied, so that the motion of the nuclei can be approximated by a classical trajectory $r = r(t)$. On the basis of this and the perturbation theory (which is applicable, since $R/r \sim 0.15 \ll 1$) the probability that the mu-molecule breaks up is determined by the expression

$$W_b(E) = \frac{1}{3} \int d^2(\varepsilon_p) |F(\omega)|^2 \frac{d^3p}{(2\pi)^3} = \frac{\beta^2 C_a^2}{\pi x^2} \int_0^\infty x^{1/2} \frac{3x^2 + 2x + 3}{(x+1)^4} |F(\omega)|^2 dx, \tag{3.27}$$

where $\mathbf{d}(\varepsilon_r)$ is the transition dipole moment of the mu-molecule,

$$F(\omega) = \int_{-\infty}^{\infty} F(t) e^{-i\omega t} dt, \quad F(t) = -\frac{dU(t)}{dr}, \quad r = r(t).$$

We shall approximate $U(r)$ by the Morse potential $U(r) = U_0(e^{-2\alpha x} - 2e^{-\alpha x})$, where $x = r - \rho_0$, $\rho_0 = 1.4$, $U_0 = 4.5$ eV $= 0.17$, $\alpha = 1.1$ (here and below we omit the reference to atomic units). The nuclei move according to the law

$$t = \frac{1}{\alpha V} \ln \frac{1+\tau}{1-\tau}, \quad \tau = \left(\frac{e^{\alpha x} - z_-}{e^{\alpha x} + z_+}\right)^{1/2}, \quad z_\pm = (y^2 + y)^{1/2} \pm y, \quad y = \frac{U_0}{E}.$$

From here we obtain

$$F(\omega) = \frac{2\pi M\omega}{\alpha} \frac{\operatorname{ch}(2\xi\Psi)}{\operatorname{sh}(\pi\xi)}, \tag{3.28}$$
$$\Psi = \operatorname{arctg}[y^{1/2} + (1+y)^{1/2}], \quad \xi = \frac{\omega}{\alpha v}.$$

We shall study an important limiting case of the formula (3.28):

$$F(\omega) \approx \frac{\pi M\omega}{\alpha \operatorname{sh}(\pi\xi/2)}, \quad y \ll 1. \tag{3.29}$$

The expression (3.29) is identical to $F(\omega)$ for the potential $U = U_0 \exp(-2\alpha x)$. From here we conclude that for $y \ll 1$ the region near the turning point $r = r_1$ makes the main contribution to $F(\omega)$ (see Fig. 15). In this region, however, the Morse potential is inapplicable, so that we shall approximate $U(r)$ by the more accurate expression $U(r) = r^{-1} - r_0^{-1}$, for which

$$F(\omega) = P_0 E_0, \quad P_0 = \pi\omega(\tilde{v})^{-2} H_{i\nu}^{(1)}(i\nu), \quad E_0 = e^{-2\pi\nu}, \tag{3.30}$$
$$\nu = \frac{\omega}{M\tilde{v}^3}, \quad \tilde{v}^2 = v^2 + \frac{2}{r_0 M}.$$

In what follows we shall use for the exponential factor E_0 the more accurate expression[5,11]

$$E_0 = \exp \operatorname{Im} \int (K(r) - K'(r))\, dr \approx \exp(-\omega M^{1/2} \tau(E)),$$
$$\tau(E) = \int (2(U(r) - E))^{-1/2} dr, \tag{3.31}$$

where $U(r)$ is the exact potential energy of the atoms. In the formula (3.31) the relation $\omega \sim |\varepsilon_{11}| \ll E + U_0$ was used and the following notation was introduced: $K(r) = [2M(E-U)]^{-1/2}$, $K'(r) = [2M(E'-U)]^{1/2}$, $E' = E - \omega$. The values of $\tau(E)$ are presented in Ref. 5. The computational results of Refs. 114 and 115 were used for $U(r)$.

So, for $E \sim U_0$ the probability $W_b(E)$ that the mu-molecule breaks up is determined by the expressions (3.27), (3.30), and (3.31), while for low energies $E \leqslant U_0$ the breakup probability is given by the expressions (3.27) and (3.28). The values of $W_b(E)$ and $\lambda_b(E) = \eta N_0 v \sigma_{cap}(v) W_b(E)$ are presented in Figs. 16 and 17. For $E \sim U_0$ interpolation was performed. For $E \geqslant 0.5$ a.u. the formula (3.27) gives the meaningless result $W_b \geqslant 1$, i.e., the perturbation theory is no longer applicable. In this case, in reality, $W_b \approx 1$.

According to Eqs. (3.13) and (3.25) the rate of formation of mu-molecules by the neutral + neutral mechanism (3.11) is determined by the expressions

$$\lambda_{form}(T) = \alpha_{dis}^2 \varphi^2 C_d \lambda_{form}^{(0)}, \tag{3.32}$$
$$\lambda_{form}^{(0)} = 3N_0 \left(\frac{2\pi}{\mu_a T}\right)^{3/2} e^{|\varepsilon_{11}|/T} \langle \lambda_b(E)\rangle,$$

where α_{dis} is the probability that the atom is not a constitutent of the molecule (degree of dissociation), i.e., the density of atoms is equal to $\alpha_{dis} N = \alpha_{dis} N_0 \varphi$. An interesting feature of the mechanism (3.11) is that because $W_b(E)$ increases rapidly already for $T \leqslant 1$ eV collisions with higher energy $E \sim 10$ eV make the main contribution to $\lambda_b(T)$ and hence to $\lambda_{form}(T)$ also.

The rate of formation of mu-molecules by the ion + neutral mechanism (3.8) and (3.9) can be calculated

analogously. It can be written in the form

$$\lambda_{\text{form}}(T) = \alpha_i (1 - \alpha_н) \varphi^2 C_d \lambda^{(0)}_{\text{form}}(T), \tag{3.33}$$

$$\lambda^{(0)}_{\text{form}}(T) = 6N_0 \left(\frac{2\pi}{\mu_a T}\right)^{3/2} \langle \lambda_b(E) \rangle, \tag{3.34}$$

where $\lambda_p(E) \sim \eta N_0 v \sigma_{\text{cap}}(v) W_b(E)$, $\eta = 1/2$ is the probability of motion along an attractive g-term, and $\sigma_{\text{cap}}(v) = 2\pi v^{-1}(\alpha/M)^{1/2}$ is the cross section for capture by polarization forces $U(r) = -\alpha/(2r^4)$, $\alpha = 4.5$. An additional factor of two, which accounts for the possibility of formation of mu-molecules in the two reactions (3.8) and (3.9), was introduced into the formula (3.33). The values of $\tau(E)$, corresponding to an H_2^+ ion are presented in Ref. 5. The potential energy $U(r)$ ($1s\sigma$ term of the H_2^+ ion) was taken from Ref. 16. The probability $W_b(E)$ and the rate of break-up of mu-molecules $\lambda_b(E)$ are presented in Figs. 16 and 17.

The reduced rates $\lambda^{(0)}_{\text{form}}(T)$ for the above-studied mechanisms of formation of mu-molecules are presented in Fig. 18.

Figure 19 shows the observed rate of the neutral + neutral process, calculated from Eqs. (3.12), (3.13), and (3.32), for different φ. The following well-known expression was used for the degree of dissociation:

$$\alpha_{\text{dis}} = [1 + K_д(1 + \alpha_д)]^{-1/2}, \tag{3.35}$$

$$K_{\text{dis}} = \pi^{3/2}\rho_0^2 N_0 \varphi \left(\frac{2T}{K}\right)^{1/2} e^{D/T},$$

where $D \approx 4.5$ eV is the dissociation energy, $\rho_0 = 14$ a.u., and $K = 0.62$ a.u. is the "rigidity" of the molecule. For $\rho \approx \rho_0$ $U(\rho) \approx K(\rho - \rho_0)^2/2$. Vesman's mechanism (see Figs. 2 and 3) and the ion-neutral and electronic mechanisms are activated to the left and right of the maximum of $\lambda_{dt\mu}$ in Fig. 19. From here we conclude, in particular, that for $\varphi \sim 5$ and $T \leqslant 2$ eV $\lambda_{dt\mu} \geqslant 2 \times 10^9$, and the maximum rate $\lambda_{dt\mu} \sim 10^{19}$ is obtained for $T \sim 0.3$ eV.[5-7]

In concluding this section we shall discuss muon catalysis in deuterium. In the case of $dd\mu$-molecules the most important mechanism is the neutral + neutral mechanism, for which $\lambda_d = 0.8 \cdot 10^9 \varphi \alpha_{\text{dis}}^2$,[5]

$$\tilde{\lambda}_{dd\mu} \approx \frac{4.7 \cdot 10^5 \varphi^2 \alpha_d^2}{T^{3/2}(1 + 1.7\varphi\alpha_d^2)} e^{1.97/T}, \tag{3.36}$$

where T is given in eV. from Eqs. (3.35) and (3.36) we conclude that under equilibrium conditions the rate $\lambda_{dd\mu}$ is low; this is explained by the smallness of the rate λ_f^{dd} of the nuclear reaction at equilibrium. To achieve $\lambda_{dd\mu} \sim 10^9$ it is necessary to create nonequilibrium conditions with high degree of dissociation of the molecules. In particular, for $\varphi = 5$ and $T = 0.4$ eV it is necessary that $\alpha_{\text{dis}} \geqslant 0.1$ (at equilibrium $\alpha_{\text{dis}} \sim 2 \times 10^{-3}$). We note, however, that even if it were possible to create such conditions, muon catalysis in deuterium is not promising because of the high initial sticking probability in deuterium (2.10).

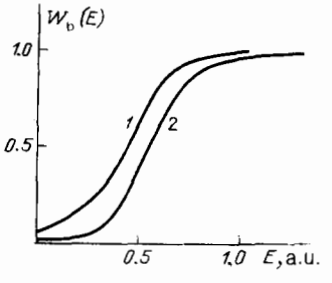

FIG. 16. The break-up probability $W_b(E)$ of the mu-molecules $dt\mu$ for the mechanisms (3.11) (*1*) and (3.8) and (3.9) (*2*).

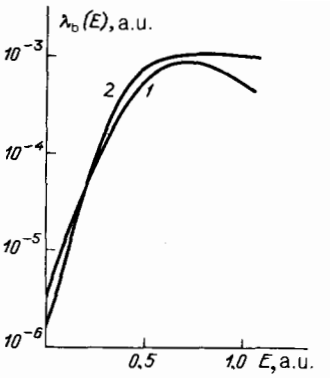

FIG. 17. The break-up rate $\lambda_b(E)$ of the mu-molecules $dt\mu$ for the mechanisms (3.11) (*1*) and (3.8) and (3.9) (*2*) (1 a.u. $= 4.16 \times 10^{16}$ s^{-1}).

3.3. Probability of muon shakeoff from $\alpha\mu$ ions in plasma

As the plasma temperature increases the stopping power $\varkappa$ of the plasma decreases,[117,118] so that according to Eq. (2.13) the shakeoff probability increases. For a fully ionized plasma[118] ($e = \hbar = m_e = 1$)

$$\varkappa(E) = -4\pi\Lambda(v)\frac{d\Psi(v)}{dv}, \tag{3.37}$$

$$\Psi(v) = \int \frac{f(\mathbf{v}_e)}{|\mathbf{v} - \mathbf{v}_e|} d^3v_e,$$

where $f(\mathbf{v}_e)$ is the electron velocity distribution function, $\int f(\mathbf{v}_e) d^3\mathbf{v}_e = 1$, $\Lambda(v) = \ln(2r_0/e_0^{1/2})$, $e_0 = 2.718...$ The expression (3.37) is most simply derived starting from Rutherford's formula, and calculating in the rest system of the $\alpha\mu$ ion the momentum transferred to the ion per unit time by the electrons.

Since $f(\mathbf{v}_e)$ is isotropic, Eq. (3.37) can be represented in the form

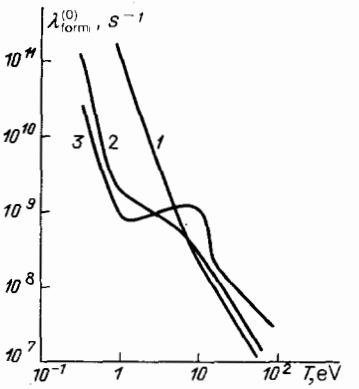

FIG. 18. The reduced formation rates $\lambda^{(0)}_{\text{form}}$ of the mu-molecules $dt\mu$ in triple collisions. The curves *1–3* correspond to the electronic mechanism (3.6) and (3.7), the neutral + neutral mechanism (3.11), and the total reaction rate (3.8) and (3.9), respectively.

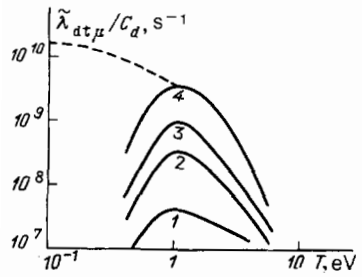

FIG. 19. The effective (observed) formation rate $\lambda_{dt\mu}$ of the mu-molecules $dt\mu$ by the mechanism neutral + neutral (3.11). $\varphi = 0.2$ (*1*), 1 (*2*), 2(*3*), and 5(*4*). The dashed curve corresponds to Vesman's mechanism for $\varphi = 5$ (see Fig. 2).

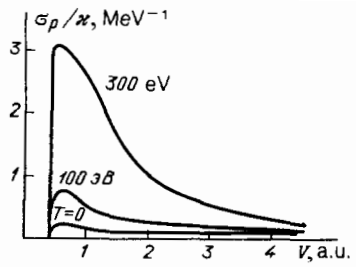

FIG. 21. The dependence of the quantity $\delta = \sigma_b(E)/\varkappa$ from Eq. (2.13) on the velocity of the $\alpha\mu$ ions (the numbers on the curves indicate the plasma temperature).

$$\varkappa(E) = 16\pi^2\Lambda(v)\,v^{-2}\int_0^v v_e^2 f(v_e)\,dv_e = 4\pi\Lambda(v)\,v^{-2}\mu\left(\frac{v}{(2T)^{1/2}}\right), \tag{3.38}$$

where

$$\mu(x) = 4\pi^{-1/2}\int_0^x y^2 e^{-y^2} dy.$$

From Eq. (3.38) we conclude that because of the specific nature of the Coulomb interaction, only electrons with $v_e < v$ make a nonzero contribution to $\varkappa$. Therefore, for a sufficiently high plasma temperature ($T \geqslant 100$ eV), when the thermal velocity of the electrons is high ($v_{Te} \geqslant v$), the stopping of the $\alpha\mu$ ions drops appreciably (Fig. 20).

Figure 21 shows a plot of the quantity $\delta(E)$ from the expression (2.13) as a function of the energy of the $\alpha\mu$ ion. The cross section σ_b corresponds to the curve 2 in Fig. 14. It is obvious that as the plasma temperature increases the muons are shaken off primarily at the end of the stopping path. Since in this case $\sigma_i \ll \sigma_{ct}$, the charge-transfer process (2.4) has the highest probability (~ 0.9), i.e., the muon immediately transfers from the $\alpha\mu$ ion to the nuclei of the DT mixture, bypassing the state in which a mesic atom is formed and subsequently deexcited. These results will also remain valid for the curve 1 (see Fig. 14).

The muon shakeoff probability R_0 in a plasma, calculated in Ref. 6 from Eqs. (2.12) and (3.38) with the cross section 2 (see Fig. 14), is presented in Figs. 22 and 23. We note that in a plasma the process of step ionization $(\alpha\mu)_{1s} \to (\alpha\mu)^* \to \alpha + \mu$ is much more important than in a molecular medium.[6]

4. MUON CATALYSIS OF NUCLEAR FUSION REACTIONS IN A NONUNIFORM DT PLASMA

4.1. General scheme of the processes. The effective sticking coefficient

As one can see from Figs. 19, 22, and 23, the number of cycles X_c cannot be appreciably increased in a uniform plasma, because there does not exist a temperature interval in which ω_s and $1/\lambda_{dt\mu}$ are small simultaneously.

If the hot ($T \geqslant 100$ eV) deuterium plasma contains comparatively cold dense drops of DT mixture, in which $T < 2$ eV, $\varphi \equiv \varphi_m \geqslant 1$, $C_t \sim 0.1$–0.3, then in such a nonuniform plasma it is possible to achieve values of X_c that are an order of magnitude larger than in the case of a molecular DT mixture,[5,7] i.e., up to $X_c \sim 1000$–1500.[7] Here and below φ_m is the density of the matter in drops.

For drop diameter $d = 2R$ less than or of the order of the stopping distance of $\alpha\mu$ ions in a molecular DT mixture $L_{\alpha\mu}$ (cm) $\sim 0.03/\varphi_m$, nuclear reactions occur in the drops and the $\alpha\mu$ ions are stopped in the plasma. As was shown in the preceding section, for $\alpha\mu$-ion energies $\leqslant 0.5$ MeV muon shakeoff in a plasma occurs primarily at the end of the stopping path. As $\alpha\mu$ ions move through the molecular matter of a drop they also lose muons with probability R_m. Based on these remarks, we conclude that the effective sticking coefficient in a nonuniform plasma is equal to

$$\omega_s \approx \omega_s^M(1 - R_0), \tag{4.1}$$

where $\omega_s^M = \omega_s^0(1 - R_M)$ and R_0 is the shakeoff probability in the case of stopping in a plasma. According to Figs. 22 and 23

$$R_0 \approx 0.6,\ 0.7,\ 0.8,\ 0.87 \tag{4.2}$$

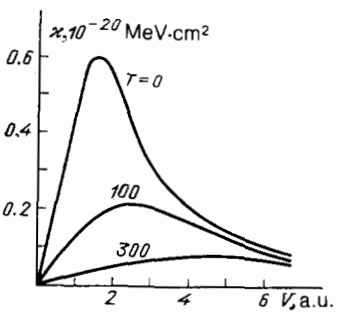

FIG. 20. The effective stopping of $\alpha\mu$ ions as a function of their velocity for different plasma temperatures (indicated in eV on the curves.

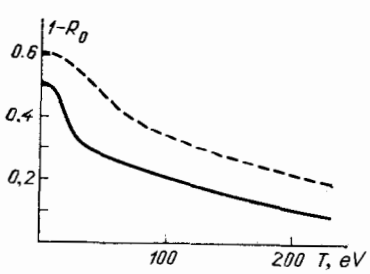

FIG. 22. The temperature dependence of the muon shakeoff probability in a DT plasma with $\varphi = 1$ (solid curve). The broken curve corresponds to the calculation with the cross section 1 (see Fig. 14).

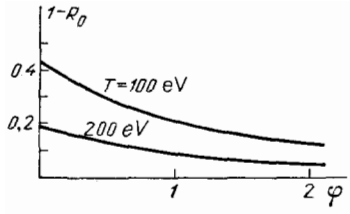

FIG. 23. The muon shakeoff probability as a function of the density of the DT plasma for different plasma temperatures.

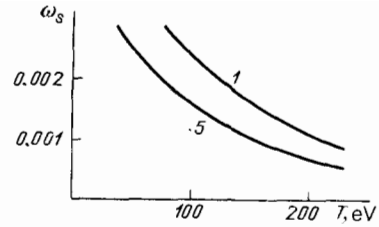

FIG. 24. The effective coefficient of sticking of muons to α particles ($dt\mu \to \mu^4He + n$) in a nonuniform plasma with different density φ_m of matter in drops (indicated by the numbers of the curves).

at temperatures $T = 100$, 1250, 200, and 250 eV, respectively (it was assumed that $\varphi \sim 0.05$–0.1; see below).

Since $d \leqslant 1_{a\mu}$ and for molecular matter $\delta(E) \approx \text{const}$,[89] we find

$$\omega_s^M \sim 0.006 \quad \text{if} \quad \varphi_m \sim 1, \tag{4.3}$$

$$\omega_s^M \sim 0.004 \quad \text{if} \quad \varphi_m \sim 5. \tag{4.4}$$

The decrease in ω_s^m as φ_m increases is explained by step ionization processes.[100-102]

The effective sticking coefficient in a plasma, calculated from the formulas (4.1)–(4.4), is presented in Fig. 24. Comparing Figs. 24 and 13 one can see that the effective muon sticking coefficient in a nonuniform plasma is an order of magnitude lower than in a molecular DT mixture. As we have seen, there are several approximately equivalent reasons for this: 1) the Belyaev-Budker effect (decreases of $\varkappa$ as T increases); 2) high muon shakeoff cross section at low energies owing to nonadiabatic effects; 3) compression of the drop material to $\varphi_m \sim 5$ under the action of the static pressure of the plasma $p \sim 10^6$ atm (see Sec. 4.2); 4) step ionization of $\alpha\mu$ ions plays an important role; and, 5) muon shakeoff in the plasma occurs at the end of the stopping path of $\alpha\mu$ ions.

Thus in a nonuniform plasma it is hypothetically possible to achieve $X_c \sim 1/\omega_s \sim (1-2)\cdot 10^3$. This is proved in Secs 4.3 and 4.4.

Once a muon has entered a drop (the mechanisms for reaching the drops are discussed in Secs. 4.3 and 4.4) it catalyzes in it of the order of $1/\omega_s^m$ of nuclear reactions over a time

$$\tau_M \approx (\omega_s^M \lambda_{dt\mu})^{-1} \sim (0.2-1)\times 10^{-7} \text{ s}. \tag{4.5}$$

After this the muon leave the drop as a constituent of an $\alpha\mu$ ion, is freed from the ion with a significant probability R_0 in the plasma, and once again enters a drop.

4.2. Drop lifetime

The number of cycles X_c achievable in a nonuniform plasma depends strongly on the drop evaporation time τ_{evap} (Refs. 5–7 and 106; in the discussion below we follow Ref. 106).

We shall first study the case when the heat flux S_{el} transferred to the drop by the electrons is large compared with the heat flux S_{ph} owing to the bremmstrahlung photons: $S_{ph} \ll S_{el}$. In the case of interest to us, that of a dense plasma, $T_e \approx T_i \equiv T$, $r_D \ll R$, where $R \sim 3\cdot 10^{-3}$ cm is the radius of the drops (see below), the plasma is quasineutral, and the single-fluid-hydrodynamics approximation is applicable (see, for example, Ref. 119). For a sufficiently low plasma temperature [$T \ll 1$ keV (Ref. 106)] quasistationary evaporation is realized. In this regime the heat supplied by the electrons is carried off by the matter evaporated from a drop:

$$\varkappa(T)\frac{dT}{dr} \approx 2C_p JNv, \tag{4.6}$$

$$4\pi r^2 Nv = J = \text{const}; \tag{4.7}$$

here J is the number of nuclei escaping from the surface of a drop per unit time, v is the average velocity of the matter, r is the distance to the center of the drop, N is the density of nuclei, M is the mass of the nuclei, $C_p = 5/2$, $\varkappa(T) = 2\cdot 10^{25}\tilde{T}^{5/2}$ is the electronic thermal conductivity of the plasma (here and below cgs units are employed), and $\tilde{T} = T\,(\text{eV})/100$.

It is well known[119] that for a power-law dependence of $\varkappa(T)$ a heat wave propagates inside the drop (for $T \geqslant 1$ keV $v \sim C_s = (T/M)^{1/2}$, so that the heat wave apparently transforms into a shock wave[106] and the ablation regime is realized), so that $T \approx 0$ for $r < R(t)$, where $R(t)$ is the drop radius which decreases as a result of evaporation; $T = T(r,t) \neq 0$ for $r > R(t)$; $T \to T_0$ as $r \to \infty$, where T_0 is the plasma temperature far from the drop:

$$4\pi R^2(t) N_m \frac{dR}{dt} = -J, \tag{4.8}$$

where N_m is the concentration of nuclei in a drop.

In this connection we note that here and below we shall study the most interesting case, when the drops make up a small fraction of the volume of the plasma and the fraction of matter ω_m in the drops is small: $\omega_m \ll 1$. This condition must be satisfied in order for $\alpha\mu$ ions to stop in the plasma and not in the drops. More accurately, if this condition is satisfied, the terminal point of the path of an $\alpha\mu$ ion, where muons are primarily shaken off in the plasma (see Sec. 3.3), lies inside the plasma and not inside a drop. We assume that the pressure in a drop is balanced ($P_0 = \text{const}$), since under real conditions the growth time of the pressure in the plasma (the time over which the drop enters the plasma or the time in which the plasma is created in an aerosol) is much longer than the characteristic pressure equilibration time $\sim R/c_m$, where c_m is the velocity of sound in a drop.

From Eqs. (4.6)–(4.8) and the boundary condition $T(\infty) = T_0$ we obtain

$$\varkappa(T_0) - \varkappa(T) = \frac{5C_p J}{4\pi r}, \tag{4.9}$$

$$J = \frac{4\pi R}{5C_p}\varkappa(T_0), \tag{4.10}$$

$$\tau_{evap} = \frac{5C_s N_m R^2}{2\varkappa} = \frac{25 N_m R^2}{4\varkappa}, \quad (4.11)$$

where $\varkappa \equiv \varkappa(T_0)$ and $R \equiv R_0$ is the initial radius of a drop. In what follows we shall write T instead of T_0.

In the case of interest to us, that of muon-catalysis in a plasma, the drop diameter must be shorter than the stopping distance of $\alpha\mu$ ions: $N_m R \leqslant 1 \cdot 10^{20}$ cm^{-2}. The pressure in the plasma is high ($P \sim 10^6$ atm), so that the drops are compressed: $N_m \sim 2 \times 10^{23}$ cm^{-3}, i.e., $\varphi_m \sim 5$ (this estimate can be easily obtained starting from the intermolecular interaction law $U \approx U_0 \exp(-2\eta R)$, $U_0 = 250$ eV, $\eta = 0.85$ a.u.).[70] From here and from Eq. (4.11) we obtain

$$R \sim 3 \cdot 10^{-3}, \quad \tau_{evap} \approx \frac{0.7 \cdot 10^{-6}}{\tilde{T}^{5/2}}, \quad (4.12)$$

The physical meaning of the formula (4.11) is as follows. The amount of heat $Q_{el} \sim 4\pi R^2 S_{el}$, where $S_{el} = \varkappa |\nabla T| \sim \varkappa T/R$, arrives at a drop per unit time. The evaporating matter carries off energy $Q_{evap} \sim 2C_p TJ$ per unit time. From the condition of quasistationary equilibrium $Q_{evap} \approx Q_{el}$ we obtain the estimates (4.10) and (4.11). From here it is obvious that taking bremmstrahlung into account

$$\tau_{evap} \approx \frac{25 N_m R^2}{4\left(\varkappa + S_{ph}\frac{R}{T}\right)}, \quad (4.13)$$

where $S_{ph} \approx 10^{21} d_p \varphi^2 \tilde{T}^{1/2}$ and d_p is the characteristic size of the plasma (diameter of the pinch).

We shall discuss the dependence of N, v, and the pressure P on r.[106] For $r = R$, $N = N_m$, $v = 0$, and $P = P_0$. As r increases the density N decreases rapidly to the density of the hot plasma. The velocity v of the matter at first increases, after which, according to Eq. (4.7), it decreases and approaches zero as $r \to \infty$. The pressure at first drops by a small amount; then at $r \sim R$ it increases up to the pressure of the surrounding plasma P. Because of the reactive forces arising as the matter evaporates (ablation effect), the pressure in the drop is much higher than in the plasma:

$$\frac{P_0 - P}{P} \sim 0.01 \tilde{T}^2. \quad (4.14)$$

Some of the bremsstrahlung photons penetrate into the drop, are absorbed in the process of photoionization, and heat up the interior of the drop. The time over which a drop of the radius indicated above is heated up to $T \sim T_m \sim 2$ eV, when mesicmolecules are no longer formed, is of the order of[7]

$$\tau_H \sim 10^{-11} \tilde{T}^{1/4} \varphi^{-2} d_p^{-1} e^{3.7/\tilde{T}^{3/4}}. \quad (4.15)$$

In the derivation of the relation (4.15) the cross section for the photoionization of a hydrogen atom, as presented, for example, in Ref. 120, was employed and the frequency spectrum of the bremsstrahlung photons was taken into account.

The time during which nuclear reactions occur in the drop (the lifetime of a drop), is evidently determined by the expression

$$\tau_{drop} = \min(\tau_{evap}, \tau_H). \quad (4.16)$$

We note that in the region $\varphi \sim 0.05$–0.1, in which X_c is maximum (see below), $\tau_{drop} \approx \tau_{evap}$.

The α-particles produced in the nuclear reactions also heat the drops, leaving in the drops the fraction $\xi \sim 1/2$ of their energy. As the temperature increases up to $\sim T_m$, allowing for the dissociation of the molecules energy ~ 5 eV is expended per atom. From here it is easy to see that not more than $n_f \sim 10^{11}$ fusion reactions can occur in a drop. For this reason, in particular, for drops with $R \sim 3 \times 10^{-3}$ cm, a positive energy balance on fusion reactions only cannot be achieved, i.e., such a nonuniform plasma can serve only as a source of neutrons. It is true that there exists the possibility, which we have not studied in detail, of decreasing ξ by decreasing the radius of the drops. According to Eq. (4.13) τ_{evap} decreases sharply in this case, and this makes the conditions of muon catalysis more stringent.

4.3. Evaporation of drops in a strong magnetic field

Following Ref. 106, we shall calculate τ_{evap} in the magnetic field of a pinch $H \sim 10^6$–10^7 G, in which the electrons are magnetized and the ions are not:

$$\omega_e \tau_e \sim 0{,}3 \tilde{H} \tilde{T}^{3/2} \varphi^{-1} \gg 1, \quad (4.17)$$

$$\omega_i \tau_i \sim 0{,}8 \cdot 10^{-2} \tilde{H} \tilde{T}^{3/2} \varphi^{-1} \ll 1,$$

where ω_e and ω_i are the electron and ion cyclotron frequency τ_e and τ_i are the free flight times, and $\tilde{H} = H(G)/10^7$. According to Eq. (4.14) the evaporating matter introduces a small perturbation in the pressure of the plasma. Since in the pinch Bennet's condition

$$\frac{H^2}{8\pi} \sim 2NT \equiv P \quad (4.18)$$

is satisfied, we conclude that the magnetic field is not distorted much by the evaporating matter: $\mathbf{H}(r) \approx$ const.

In Sec. 4.2 it is shown that for $T \ll 1$ keV the evaporation time can be calculated by analyzing only the quasistationary region, i.e., starting from the equations of balance of particles and energy. These equations, in the presence of a magnetic field, have the form[110,121]

$$\nabla \mathbf{j} = 0, \quad (4.19)$$

$$2C_p T \mathbf{j} = \varkappa_\perp \nabla_\perp T + \varkappa_\parallel \nabla_\parallel T + \frac{5CNT}{2eH^2}[\mathbf{H}\nabla T], \quad (4.20)$$

where $\mathbf{j}$ is the flux density of nuclei, $\varkappa_\parallel \approx \varkappa$, and $\varkappa$ is the thermal conductivity in the absence of a magnetic field (see the preceding section):

$$\varkappa_\perp = \frac{4{,}66NT}{m_e \omega_e^2 \tau_e}, \quad \frac{\varkappa_\perp}{\varkappa_\parallel} \sim (\omega_e \tau_e)^{-2}; \quad (4.21)$$

where the symbols $\parallel$ and $\perp$ in Eqs. (4.20) and (4.21) denote directions parallel (the Z axis) and perpendicular to the magnetic field.

The last term in Eq. (4.20) can be dropped, since it describes the azimuthal nondissipative heat flux, which is not important for our further discussion.

According to Eqs. (4.17), (4.18), and (4.21) $\varkappa_\perp \ll \varkappa_\parallel$, so that it is reasonable to study the case $\varkappa_\perp = 0$ as the zeroth-order approximation. In this approximation $j_\perp = 0$ and $j_\parallel \neq 0$, i.e., the evaporating matter moves in both directions along the Z axis inside a "tube" containing a drop with $T = 0$. In this case there is a unique characteristic length—the length L of the tube, so that $|\nabla T| \sim T_0/L$. As H increases

the effective length L of the tube increases (see below), so that $S_{el} = \varkappa|\nabla T|$ decreases and τ_{evap} increases.

From Eqs. (4.19) and (4.20) there follow the relations (ρ is the distance from the axis of the tube)

$$j_{\parallel} = \varkappa_{\parallel}(2C_pT)^{-1}\frac{\partial T}{\partial z}, \tag{4.22}$$

$$j_{\perp} = \varkappa_{\perp}(2C_pT)^{-1}\frac{\partial T}{\partial \rho}, \tag{4.23}$$

$$\frac{\partial j_{\parallel}}{\partial z} + \frac{1}{\rho}\frac{\partial \rho j_{\perp}}{\partial \rho} = 0. \tag{4.24}$$

$$\frac{\partial}{\partial z}\left(\frac{\varkappa_{\parallel}}{T}\frac{\partial T}{\partial z}\right) + \frac{1}{\rho}\frac{\partial}{\partial \rho}\left(\frac{\rho\varkappa_{\perp}}{T}\frac{\partial T}{\partial \rho}\right) = 0. \tag{4.25}$$

For $|z| \sim L$, where $T \sim T_0/2$, it is obvious that $\partial T/\partial z \sim T/L$ and $\partial T/\partial \rho \sim T/\rho$, so that we obtain from Eqs. (4.22)–(4.25)

$$L' \sim R\left(\frac{\varkappa_{\parallel}}{\varkappa_{\perp}}\right)^{1/2} \gg R, \tag{4.26}$$

$$\frac{j_{\perp}}{j_{\parallel}} \sim \left(\frac{\varkappa_{\perp}}{\varkappa_{\parallel}}\right)^{1/2} \ll 1, \tag{4.27}$$

$$j_{\parallel} \sim j\left(\frac{\varkappa_{\perp}}{\varkappa_{\parallel}}\right)^{1/2} \ll j, \tag{4.28}$$

where $j \sim \varkappa/2C_pR$ is the flux density of the evaporating matter for $H = 0$ (see the preceding section).

One can see from Eqs. (4.21), (4.27), and (4.28) that in a strong magnetic field the evaporation time increases in proportional to H. Combining this result with Eq. (4.13) we obtain the following interpolation expression

$$\tau_{evap} \approx \frac{25N_mR^2}{4[\varkappa + (S_fR/T)]}[1 + (\omega_e\tau_e)^2]^{1/2}. \tag{4.29}$$

Because of the smallness of the Larmor radius of the electrons ($r_H \ll d_p$) the nonuniformity of the magnetic field is not important.

So, it has been shown in this section that a strong magnetic field changes the character of the motion of the evaporating matter. This results in a decrease of the heat flux from the plasma, i.e., the evaporation time increases. Under typical conditions of muon catalysis in plasma (see below) and for the magnetic field from Eq. (4.18) τ_{evap} increases by a factor of ~3–10.

It is interesting that in spite of the anisotropy of the problem the normal component of the current density j_n at the surface of a drop is constant, i.e., the drop remains spherical as it evaporates. This is most simply proved by solving Eq. (4.25) in the simple case $\varkappa_{\perp}(\mathbf{r}) = \text{const}$ and $\varkappa_{\parallel}(\mathbf{r}) = \text{const}$. After redefining the variable $z = z'(\varkappa_{\parallel}/\varkappa_{\perp})^{1/2}$ Eq. (4.25) takes the same form as the Laplace equation describing the field of a charged conducting ellipsoid of revolution.

We mention also that because there exists a plasma layer of evaporating matter between the drop and the plasma the electric floating potential of the drop is close to zero.

4.4. Nonstationary regime of muon catalysis in plasma

In the nonstationary regime[7] (NR below) the fusion reactions stop as the stationary drops evaporate or are heated. In this case the muon enters a drop from the plasma only as a constituent of a mu-atom. The point is that the diffusion coefficient of charged muons D_{μ} in a plasma is small—$\sim (m_{\mu}/m_e)^{1/2}$ times smaller than for electrons, i.e., the electrons reach the drop ~15 times more quickly than do muons. Each time an electron enters a drop it gives to the drop its energy $\sim T$. As a result the drops evaporate before a charged muon can reach them. From here we conclude that a necessary link in muon catalysis in the nonstationary regime is the formation of mesicatoms in the plasma. The rate of this process is determined from Eq. (3.3).

The rate of diffusion of mu-atoms to drops is determined by the expression[7]

$$\lambda_D^a = \min(4\pi D_a N_{\kappa} R,\ \pi R^2 N_{\kappa} v_{mes}) \approx 0.7 \cdot 10^8 \omega_M \tilde{T}^{1/2} \min(1, 10\varphi), \tag{4.30}$$

where $D_a \approx (3N\sigma_{mes})^{-1} v_{mes}$ is the diffusion coefficient of mesicatoms in plasma (Chapman-Enskog approximation), $\sigma_{mes} \sim 0.5 \cdot 10^{-19}$ cm^2 is the cross section for scattering of mesicatoms by nuclei at energies $\sim 3T/2 \geqslant 150$ eV,[28] $v_{mes} \approx 10^7 \tilde{T}^{1/2}$ is the thermal velocity of the mesicatoms, and N_d is the number of drops in 1 cm^3. Equation (4.30) takes into account the fact that for $\varphi \leqslant 0.1$ the range of mesicatoms $(N\sigma_{mes})^{-1}$ is greater than the diameter of the drops.

The number of cycles in the nonstationary regime is determined by the expression[7]

$$X_c = \frac{\lambda_D^a \lambda_{mes}}{\omega_s^M(\lambda_2 - \lambda_1)}\left[\frac{1 - \exp(-\lambda_1\tau_K)}{\lambda_1} - \frac{1 - \exp(-\lambda_2\tau_K)}{\lambda_2}\right], \tag{4.31}$$

where $\lambda_1 = \lambda_0 + (1 - R_0)\lambda_0^3$ and $\lambda_2 = \lambda_0 + \lambda_{mes}$. In deriving Eq. (4.31) we neglected the residence time τ_m (4.5) of the muons in the drops. In the nonstationary regime this time is much shorter than the characteristic times of other processes. The transfer of muons in the process of charge transfer (2.4) (see Sec. 2) was also taken into account. From Eqs. (3.3), (4.1), (4.2), (4.4), (4.15), (4.16), (4.18), and (4.29)–(4.31) we conclude that the maximum number of cycles in the nonstationary regime[6,7]

$$X_c \approx 500 \tag{4.32}$$

is reached under the conditions

$$T \approx 100 \text{ eV}, \quad \omega_M \approx 0.2, \quad \varphi \approx 0.08, \quad d_p \approx 0.1 \text{ cm}. \tag{4.33}$$

The lifetime τ_{pl} of the plasma must be quite long [$\tau_{pl} \geqslant 1.5/\lambda_{12}$, $\lambda_{12} = \min(\lambda_1, \lambda_2)$]. Under the conditions (4.33)

$$\tau_n \geqslant 2 \cdot 10^{-7} \text{ s}. \tag{4.34}$$

The question of the confinement of α particles, $\alpha\mu$ ions, pions, and muons in plasma is analyzed in Sec. 5.4.

4.5. Steady-state regime of muon catalysis in plasma

To increase further X_c it is necessary to reduce ω_s, i.e., the plasma temperature must be increased (see Fig. 24). In the process, the lifetime of the drops τ_{drop} decreases and the number of cycles in the time-dependent regime (4.31) decreases. We shall study the quasi-steady-state regime[7] (QR), when the drops of liquid or solid DT mixture are injected with a high velocity $v_{drop} \sim 10^6$ cm/s (see below) into a plasma or the plasma itself flows through an aerosol. In this case the evaporated drops are replaced by new drops.

It is obvious that the condition

$$\tau_M \leqslant \frac{d_p}{v_{drop}} \tag{4.35}$$

must be satisfied, otherwise the muons, having penetrated into a drop, will be carried out of the region of the pinch together with the drops. For $T\sim 200$ eV and $\varphi\leqslant 0.1$ the range of $\alpha\mu$ ions in plasma ($\geqslant 1$ cm) is greater than the diameter of the pinch $d_p\sim 0.1$ cm and the Larmor radius of their trajectories in the field of the pinch is smaller than the pinch diameter. Therefore, first, the $\alpha\mu$ ions escaping from the drops are confined by the pinch (see below) and, second, the $\alpha\mu$ ions are uniformly mixed throughout the volume of the pinch.

It is also necessary to require that the drops penetrate into the volume of the pinch:

$$\tau_{\text{drop}} \geqslant \frac{d_p}{v_{\text{drop}}}. \tag{4.36}$$

From Eqs. (4.35) and (4.36) there follows the requirement that $\tau_m \leqslant \tau_{\text{drop}}$, whence for $\lambda_{\text{d}t\mu}\sim 10^{10}$ (see Fig. 19) we conclude that $\tau_{\text{drop}}\geqslant 2\cdot 10^{-8}$ s. This limits the possible temperatures of muon catalysis in plasma: $T\leqslant 400$ eV.

Because of the motion of the drops the rate of diffusion of muons and mesic atoms toward the drops acquires the additional term [the relation (4.36) was used]

$$\lambda_{\text{D}}^{\mu} = \pi R^2 N_{\text{K}} v_{\text{drop}} \approx \frac{50 d_p \varphi \omega_M}{\tau_{\text{K}}}. \tag{4.37}$$

In contradistinction to the time-dependent regime, in the quasi-steady-state regime the muons themselves evidently diffuse toward the drops at the rate[5]

$$\lambda_{\text{D}}^{\text{K}} = 4\pi D_{\mu} R N_{\text{K}} \approx 10^6 \omega_{\text{M}} \tilde{T}^{5/2}, \tag{4.38}$$

where D_{μ} is the diffusion coefficient of muons in plasma.

The number of cycles in the quasi-steady-state regime is determined by the expression[7]

$$X_{\text{c}}^{-1} = \omega_{\text{s}}^{\text{M}} (1 - R_0 + \eta)(1 + \gamma), \tag{4.39}$$
$$\eta = \frac{\lambda_0}{\lambda_{\text{D}}^{\text{a}} + \lambda_{\text{D}}^{\text{K}}}\left(1 + \frac{\tau_{\text{M}}}{\tau_{\text{K}}}\right), \quad \gamma = \frac{\lambda_0}{\lambda_{\text{mes}} + \lambda_{\text{D}}^{\mu} + \lambda_{\text{D}}^{\text{K}}}.$$

Comparing Eqs. (3.3) and (4.38) we conclude that for $T\geqslant 200$ eV in the quasi-steady-state regime the muons penetrate into the drops before mu-atoms are formed. Further, for $\varphi\leqslant 0.1$ we have $(1 - R_0)/\eta \sim 70\varphi$, so that for $\varphi\geqslant 0.02$ we can set in Eq. (4.39) $\eta = 0$. For $\varphi\leqslant 0.02$ the number of cycles decreases in proportion to φ.

From Eq. (4.39) and the estimates of the rates and times obtained above there follows the conclusion that in the quasi-steady-state

$$X_{\text{c}}\sim 1000\text{—}1500 \tag{4.40}$$

cycles are achieved[7,160] under the conditions

$$T\sim 200\text{—}250 \text{ eV}, \quad \varphi\sim 0.03\text{—}0.05, \tag{4.41}$$
$$\omega_{\text{M}}\sim 0.1\text{—}0.2, \quad v_{\text{drop}}\sim 10^6\text{—}10^7 \text{ cm/s},$$
$$d_p\sim 0.1\text{—}0.5 \text{ cm}, \quad \tau_{\text{pl}}\leqslant 3\cdot 10^{-7} \text{ s}.$$

Thus the number of cycles achieved in a plasma is an order of magnitude higher than in a molecular DT mixture.

5. POSSIBLE EXPERIMENTS ON DETERMINING THE BASIC CHARACTERISTICS OF MUON CATALYSIS IN PLASMA

Investigations of muon catalysis are currently being conducted by experimental groups at the Joint Institute of Nuclear Research (Dubna), Leningrad Institute of Nuclear Physics (Leningrad), Los Alamos (USA), TRIUMF (Canada), PSI (Switzerland), KEK (Japan), and the Rutherford Laboratory (England). Quite a large number of experiments devoted to this subject have now been performed. The basic results of these investigations are as follows:

a) the effective coefficient of sticking ω_{s} of a muon to charged products of a fusion reaction in a $\text{d}t\mu$ molecule is equal to $(0.45 \pm 0.05)\times 10^{-2}$;

b) the cycle rate of muon catalysis increases as the temperature of the mixture $D_2 + T_2$ increases and is equal to $\sim 1.5\times 10^3 \text{ s}^{-1}$ at $T = 600$ K (the maximum cycle rate has not been established owing to the difficulty of making targets that operate at temperatures of the $D_2 + T_2$ mixture higher than 600 K); and,

c) the number of cycles X_{c} at the temperatures and pressures of the $D_2 + T_2$ mixture which have been studied cannot exceed ~ 200.

The results obtained thus far apparently indicate that this phenomenon cannot be used in practice to produce energy. Nonetheless, the beauty of the physics of muon processes in cold hydrogen will stimulate for along time theoretical physicists as well as experimenters to perform further investigations.

In our view the most promising areas of research are muon catalysis processes in plasma, a completely unstudied and interesting area at the junction point of different sciences.

We shall examine experiments that can be performed in a meson factory with a storage ring (for example, in the meson factory under construction at Troitsk (Institute of Nuclear Research) or on existing accelerators in Los Alamos, KEK, and the Rurtherford Laboratory) using installations—ultrahigh electric power (UHEP) generators[122] - intended for producing plasma with the required parameters [for example, an updated Angara-5-1 module (Troitsk) and high-current electron and ion accelerators]. We shall begin this section with an examination of such installations (we thank S. L. Nedoseev for explaining this question to us).

5.1. Technology of generation and concentration of ultrahigh electric power (UHEP)

The well-developed technology for generating and concentrating ultrahigh electric power (power $W > 10^{12}$ W, rise time of the current pulse $\tau_p\sim 0.1\text{–}0.3$ μs, and energy $E\sim (0.1\text{–}0.5)\times 10^6$ J) is best suited for forming media with pressure $p\sim NT$ on the order of megabars with densities and temperatures in the ranges $10^{19}\leqslant N\leqslant 10^{23}$ cm^{-3} and $1\leqslant T\leqslant 10^3$ eV.

Ultrahigh electric power is generated with the help of megavolt forming lines. The energy carrier that excites the medium can be an electron or ion beam, a high-current self-compressed electric discharge—a Z-pinch ($I\sim 1\text{–}10$ MA), a low-mass liner accelerated by the magnetic field generated by a current, or a flux of $\sim 0.1\text{–}0.3$ keV soft x-rays with $W\sim 10^{12}$ W. Most of these energy carriers are convenient for producing media in the form of long cylinders $1/d\geqslant 10$ (see below).

In the case of narrow pulses applied to the starting condensed medium ($N\sim N_0$) it is entirely possible for heterogeneous states, containing simultaneously hot plasma ($T\sim 10^2$ eV, $N\sim 10^{19}\text{–}10^{21}$ cm^{-3}) and a highly dense "drop" component ($T\sim 0.1$ eV, $N\sim 10^{23}$ cm^{-3}), to form. It

will apparently be possible to vary the ratio of the masses of these components over very wide limits depending on the initial conditions of the experiment and the duration of the process.

Experimental investigations following the program of inertial-confinement thermonuclear fusion based on imploding emitting liners ($E_{rad} \sim 10^5$ J) and based on a deuterium Z-pinch ($Y \sim 10^{12}$ N/pulse) are now being conducted on the Angar-5-1 complex built at OIRT FIAE (Division of Research Reactors and Technology, Branch of the Institute of Atomic Energy).[122] The plasma parameters achieved in the Z-pinches on Angara-5-1

$$T \sim 10^3 \text{ eV}, \quad N_i \geqslant 10^{20} \text{cm}^{-3}, \quad l \sim 1 \text{ cm}, \quad \frac{l}{d} \sim 10$$

meet all the requirements formulated in Sec. 4 and below. The duration of the process is several times shorter than required. The "drop" phase was absent because the jet of deuterium gas was compressed.

In the Angara-5 program it is expected that the complex will be modernized by building a new modular generator for generating ultrahigh electric power with $W \sim 5$ TW in order to increase the total power of the eight-module Angara-5-1 generator up to 40 TW. The new module could become the power base for the experiment on the production of a heterogeneous medium.

To perform experiments in which the target is heated up to $T \sim 1$ eV a high-current electron accelerator of the type Triton (FIAE-Branch of the Institute of Atomic Energy) with the following characteristics can be employed: electron energy ~ 1 MeV, pulse width ~ 30 ns, average current ~ 100 kA, and total electron-beam energy 2 kJ. The proposed experiments are examined in Ref. 107.

5.2. Experiment on determining the cycle rate of muon catalysis for mixture temperatures of ~1 eV

The deuterium-tritium target discussed in Sec. 1.5 is not suitable for performing measurements of $\lambda_{dt\mu}$ in the region $T \sim 0.1$–2 eV and $\varphi \sim 0.1$.–1. Because of the high pressures and temperatures such measurements can be performed only on short-lived targets ($\tau \sim 1\ \mu$s).

The computed rate of formation of muon molecules $dt\mu$ (see Sec. 3.2) exceeds 10^9 s^{-1} for mixture temperatures $T \leqslant 2$ eV. A detailed investigation of these reactions requires measurements of the formation rate of mu-molecules in wide intervals of the temperature and density of the DT mixture ($0.1 < T < 2$ eV, $0.1 \leqslant \varphi \leqslant 1$). To do this it is proposed that a deuterium-tritium target heated with a high-current electron beam up to temperatures of 0.1–2 eV with mixture density $5 \cdot 10^{21} \leqslant N \leqslant 5 \times 10^{22}$ cm^{-3} and a working volume of 0.1–0.5 cm^3 be made. The relative volume concentration of impurities (N_2, O_2, CO_2, etc.) in the D_2T_2 mixture should not exceed 10^{-6}.

We shall list the main processes and indicate their characteristic times. An electron beam entering a frozen or liquid deuterium-tritium target with a volume of the order of 0.1 cm^3 and density $\varphi \sim 1$ uniformly heats it up to a temperature of 1 eV within ~ 30 ns. Then a muon beam (pulse width $\Delta t < 300$ ns, muon energy $E_\mu = 60$ MeV, and the total number of muons per pulse incident on the target $I > 10^3$) from the storage ring of a meson factory or from an accelerator of the type KEK or the accelerator built at the Rutherford Laboratory ($\Delta t \sim 50$ ns, $I \sim 10^4$ on a target area ~ 0.2 cm^2) is passed through the target. Approximately 10^{-3} I muons stop in the volume of the target. These muons in turn generate in fusion reactions $\sim 10^{-3} I \times 10^2 = 10^{-1}$ I neutrons, i.e., for the muon beam intensities presented, of the order of 10^3 neutrons will be generated per muon pulse. For a neutron detection efficiency of $\sim 10\%$, approximately 100 neutrons per pulse will be detected, which is sufficient for obtaining an acceptable statisical sample. The experiment can also be performed using a cold target; this will make it possible to calibrate the apparatus.

We note that the neutron background is generated only when muons stop in the walls of the vessel surrounding the target and it can be easily discriminated.

5.3. Experiment on determining the number of cycles X_c and the effective muon sticking coefficient ω_s for extreme D_2+T_2 mixture densities

In this experiment $\lambda_{dt\mu}$ and X_c are measured in the stationary regime of muon-catalysis with $T \sim 1$ eV and $\varphi \sim 5$. To achieve the indicated density of matter the solid drop or cylinder of DT mixture must be compressed by a Z-pinch on an installation of the Angara-5-1 type. The pressure in the Z-pinch reaches $\sim 10^5$ atm, so that (see Sec. 4.2) the mixture is compressed to $\varphi \sim 5$. The computed effective rate of formation of mu-molecules is presented in Fig. 19.

5.4. Experiment on determining the effective sticking coefficient ω_s and the number of cycles X_c in a nonuniform plasma

To study the dependence of ω_s and X_c on the temperature and density of a nonuniform plasma it is necessary to develop an experimental apparatus in which plasma is heated from 50 to 250 eV in a volume of 0.01–0.03 cm^3 with plasma density $5 \cdot 10^{20} \leqslant N \leqslant 10^{22}$ cm^{-3}. The lifetime of the plasma column is $\geqslant 3 \times 10^{-7}$ s. Plasma ignition must be synchronized with the operation of the storage ring with an accuracy of 5×10^{-8} s.

A plasma column with the indicated parameters (Z-pinch) is produced by compression of a linear, consisting of an assembly of solid deuterium filaments with total mass $\sim 600\ \mu$g and length ~ 1–5 cm, under the action of a current of the order of 3–5 MA flowing through it. A filament ~ 2 cm long and 0.02 cm in diameter consisting of a solid DT mixture with a mass of $100\ \mu$g must be placed at the center of the liner. We note that tritium is contained only in this filament and the total mass of the tritium is ~ 20–$50\ \mu$g.

The mass of the assembly was determined from Bennet's relation $J^2 = \pi c^2 N_i T d_p^2 V_g$, from which the diameter of the pinch is actually found, because J, N_i, and T are given. The current strength $J \sim 3$–5 MA, in particular, is determined from the condition for the pions and muons formed to be confined in the pinch (see below).

At first a preliminary voltage pulse is applied to the central filament. This explodes the filament into $\sim 10^3$ fragments, which form the drops of required size. Next, the main pulse is applied to the liner, accelerating it up to velocity $v \sim 5 \times 10^7$ cm/s. The Z-pinch collapses at the moment the fragments of the filament occupy a cylindrical region of the order of 0.1 cm in diameter. With the collapse, at the center the kinetic energy of the liner is transformed into heat within $3 \cdot 10^{-8}$ s. In this manner a plasma with the required param-

eters is obtained. Next, a proton beam from the storage ring of the meson factor is passed along the axis of the pinch. The pulse width is ~200–300 ns, the number of protons per pulse is $(3–6)\times10^{13}$, and the proton energy is 600 MeV. The Larmor radius of the protons with the indicated energy in the magnetic field of the pinch is greater than the diameter of the pinch, so that the proton beam enters the pinch. We note that the protons do not destroy the drops; they heat the drops by only ~50 K.

The cross section for the production of negative pions in collisions of protons with nuclei at the indicated energy is $\sim2\times10^{-27}$ cm^2, so that $\sim10^9$ negative pions are produced per pulse in a pinch with density $N_i\sim3\times10^{21}$ and length ~3 cm; the pions in turn decay into muons. Because of the smallness of the Larmor radius of the pions and muons in the magnetic field of a pinch with a current of ~5 MA the probability that they will stop in the matter of the pinch is high,[107] as a result of which $\sim10^9$ muons remain in the plasma. To increase the number of muons stopping in the plasma the pinch should have the form of a spindle with the ratio of the length to the greatest diameter

$$\frac{l}{d_p}\geqslant 10. \tag{5.1}$$

Actually, the probability of confinement of a particle created in the Z-pinch depends primarily on the parameter (m is the particle mass, v is the particle velocity, and $\gamma=[1-(v^2/c^2)]^{-1/2}$)

$$\xi=\frac{r_p}{r_H}=\frac{2eJ}{mc^2\gamma v}, \tag{5.2}$$

which is the ratio of the pinch radius r_p to the Larmor radius r_H of the particle orbit. The particles escape primarily from the ends of the pinch. To confine the particles the ratio of the pinch length l to the pinch diameter must be quite large:[107]

$$\frac{l}{d_p}\geqslant 0{,}14e^{(7{,}5/\xi)}. \tag{5.3}$$

From Eqs. (5.2) and (5.3) it follows that under the condition (5.1) the π^- and μ^- mesons produced are confined by the pinch. This conclusion is confirmed by numerical calculations.[107] The required form of the pinch is achieved with a special distribution of the liner mass (light ends).

To obtain a plasma with the above-indicated properties the liner can be compressed with the help of a fast capacitor bank storing 100–200 kJ of energy, $I=3–5$ MA, and $\tau_f=0.6\,\mu$s.[123,124]

This experiment is difficult to perform and requires preliminary investigations. It is necessary to measure the lifetime of the drops in the plasma. The key question in this scheme is the lifetime of the pinch, which must be $>3\times10^{-7}$ s. This time agrees with experiments (see Refs. 125 and 126 and the references cited here), according to which the lifetime of the pinch (i.e., the current in the pinch) $\tau\sim kd_p/c_s$, where $k\sim10–100$ is a dimensionless factor. For the parameters indicated above $\tau\sim0.5–1\,\mu$s, which is greater than the required lifetime of the pinch. We note, however, there is still no final theory explaining such a long lifetime of the pinch.

An important problem is the problem of separating the neutrons ($\sim10^{11}-10^{12}$) produced in the fusion reaction in the mu-molecules $dt\mu$ from the background created by neutrons generated by the pinch itself; the expected number of pinch neutrons at $T\sim100–200$ eV is $10^{10}-10^{11}$.[126,127] We note that this background can be significantly reduced by applying a magnetic field along the axis of the pinch; this field would prevent the development of necks in the pinch.

To measure X_c in the time-dependent regime of muon catalysis (see Sec. 4.5) it is necessary to develop a setup with a pinch moving along an aerosol with a velocity of $10^6–10^7$ cm/s.

CONCLUSIONS

Thus the mechanisms of muon processes in cold hydrogen have, on the whole, been studied. Based on the results obtained it can be concluded[128] that the number of cycles $X_c\sim150$ achieved in traditional muon catalysis is too small for using this phenomena to produce electricity (an opposing view is presented in Ref. 129). In any variant—molecular or plasma—the power generating installation based on muon catalysis is unpromising compared with tokamaks, since it can use only schemes with breeding, which is bad ecologically, not to mention the difficulty of the scheme itself. Another drawback is the large quantity of tritium required in the molecular variant.

With regard to practical applications, muon catalysis can be used as one possibility for producing a powerful pulsed neutron source with intensity $\sim10^{16}-10^{19}$ neutrons per pulse of width $\sim10^{-7}-10^{-8}$ s.[130]

Among applications of the results of the theory and experiments on muon-catalysis in a molecular medium, we call attention, for example, to the possibility of measuring the corrections, associated with the polarization of the e^-e^+ vacuum, to the energy levels of a mu-molecule.[3,4] The most realistic candidate for this is the $dd\mu$ molecule, since in this case the extraneous effects are weakest (see Sec. 1.3) and, as a consequence, the best agreement is achieved between theory and experiment.

Interesting and completely unstudied fields of physical research at the junction point of different sciences open up in the study of the processes occurring when muons stop in plasma, where $X_c\sim1500$ can be achieved (see Secs. 2–5). The possibility of using the sharp temperature dependence of the formation rates of mu-atoms in plasma (see Sec. 3.1) for plasma diagnostics at $T\sim100$ eV is interesting.

It should be noted that the production and investigation of a heterogeneous plasma in Z and θ pinches is also of interest in itself, since the behavior of a nonuniform plasma can elucidate the essence of the physical processes occurring in a pinch as it is formed.

From what was said above it follows that the experimental study of the processes examined above is very important and is undoubtedly of great interest from both the theoretical and practical viewpoints.

APPENDIX: SUCCESSIVELY RECORDED EVENTS IN THE PROCESS OF MULTIPLE MUON CATALYSIS

In the experimental investigation of multiple muon catalysis of fusion reactions of hydrogen isotope nuclei there arises the problem of analyzing the integrated yields and temporal distributions of successively recorded reactions events:

$$\mathrm{d}+\mathrm{d}\begin{cases}\rightarrow \mathrm{t}+p+4\,MeV,\\ \rightarrow {}^3\mathrm{He}+\mathrm{n}+3{,}3\,\mathrm{MeV},\end{cases} \tag{A1}$$

$$\mathrm{t}+\mathrm{t}\rightarrow{}^4\mathrm{He}+2\mathrm{n}+11{,}3\ \mathrm{MeV}, \tag{A2}$$

$$d+t\rightarrow{}^4He+n+17{,}6\ \text{MeV}. \qquad (A3)$$

A characteristic feature of these processes is their multiplicity—the same muon can give rise to many cycles of the indicated reactions. (A cycle is a collection of processes resulting in the fusion reaction of interest, whose products are recorded.) Figure 25 shows the general scheme of multiple muon catalysis. The muon gives rise successively to a periodically repeating chain of processes (cycles), at the end of which the fusion reaction of interest occurs. As a result of the reaction (at the end of the cycle) fusion products form, and the muon itself is freed with probability $(1-\omega)$ and gives rise to a new cycle of muon catalysis. This suggests that if the temporal distributions of the first, second, etc., events are also recorded, then this additional experimental information will make it possible to determine more completely the characteristics of the process of muon catalysis than in the case when only all events are recorded. In this section we shall examine the kinetics of muon catalysis in pure deuterium (Fig. 26), i.e., we shall find analytic expressions for the yields and the temporal distributions of the first, second, etc., events of muon-catalysis reactions recorded with efficiency $\varepsilon < 1$.

The kinetics of muon catalysis in pure deuterium is the simplest case, when the entire process of muon-catalysis is characterized by only two parameters: the formation rate of muonic molecules and the probability that a muon sticks to one of the reaction products, namely, to ^{3}He. We studied the kinetics of muon-catalysis theoretically earlier. We derived expressions for the yields and the temporal distributions of the products of the fusion reactions in muonic molecules. For example, the temporal distribution of acts of catalysis of the reaction, namely, the yield of neutrons from the reaction (A1) (here we neglect the effects associated with the hyperfine structure of the $d\mu$ atom)

$$d\mu+d\rightarrow dd\mu\rightarrow{}^3He+n+\mu \qquad (A4)$$

has the form (in what follows we write, for brevity, λ instead of $\tilde{\lambda}$)

$$\frac{dn}{dt}=\beta\lambda_{dd\mu}\exp\left[-(\lambda_0+\beta\omega_d\lambda_{dd\mu})\,t\right], \qquad (A5)$$

and their average multiplicity

$$\bar{n}=\frac{\beta\lambda_{dd\mu}}{\lambda_0+\beta\omega_d\lambda_{dd\mu}}. \qquad (A6)$$

The expressions (A5) and (A6) are normalized to the number of muons initiating reactions. The derivation of these expressions took into account the fact that the nuclear reaction (d + d) occurs instantaneously, i.e., its rate $\lambda_f^{dd}\gg\lambda_0$, $\lambda_{dd\mu}$.

Under real experimental conditions the products of the

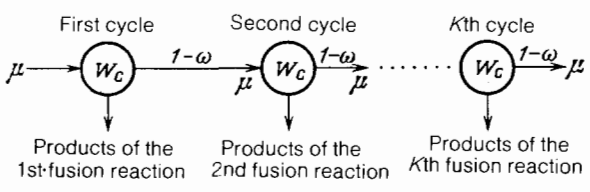

FIG. 25. Diagram of successive cycles of the muon catalysis reaction.

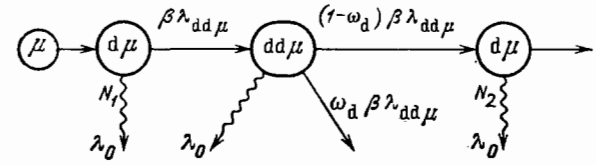

FIG. 26. Diagram of successive muon catalysis of fusion reactions in a $dd\mu$ molecule.

reactions occurring in muon catalysis are recorded with efficiency $\varepsilon < 1$. It is easy to show that the temporal distribution of all (i.e., obtained without introducing additional selection criteria) recorded acts of catalysis will have the form

$$\frac{dn^{exp}}{dt}=\varepsilon\beta\lambda_{dd\mu}\exp\left[-(\lambda_0+\beta\omega_d\lambda_{dd\mu})\,t\right], \qquad (A7)$$

and their yield ("experimental multiplicity") will be

$$\bar{n}^{exp}=\frac{\varepsilon\beta\lambda_{dd\mu}}{\lambda_0+\beta\omega_d\lambda_{dd\mu}}, \qquad (A8)$$

i.e., they are identical (to within a normalization factor) to the "physical" expressions (A5) and (A6). As one can see from the expression (A7) and (A8), their use in analysis of experimental data will make it possible to find only the products $\beta\omega_d\lambda_{dd\mu}$ and $\beta\varepsilon\lambda_{dd\mu}$, i.e., to determine ω_d and $\beta\lambda_{dd\mu}$ independently it is necessary to know the detection efficiency ε. The direct determination of ε is a difficult problem. As a rule, in such cases the efficiency is calculated by the Monte Carlo method taking into account the parameters of the process of interest and the geometry of the experimental apparatus. We shall show that to determine ω_d and $\beta\lambda_{dd\mu}$ independently it is sufficient to use only data on the yield and the temporal distribution of the "first" and on the yield of the "second" detected neutrons.

The scheme of successive muon catalysis of the reaction (A1) is presented in Fig. 26. The muon freed in the reaction (A4) forms instantaneously ($\lambda_a\gg\lambda_0$, $\lambda_{dd\mu}$) a $d\mu$ atom and then, with the rate $\beta\lambda_{dd\mu}$, a $dd\mu$ molecule. We denote by Ni the number of $d\mu$ atoms remaining up to the ith act of the fusion reaction. The functions satisfy the system of equations

$$\begin{aligned}
&\frac{dN_1}{dt}=-\lambda N_1,\\
&\frac{dN_2}{dt}=-\lambda N_2+(1-\omega_d)\,\beta\lambda_{dd\mu}N_1,\\
&\cdots\cdots\cdots\cdots\cdots\\
&\frac{dN_i}{dt}=-\lambda N_i+(1-\omega_d)\,\beta\lambda_{dd\mu}N_{i-1},
\end{aligned}$$

where $\lambda\equiv\lambda_0+\beta\lambda_{dd\mu}$. The solutions of this system for the boundary condition $N_i(0)=1$ have the form

$$N_i(t)=[(1-\omega_d)\,\beta\lambda_{dd\mu}]^{i-1}t^{i-1}e^{-\lambda t}\frac{1}{(i-1)!}$$

Since the rate of the reaction (A1) is $\lambda_f^{dd}\gg\lambda_{dd\mu}$, λ_0 the temporal distribution of the neutrons from the ith act is

$$f(t)=\frac{dn_i}{dt}=\beta\lambda_{dd\mu}N_i(t)=\beta^i\lambda_{dd\mu}^i(1-\omega_d)^{i-1}e^{-\lambda t}[(i-1)!]^{-1}. \qquad (A9)$$

The yield of neutrons from the ith act is

$$n_i=\int_0^\infty f_i(t)\,dt=(1-\omega_d)^{i-1}\left(\frac{\lambda_{dd\mu}}{\lambda}\right)^i. \qquad (A10)$$

With the help of the expression (A10) it is also possible to obtain relations for the yields of single, double, etc., reactions:

$$n(i) = n_i - n_{i-1} = (1-\omega_d)^{i-1}\beta^i\lambda_{dd\mu}^i(\lambda_0+\omega_d\lambda_{dd\mu})\frac{1}{\lambda^{i+1}}. \quad (A11)$$

It is easy to show that the temporal distribution of all atoms is identical to the expression (A5), and the yield of all acts of fusion reactions

$$n = \sum_{i=1}^{\infty} n_i = \int_0^{\infty} n(t)\,dt = \frac{\beta\lambda_{dd\mu}}{\lambda_0+\beta\omega_d\lambda_{dd\mu}}$$

is identical to the expression (A6).

We shall now take into account the finite detection efficiency $\varepsilon < 1$. Here there arises the possibility that the neutron from the ith act of catalysis will be recorded first under the condition that the neutrons from the preceding $i-1$ reaction acts will not be recorded. Taking this into account, the temporal distribution of the first detected neutrons can be represented as a sum:

$$\begin{aligned} f_1^{exp}(t) &= \varepsilon f_1(t) + (1-\varepsilon)\{\varepsilon f_2(t) + (1-\varepsilon)[\varepsilon f_3(t) + \dots]\} \\ &= \varepsilon[f_1(t) + (1-\varepsilon)f_2(t) + (1-\varepsilon)^2 f_3(t) + \dots] \\ &= \varepsilon\sum_{i=1}^{\infty}(1-\varepsilon)^{i-1}f_i(t). \end{aligned} \quad (A12)$$

Substituting here the expression (A9) for $f_i(t)$ we obtain in explicit form

$$f_1^{exp}(t) = \varepsilon\beta\lambda_{dd\mu}\exp\{-[\lambda_0+(\varepsilon+\omega_d-\varepsilon\omega_d)\beta\lambda_{dd\mu}]t\}. \quad (A13)$$

The yield of the first detected neutrons is

$$n_1^{exp} = \int_0^{\infty} f_1^{exp}(t)\,dt = \varepsilon\beta\lambda_{dd\mu}[\lambda_0+(\varepsilon+\omega_d-\varepsilon\omega_d)\beta\lambda_{dd\mu}]^{-1}. \quad (A14)$$

The same expression can be derived with the help of the formula (A6), if in it n_i from the relation (A11) is substituted for $f_i(t)$.

In deriving an expression for the yield of the second detected reaction acts it is necessary to take into account the fact that neutrons from the following pairs of catalysis acts can be detected:

$$(1,2),\ (1,3),\dots(1,i);\ (2,3),\ (2,4),\dots,\ (2,i);\dots$$

Correspondingly the yield is

$$\begin{aligned} n_2^{exp} &= \varepsilon^2 n_2 + \varepsilon^2(1-\varepsilon)n_3 + \dots \\ &\quad + \varepsilon^2(1-\varepsilon)^{i-2}n_i + \dots + \varepsilon^2(1-\varepsilon)n_3 + \dots \\ &= \varepsilon^2[n_2 + 2(1-\varepsilon)n_3 + 3(1-\varepsilon)^2 n_4 + \dots \\ &\quad + (i-1)(1-\varepsilon)^{i-2}n_i + \dots] \\ &= \varepsilon^2(1-\omega_d)\left(\frac{\lambda_{dd\mu}}{\lambda}\right)^2 \\ &\quad \sum[(1-\varepsilon)(1-\omega_d)^{-1}\left(\frac{\beta\lambda_{dd\mu}}{\lambda}\right)^{-1}]^{i-2}(i-1) \\ &= \varepsilon^2\beta^2\lambda_{dd\mu}^2(1-\omega_d)[\lambda_0+(\varepsilon+\omega_d-\varepsilon\omega_d)\beta\lambda_{dd\mu}]^{-2}. \end{aligned} \quad (A15)$$

We note that the expression (A15) can also be derived with the help of a relation analogous to (A11) for $i=1$

$$n_1^{exp} - n_2^{exp} = n^{exp}(1), \quad (A16)$$

where $n^{exp}(1)$ is the yield of single detected events. Indeed, the formula for the yield of m events can be written in the form

$$n^{exp}(m) = \sum_{i=1}^{\infty} n(i)P_i^m, \quad (A17)$$

where P_i^m is the binomial probability of detecting m out of i events

$$P_i^m = C_i^m \cdot \varepsilon^m(1-\varepsilon)^{i-m}, \quad (A18)$$

and C_i^m are the binomial coefficients.

Substituting into the formula (A17) the expression for $n(i)$ from (A11) and the expression (A18) for P_i^m we obtain

$$n^{exp}(m) = \varepsilon^m(1-\omega_d)^{m-1}\frac{(\lambda_0+\omega_d\beta\lambda_{dd\mu})\beta\lambda_{dd\mu}^m}{[\lambda_0+(\varepsilon+\omega_d-\varepsilon\omega_d)\beta\lambda_{dd\mu}]^{m+1}}. \quad (A19)$$

For $m=1$

$$n^{exp}(1) = \frac{\varepsilon\beta\lambda_{dd\mu}(\lambda_0+\omega_d\beta\lambda_{dd\mu})}{[\lambda_0+(\varepsilon+\omega_d-\varepsilon\omega_d)\beta\lambda_{dd\mu}]^2} \quad (A20)$$

Substituting into the formula (A16) the expressions (A20) and (A14) we obtain the relation (A15) for n_2^{exp}.

The expressions (A13)–(A15) and (A19) are sufficient for analysis of experimental data for purposes of determining independently ω_d and $\beta\lambda_{dd\mu}$. The following algorithm is most convenient.

1. The quantity

$$a \equiv \lambda_0 + (\omega_d + \varepsilon - \varepsilon\omega_d)\beta\lambda_{dd\mu}$$

is determined from analysis of the temporal distribution of the first recorded events (A13).

2. From the measured values of a, n_1^{exp}, and n_2^{exp}

$$b \equiv \lambda_0 + \omega_d\beta\lambda_{dd\mu}.$$

is determined with the help of the relations $n_1^{exp}(\lambda_0+\omega_d\beta\lambda_{dd\mu})/a = n^{exp}(1) = n_1^{exp} - n_2^{exp}$.

3. The quantity ω_d is determined from the relation

$$1-\omega_d = \frac{n_2^{exp}}{(n_1^{exp})^2}$$

4. The quantity $\beta\lambda_{dd\mu}$ is determined by substituting ω_d obtained in step 3 into the expression for the known quantity $b = \lambda_0 + \omega d\beta\lambda_{dd\mu}$.

Thus the quantity sought ω_d and $\beta\lambda_{dd\mu}$ can be determined without using the detection efficiency. Obviously, the detection efficiency itself can also be determined starting from the foregoing analysis; this is of interest in itself. This method of determining the muonic-molecular constants of catalysis in deuterium was employed to analyze the experimental data obtained in Ref. 132.

[1] S. S. Gershteĭn and Ya. B. Zel'dovich, Usp. Fiz. Nauk **71**, 581 (1960) [Sov. Phys. Usp. 3(43), 593 (1961)].
[2] S. S. Gersteĭn and L. I. Ponomarev, in *Muon Physics*, Eds. V. W. Hughes and C. S. Wu, Academic Press, London, 1975, Vol. 3, p. 141.
[3] L. Bracci and G. Fiorentini, Phys. Rep. **86**, 175 (1982).
[4] L. I. Ponomarev and G. Fiorentini, Muon Catal. Fusion **1**, 3 (1987).
[5] L. I. Men'shikov, *Muon catalysis in dense low-temperature plasma*, (in

Russian), Preprint No. 4589/2, Institute of Atomic Energy, Moscow, 1988.
[6]L. I. Men'shikov and V. A. Shakirov, Zh. Eksp. Teor. Fiz. **95**, 458 (1989) [Sov. Phys. JETP **68**, 258 (1989)].
[7]L. I. Men'shikov, Fiz. Plazmy **16**, 386 (1990) [Sov. J. Plasma Phys.].
[8]F. C. Frank, Nature **160**, 525 (1947).
[9]G. M. G. Lattes, G. P. S. Occhialini, and C. F. Powell, *ibid.*, 453.
[10]L. W. Alvarez, H. Brander, and F. S. Crawford, Phys. Rev. **105**, 1127 (1957).
[11]L. D. Landau and E. M. Lifshitz, *Quantum Mechanics*, Pergamon Press, N.Y., 1977. [Russ. original, Nauka, M., 1974].
[12]H. A. Bethe, Ann. Phys. (Leipzig) **5**, 325 (1930).
[13]A. S. Wightman, Phys. Rev. 77, 521 (1950).
[14]V. V. Balashov, V. K. Dolinov, and G. Ya. Korenman, Muon Catal. Fusion **2**, 105 (1988).
[15]H. A. Bethe and M. Leon, Phys. Rev. **127**, 636 (1962).
[16]L. I. Men'shikov and L. I. Ponomarev, Pis'ma Zh. Eksp. Teor. Fiz. **39**, 542 (1984) [JETP Lett. **39**, 663 (1984)].
[17]L. I. Men'shikov and L. I. Ponomarev, *Quasiresonance charge exchange between mesoatoms of hydrogen isotopes in excited states* (in Russian) Preprint No. 4006/12, Institute of Atomic Energy, Moscow (1984).
[18]L. I. Men'shikov and L. I. Ponomarev, Z. Phys. Kl D **2**, 1 (1986).
[19]L. I. Men'shikov and L. I. Ponomarev, Pis'ma Zh. Eksp. Teor. Fiz. **42**, 12 (1985) [JETP Lett. **42**, 13 (1985)].
[20]A. P. Bukhvostov and N. P. Popov, Zh. Eksp. Teor. Fiz. **82**, 23 (1982) [Sov. Phys. JETP. **55**, 13 (1982)].
[21]L. I. Men'shikov, *Kinetics of mesoatoms of hydrogen isotopes in excited states*, (in Russian), Preprint No. 4531/2, Institute of Atomic Energy, Moscow (1987).
[22]L. I. Men'shikov, Muon Catal. Fusion **2**, 173 (1988).
[23]A. V. Kravtsov, A. Yu. Mayorov, A. I. Mikhailov, N. P. Popov, and E. A. Soloviev, Quasiresonant charge—exchange of the excited mesic hydrogen in the mixture of hydrogen isotopes (in Russian), Preprint No. 1272, Leningrad Institute of Nuclear Research, Leningrad, 1987.
[24]E. A. Solov'ev, Yad. Fiz. **43**, 784 (1986) (*sic*).
[25]W. H. Breunlich, M. Cargenelli, J. Marton, and P. Kammel, *Muon catalyzed fusion*, Preprint No. 21174, Lawrence Laboratory, University of California, Berkely, 1986.
[26]S. E. Jones, A. N. Anderson, and A. J. Gaffrey, Phys. Rev. Lett. **56**, 588 (1986).
[27]S. I. Vinitskiĭ and L. I. Ponomarev, Fiz. Elem. Chastits At. Yadra **13**, 1336 (1982) [Sov. J. Part. Nucl. **13**, 557 (1982)].
[28]M. Bubak and M. P. Faifman, *Cross section for hydrogen muonic atomic processes in two-level approximation of the adiabatic framework*, Preprint JINR E4-87-464, Dubna (1987).
[29]A. V. Matveenko and L. I. Ponomarev, Zh. Eksp. Teor. Fiz. **59**, 1953 (1970) (*sic*).
[30]V. B. Belyaev, S. S. Gershtein, V. N. Zakhar'ev, and S. P. Lomnev, *ibid.* **37**, 1652 (1959) [Sov. Phys. JETP **10**, 1171 (1959)].
[31]A. V. Kravtsov, A. I. Mikhaĭlov, and N. P. Popov, *Muonic atoms scattering on atoms*, Preprint No. 1037, Leningrad Institute of Nuclear Physics of the Academy of Sciences of the USSR, Leningrad (1985).
[32]A. Adamczak, V. S. Melezhik, and L. I. Men'shikov, Z. Phys. K1. D **4**, 153 (1986).
[33]A. Adamczak and V. S. Melezhik, Phys. Lett. A **118**, 181 (1986).
[34]A. Adamczak, *Mesic atomic scattering on diatomic molecules*, Preprint No. 964, Uppsala University, Uppsala, 1988.
[35]V. S. Melezhik, Muon Catal. Fusion **1**, 205 (1987).
[36]L. I. Men'shikov, *Scattering of mesoatoms of hydrogen isotopes by hydrogen isotopes molecules* (in Russian), preprint No. 3811/12, Institute of Atomic Energy, Moscow (1983).
[37]L. I. Ponomarev and M. P. Faĭfman, Zh. Eksp. Teor. Fiz. **71**, 1669 (1976) (*sic*).
[38]É. A. Vesman, Pis'ma Zh. Eksp. Teor. Fiz. **5**, 113 (1967) [JETP Lett. **5**, 91 (1967)].
[39]S. I. Vinitskiĭ, L. I. Ponomarev, I. V. Puzynin, T. P. Puzynina, L. N. Somov, and M. P. Faĭfman, Zh. Eksp. Teor. Fiz. **74**, 849 (1978) [Sov. Phys. JETP **47**, 444 (1978)].
[40]L. I. Men'shikov, Yad. Fiz. **42**, 1184 (1985) [Sov. J. Nucl. Phys. **42**, 750].
[41]M. P. Faĭfman, L. I. Men'shikov, and T. A. Strizsh, Muon Catal. Fusion 4, 1 (1989).
[42]L. I. Men'shikov and M. P. Faĭfman, *Calculation of the rates of formation of mesomolecules taking into account the experimental data on the photoionization of hydrogen molecules*, (in Russian), Preprint No. 3849/12, Institute of Atomic Energy, Moscow (1983).
[43]Ya. B. Zel'dovich and S. S. Gerstein, Zh. Eksp. Teor. Fiz. **35**, 821 (1958) [Sov. Phys. JETP **8**, 570 (1958)].
[44]E. Zavattini in: Ref. 1, Vol. 2, p. 219.
[45]D. D. Bakalov, M. P. Faifman, L. I. Ponomarev, and S. I. Vinitsky, Nucl. Phys. A **384**, 302 (1982).
[46]D. D. Bakalov *et al.*, *μ-capture in liquid hydrogen* (in Russian), Preprint No. R4-82-633, Joint Intitute of Nuclear Research, Dubna (1982).
[47]S. S. Gerstein and L. I. Ponomarev, Phys. Lett. B **72**, 80 (1977).
[48]V. N. Ostrovskiĭ and V. I. Ustimov, Zh. Eksp. Teor. Fiz. **79**, 1228 (1980) [Sov. Phys. JETP **52**(4), 620 (1980)].
[49]A. M. Lane, Phys. Lett. A **98**, 337 (1983).
[50]L. I. Men'shikov and M. P. Faifman, A scheme for calculating decay rates of quasi-stationary states of molecular complexes, Preprint No. 4180/12, Institute of Atomic Energy, Moscow (1985).
[51]L. I. Men'shikov and M. P. Faĭfman, Yad. Fiz. **43**, 650 (1986) [Sov. J. Nucl. Phys. **43**, (3), 414 (1986)].
[52]L. I. Men'shikov, L. I. Ponomarev, T. A. Strizh, and M. P. Faĭfman, Zh. Eksp. Teor. Fiz. **92**, 1173 (1987) [Sov. Phys. JETP **65**, 656 (1987)].
[53]V. M. Perelomov, V. S. Popov, and M.V. Terent'ev, *ibid.* **50**, 1393 (1966) [Sov. Phys. JETP **23**, 924 (1966)].
[54]L. I. Men'shikov, Yad. Fiz. **42**, 1449 (1985) [Sov J. Nucl. Phys. **42**, 918 (1985)].
[55]L. I. Men'shikov, L. N. Somov, and M. P. Faĭfman, Zh. Eksp. Teor. Fiz. **94**, 6 (1988) [Sov. Phys. JETP. **67**, 652 (1988)].
[56]L. N. Somov, Muon Catal. Fusion **3**, 465 (1988).
[57]M. P. Faifman, *ibid.* **2**, 247.
[58]L. I. Men'shikov and L. I. Ponomarev, Pis'ma Zh. Eksp. Teor. Fiz. **45**, 471 (1987). [JETP Lett. **45**, 602 (1987)].
[59]M. P. Faifman, L. I. Men'shikov, and L. I. Ponomarev, Muon Catal. Fusion **2**, 285 (1988).
[60]W. H. Breunlich, M. Cargnelli, and P. Kammel, Phys. Rev. Lett. **53**, 1137 (1984).
[61]L. N. Somov, *Hyperfine structure of the energy levels of the mesicatom dμ and the mesic-molecule ddμ and the kinetics of mesic-molecular processes in deuterium* (in Russian), Preprint R4-81-851, Joint Institute of Nuclear Research, Dubna, 1981.
[62]W. H. Breunlich, M. Cargnelli, and J. Marton, Phys. Rev. Lett. **58**, 329 (1987).
[63]M. P. Faifman, L. I. Men'shikov, L. I. Ponomarev, I. V. Puzynin, and T. A. Strizsh, Z. Phys. D **1**, 79 (1986).
[64]L. I. Men'shikov and L. I. Ponomarev, Phys. Lett. B **167**, 141 (1986).
[65]Yu. V. Petrov, *Effect of the finite lifetime of a mesomolecular complex on the resonance mechanism of its formation* (in Russian), Preprint No. 1058, Leningrad Institutre of Nuclear Research, Academy of Sciences of the USSR, Leningrad, 1985.
[66]L. I. Men'shikov, Fiz. Elem. Chastits At. Yadra **199**, 1349 (1988) (*sic*).
[67]L. I. Men'shikov, Muon Catal. Fusion **2**, 273 (1988).
[68]I. I. Sobel'man, *Introduction to the Theory of Atomic Spectra*, Pergamon Press, N.Y., 1972 [Russ. original, Fizmatgiz, M., 1963].
[69]V. A. Alekseev, T. A. Andreeva, and I. I. Sobel'man, Zh. Eksp. Teor. Fiz. **62**, 614 (1972) [Sov. Phys. JETP **35**, 325 (1972)].
[70]A. A. Radtsig and B. M. Smirnov, Reference Data on Atoms, Molecules, and Ions, Springer-Verlag, Berlin, 1985. [Russ. original, Atomizdat. M., 1980 and 1986].
[71]V. M. Galitskiĭ, *Collected Scientific Works* [in Russian], Nauka, M., 1981.
[72]S. Cohen, D. L. Judd, and R. T. Riddel, Phys. Rev. **119**, 384 (1960).
[73]Ya. B. Zel'dovich and A. D. Sakharov, Zh. Eksp. Teor. Fiz. **32**, 974 (1957) [Sov. Phys. JETP **5**, 797 (1957)].
[74]L. N. Bogdanova, V. E. Markushin, V. S. Melezhik, and L. I. Ponomarev, *ibid.* **83**, 1615 (1982) [Sov. Phys. JETP **56**, 931 (1984)].
[75]L. N. Bogdanova, V. E. Markushin, V. S. Meleshik, and L. I. Ponomarev, Phys. Lett. B **115**, 171 (1982).
[76]W. H. Breunlich, M. Cargnelli, P. Kammel, J. Marton, N. Nagele, J. Werner, J. Zmeskal, C. Petitjean, J. Bistirlich, K. Crowe, J. Kurch, R. H. Sherman, H. Bossy, F. J. Hartmann, W. Neuman, and G. Smidt, Muon Catal. Fusion **1**, 121 (1981).
[77]S. I. Vinitskiĭ, L. I. Ponomarev, and M. P. Faĭfman, Zh. Eksp. Teor. Fiz. **82**, 985 (1982) [Sov. Phys. JETP. **55**, 578 (1982)].
[78]D. D. Bakalov, V. S. Melezhik, L. I. Men'shikov, and M. P. Faifman *ibid.* **94**, 61 (1988) [Sov. Phys. JETP **67**, 1769 (1988)].
[79]L. I. Men'shikov, *Muon-induced ion-molecular reactions in a mixture of hydrogen isotopes* (in Russian), Preprint No. 2810/12, Institute of Atomic Energy, Moscow, 1983.
[80]B. P. Ad'yasevich, V. G. Antonenko, and V. N. Bragin, Yad. Fiz. **35**, 1167 (1982) (*sic*).
[81]V. M. Bystritskiĭ, V. P. Dzhelepov, Z. V. Ershova, V. G. Zinov, V. K. Kapyshev, S. M. Mukhamet-Galieva, V. S. Nadezhdin, L. A. Rivkis, A. I. Rudenko, V. I. Satarov, N. V. Sergeeva, L. N. Somov, V. A. Stolupin, and V. V. Fil'chenkov, Pis'ma Zh. Eksp. Teor. Fiz. **31**, 249 (1980) [JETP Lett. **31**, 228 (1980)].
[82]V. G. Zinov, L. N. Somov, and V. V. Fil'chekov, *On the determination*

of the parameters of muonic catalysis from analysis of experimental temporal distributions of sequentially detected fusion events (in Russian), Preprint R1-81-853, Joint Institute of Nuclear Research, Dubna (1983).
[83] V. G. Zinov, L. N. Somov, and V. V. Fil'chenkov, At. Energ. **58**, 190 (1985). [Sov. At. Energy **58**, 226 (1985)].
[84] M. Bubak, V. M. Bystritsky, and A. Gula, Acta Phys. Polon. B **16**, 575 (1985).
[85] V. V. Filchenkov, L. N. Somov, and V. G. Zinov, Nucl. Instrum. Methods A **228**, 174 (1984).
[86] V. G. Zinov, L. N. Somov, and V. V. Fil'chenkov, *Method for determining the parameters of multiple muon catalysis* (in Russian) Preprint R15-82-478, Joint Institute of Nuclear Research, Dubna, 1982.
[87] A. J. Caffrey, A. N. Anderson, C. van Siclen, K. D. Watts, J. N. Bradbury, P. A. M. Gram, M. Leon, H. R. Maltrud, A. Paciotti, and S. E. Jones, Muon Catal. Fusion **1**, 53 (1987).
[88] W. H. Breunlich, M. Cargnelli, P. Kammel, J. Marton, N. Nagele, P. Pawlek, A. Scrinzi, J. Werner, J. Zmeskal, J. Bistirlich, K. M. Crowe, M. Justice, J. Kurck, C. Petitjean, R. H. Sherman, H. Bossy, H. Daniel, F. J. Hartman, W. Neumann, A. Schmidt, and T. von Egidi *ibid.*, 67.
[89] S. S. Gershteĭn, Yu. V. Petrov, L. I. Ponomarev, N. P. Popov, L. I. Presnyakov, and L. N. Somov, Zh. Eksp. Teor. Fiz. **80**, 1690 (1981) [Sov. Phys. JETP **53**, 872 (1981)].
[90] L. Bracci and G. Fiorentini, Nucl. Phys. A **364**, 383 (1981).
[91] L. N. Bogdanova, L. Bracci, G. Fiorentini, S. S. Gershtein, V. E. Markushin, V. S. Melezhik, L. I. Men'shikov, and L. I. Ponomarev, *ibid.* **454**, 653 (1986).
[92] D. Ceperly and B. J. Alder, Phys. Rev. A **31**, 1999 (1985).
[93] L. N. Bogdanova, V. E. Markushin, V. S. Melezhik, L. I. Men'shikov, and L. I. Ponomarev, Phys. Lett. B **161**, 1 (1985).
[94] D. K. Brice, Phys. Rev. **6**, 1791 (1972).
[95] G. A. Fesenko, V. L. Shablov, and V. A. Shakirov, Muon Catal. Fusion **3**, 439 (1988).
[96] E. Watt, K. F. Dunn, and H. B. Gilbody, J. Phys. B **19**, 355 (1986).
[97] J. B. Mitchel, K. F. Dunn, and G. C. Angel, *ibid.* **10**, 1897 (1987).
[98] B. Peart, R. Grey, and K. T. Dolder, *ibid.* **10**, 2675 (1977).
[99] L. A. Vaĭnshteĭn, I. I. Sobel'man, and E. A. Yukov, *Excitation of Atoms and Broadening of Spectral Lines*, Springer-Verlag, N.Y., 1981. [Russ. original, Nauka, M., 1979].
[100] L. I. Menshikov, *The muon stripping probability in $a\mu$-atom deceleration and excitation processes in matter*, Preprint No. 4206/12, Institute of Atomic Energy, Moscow, 1985.
[101] J. S. Cohen, Phys. Rev. Lett. **58**, 1407 (1987).
[102] L. I. Men'shikov and L. I. Ponomarev, Pis'ma Zh. Eksp. Teor. Fiz. **41**, 511 (1985) [JETP Lett. **41**, 623 (1985)].
[103] W. H. Breunlich, M. Cargnelli, J. Marton, P. Kammel, and C. Petitjean, Phys. Rev. Lett. **58**, 329 (1987).
[104] D. V. Balin, A. A. Vorob'ev, An. A. Vorob'ev, A. E. Il'in, E. M. Maev, V. P. Maleev, A. A. Markov, V. I. Medvedev, G. E. Petrov, L. B. Petrov, G. G. Semenchuk, and Yu. V. Smirenin, Pis'ma Zh. Eksp. Teor. Fiz. **85**, 1159 (1983).
[105] L. I. Men'shikov, Zh. Eksp. Teor. Fiz. **85**, 1159 (1983) [Sov. Phys. JETP. **58**, 675 (1983)].
[106] L. I. Men'shikov, Fiz. Plazmy **16**, 726 (1990) [Sov. J. Plasma Phys. (to be published)].
[107] L. I. Men'shikov and L. N. Somov, At. Energ. **69**, 398 (1990). [Sov. At. Energy, **69**, (1990)].
[108] S. T. Belyaev and A. I. Budker, in Plasma Physics and Problems in Controlled Thermonuclear Reactions [in Russian], Moscow, 1958, Vol. 3, p. 41.
[109] L. P. Pitaevskiĭ, Zh. Eksp. Teor. Fiz. **42**, 1326 (1962) [Sov. Phys. JETP **15**, 919 (1962)].
[110] E. M. Lifshitz and L. P. Pitaevskii, Physical Kinetics, Pregamon Press, Oxford, 1981. [Russ. original, Nauka, M., 1979].
[111] H. Bethe and E. Salpeter, *Quantum Mechanics of Atoms with One and Two Electrons*, Academic Press, N.Y., 1957 [Russ. transl., Fizmatgiz, M., 1960]
[112] G. G. Gel'man, Quantum Chemistry [in Russian], ONTI, M., 1937.
[113] R. P. Feynman, Phys. Rev. **56**, 340 (1939).
[114] W. Kolos and L. Wolnievicz, J. Chem. Phys. **41**, 3663 (1964).
[115] W. Kolos and L. Wolnievicz, *ibid.* **43**, 2429 (1965).
[116] L. I. Ponomarev and T. P. Puzynina, *Tables of the effective potentials for the three-body problem with the Coulomb interaction in the adiabatic representation*, Preprint JINR E4-83-778, Dubna, 1983.
[117] S. T. Belyaev and A. I. Budker, Dokl. Akad. Nauk SSSR **107**, 807 (1956) [Sov. Phys. Dokl. **107**, 100 (1956)].
[118] B. A. Trubnikov, Voprosy Teorii plazmy, Gosatomizdat, M., 1963, No. 1. [Rev. Plasma Phys. **1**, 105 (1965).
[119] L. D. Landau and E. M. Lifshitz, *Hydrodynamics*, Pergamon Press, N. Y., 1959 [Russ. original, Nauka, M., 1954 and 1986].
[120] V. B. Berestetskiĭ, E. M. Lifshitz, and L. P. Pitaevskiĭ, *Relativistic Quantum Theory*, Pergamon Press, Oxford, 1971 [Russ. original, Nauka, M., 1968].
[121] S. I. Braginskiĭ, *Transport phenomena in plasma* in: Ref. 118, p.183. [Rev. Plasma Phys. **1**, 205 (1983)].
[122] E. V. Grabovsky, S. L. Nedoseev, G. M. Oleynik, V. P. Smirnov, and V. Ya. Tsarfin, in *Proceedings 7th International Conference on High Power Particle* Beams (Beams-88), Karlsruhe, 1988, EC-5, p. 333.
[123] R. B. Baksht, in *Emission High-Current Electronics* [in Russian], Ed. G. A. Mesyats, Nauka, Novosibirsk, 1984.
[124] R. B. Baksht, I. M. Datsko, V. V. Loskutov, and A. V. Fedyunyn, *Subkilovolt emission of fast liners*, (in Russian), Preprint No. 34, Institute of High-Current Electronics of the Siberian Branch of the USSR Academy of Sciences, Tomsk (1988).
[125] V. V. Vikhrev, Fiz. Plazmy **12**, 454 (1986) [Sov. J. Plasma. Phys. **12**, 262 (1986)].
[126] V. F. D'yachenko and V. S. Imshennik, Voprosy teorii plazmy, Atomizdat, M., 1974, No. 8, p. 164. [Rev. Plasma Phys. **8**, 199 (1980)].
[127] B. A. Trubnikov, Fiz. Plazmy **12**, 468 (1986) [Sov. J. Plasma. Phys. **12**, 271 (1986)].
[128] V. V. Orlov, G. B. Shatalov, and K. B. Sherstnev, At. Energ. **55**, 391 (1983). [Sov. At. Energy **55**, 843 (1983)].
[129] Yu. V. Petrov, Nature **285**, 466 (1980).
[130] L. I. Men'shikov, S. L. Nedoseev, V. P. Smirnov, and L. N. Somov, *On the possibility of obtaining high-energy electron and ion rings in imploding liners* (in Russian), Preprint No. 5077/6, Institute of Atomic Energy, Moscow (1990).
[131] V. M. Bystritskiĭ, V. P. Dzhelepov, V. I. Petrukhin, A. I. Rudenko, L. N. Somov, V. M. Suvorov, V. V. Fil'chenkov, G. Khemnits, N. N. Khovanskiĭ, B. A. Khomenko, and D. Khorvat, Zh. Ekspt. Teor. Fiz. **76**, 460 (1979) [Sov. Phys. JETP **49**, 232 (1979)].
[132] V. M. Bystritsky, V. P. Dzhelepov, V. V. Filchenko, L. N. Somov, and A. V. Stolupin, Proc. Muon Catalyzed Fusion Workshop, Sanibel Island, FL., 1989, p. 17.

Translated by M. E. Alferieff